

# A NEW ROUTE TOWARDS LIGNIN-BASED POLYOLS:



## A HIGHWAY FOR LIGNIN EXPLOITATION

**Jonatan Perez-Arce**

**Donostia-San Sebastián 2020**

emari ta zabal zazu



Universidad  
del País Vasco

Euskal Herriko  
Unibertsitatea



# A NEW ROUTE TOWARDS LIGNIN-BASED POLYOLS: A HIGHWAY FOR LIGNIN EXPLOITATION

A dissertation presented by

**Jonatan Pérez Arce**

In fulfilment of the Requirements for the Degree Doctor of Philosophy

by the University of the Basque Country

In the program Renewable Materials Engineering

Advisors: **Dr. Jalel Labidi** and **Dr. Eduardo J. Garcia-Suarez**

**Chemical and Environmental Engineering Department**

**Faculty of Engineering, Gipuzkoa**

**DONOSTIA - SAN SEBASTIÁN 2020**



***“ The most exciting phrase to hear in science,  
the one that heralds new discoveries,  
is not ‘eureka’ (I found it) but ‘that’s funny.’ ”***

Isaac Asimov



## I. ACKNOWLEDGEMENTS

No se me ocurre mejor forma de empezar esta página tan especial que agradeciendo a mis directores de tesis: Eduardo J. Garcia-Suarez y Jalel Labidi, por brindarme la oportunidad de materializar estos cuatro años de doctorado. Gracias por guiarme, por el apoyo y por la confianza depositada en mí, que me han servido no solo de crecimiento académico, sino también, personal.

Quiero dedicar una mención especial a José Ramón Ochoa Gómez. Sin él toda esta aventura hubiera sido inimaginable. Gracias por poner las bases a esta tesis, compartir conmigo esa pasión por la ciencia y transmitirme parte del gran conocimiento que atesoras.

Al grupo de Química Sostenible de Tecnalia que me ha visto crecer y madurar desde que empecé con mis prácticas de máster. Quiero daros las gracias individualmente: Francisca, Olga, Soraya, Susana y Tomás, y en especial, a las que habéis compartido los laboratorios todos estos años conmigo: Ander, Belén, Cristina, Noelia, Leire y Silvia. Me habéis hecho disfrutar cada éxito y ayudado a superar los obstáculos que cada día nos pone la investigación en nuestro camino y que hace de la ella algo tan especial y emocionante.

A Amaia, Fabio, Izaskun, Rut, Patricia y Xabier daros las gracias por hacerme partícipe del grupo de BioRP. A pesar de haber trabajado en lugares diferentes, me habéis acogido como si hubiera estado haciendo el doctorado con vosotros. Gracias por esas cenas, los “Skypotes” y los viajes que compartimos.

A mis amigos y familia, en especial a mis padres, por ser ese pilar invisible durante todos estos años, apoyándome, animándome día a día y siendo tan comprensibles conmigo en esas semanas que “desaparecía” cuando estaba enfrascado en la tesis.

Y por último, me gustaría dedicar este último párrafo a la persona más importante en mi vida. Gracias Leyre por todos los años de apoyo incondicional, por estar ahí tanto en los mejores días como en los más duros. Pero, sobre todo, por haber podido compartir contigo todas las alegrías que hemos vivido y por las que nos quedan. Asko maite zaitut!





## II. MOTIVATION AND OBJECTIVES

The petrochemical boom of the second half of the last century has marked the strong development of synthetic polymers. The availability of a growing number of monomers from fossil resources has supplanted the use of biobased chemicals and their corresponding polymers gradually. However, the increase in the use of petrochemical-based products along with the oil depletion and the increasing awareness of environmental issues has led to intense research for bio-based alternatives. In this context, the synthesis of polymeric materials from renewable resources will play a crucial role, and making it industrially viable will be the greatest challenge for its future.

The growing interest in green and sustainable chemistry has focused specially in the lignocellulosic feedstock and by-products arising from agricultural, marine, and forestry activities considered as a promising, renewable, and vast resource for chemicals. In this area, lignin is one of the most promising biopolymers. Considered, until last decades, as a by-product from pulp and paper industry, lignin is gaining in importance due to its availability and exploitation possibilities.

Lignin is the second most abundant biopolymer on the earth after cellulose and the first one with an aromatic structure. It can be easily modified to make bio-based added-value products as critical intermediates for a huge field of applications. However, the use of lignin as a feedstock is still hampered by its inherent low reactivity, its brittle, and its complex structure. One way to boost the lignin is through its functionalization, yielding lignin-based polyols with better properties for industrial exploitation. Up to now, the best way to make lignin-based polyols is by lignin oxypropylation.

Nevertheless, this traditional method has several drawbacks related to the aggressive operating conditions employed. Therefore, the reaction requires special equipment to ensure safety against explosions and reaction conditions, increasing the final cost of the polyols considerably, hampering any industrial application. To circumvent these drawbacks, in this thesis, a more industrially feasible alternative route is proposed. The new process allows the synthesis of lignin-based polyols with a controlled structure under very mild conditions.

To achieve this purpose, the thesis is structured in four chapters. In **Chapter 1**, the current state of petrochemical-based polyols and the current routes to obtain bio-based alternatives are discussed with special emphasis on those obtained from lignocellulosic material and specifically from lignin.

**Chapter 2** deals with the study of the different technical lignins and the selection of the most suitable lignin to carry out a lignin polymerization according to the standard conditions used in cationic ring-opening polymerization. The selected lignin is subjected to a more exhaustive study of its chemical composition and thermal properties.

In **Chapter 3**, a study of the cationic ring-opening polymerization of oxiranes is conducted in the presence of lignin, and a polymerization mechanism is proposed to obtain lignin-based polyols. The potential of this route is studied using different reaction conditions, including the employment of different lignin sources, and possible applications are also considered for these lignin-based polyols.

**Chapter 4** extends the family of lignin-based polyols through the polymerization of different oxiranes in presence of lignin. The polyols obtained are characterized, and new structures are proposed in

accordance with the results obtained. Finally, more complex polyols are prepared by the sequential addition of different monomers.

**Chapter 5** deals with the main conclusions obtained along the previous chapters and possible future work are also presented, together with the scientific publications, patents, and publications derived from this thesis.



### III. LIST OF ABBREVIATIONS

<b>Abbreviation</b>	<b>Description</b>
<b>Lignins</b>	
Beech-OL	Organosolv lignin obtained from beech
Elm-KL	Kraft lignin obtained from elm
Eucalyptus-HL	Hydrolysis lignin obtained from eucalyptus
Eucalyptus-KL	Kraft lignin obtained from eucalyptus
GL	Lignin oligomer obtained after solvolysis in methanol
KL	Kraft lignin
Mix-OL	Organosolv lignin obtained from a mixture of woods
Olive-SL	Soda lignin obtained from olive
Pine-HL	Hydrolysis lignin obtained from pine
Poplar-HL	Hydrolysis lignin obtained from poplar
Poplar-KL	Kraft lignin obtained from poplar
<b>Lignin-based polyols and materials</b>	
CO-LBP	Lignin-based copolymer
FPU	Flexible polyurethane foam
GL-LBP	Lignin-based polyol using GL
KL-LBP	Lignin-based polyol using KL
Mix-OL-LBP	Lignin-based polyol using Mix-OL
LBP	Lignin-based polyol
LBP-FPU	LBP-based flexible polyurethane foam
LBP-RPU	LBP-based rigid polyurethane foam
LTES	Low-temperature energy storage system
PCM	Phase Change Material
PU	Polyurethane
RPU	Rigid polyurethane foam
TER-LBP	Lignin-based terpolymer
TETRA-LBP	Lignin-based tetrapolymer
<b>Reagents and catalysts</b>	
ACN	Acetonitrile
BO	Butylene oxide
BF <sub>3</sub> ·Et <sub>2</sub> O	Boron trifluoride etherate
Bu <sub>4</sub> NOH	Tetrabutylammonium hydroxide
CO	Cyclohexene oxide

DCE	Dichloroethane
DCM	Dichloromethane
DMEA	N,N-Dimethylethylamine
ECH	Epichlorohydrin
EE	1,2-Epoxy-5-hexene
EO	Ethylene oxide
GLY	Glycidol
HBF <sub>4</sub>	Tetrafluoroboric acid
H <sub>2</sub> SO <sub>4</sub>	Sulfuric acid
HO	1,2-Epoxyhexane
KOH	Potassium hydroxide
OO	1,2-Epoxyoctane
PO	Propylene oxide
SO	Styrene oxide
THF	Tetrahydrofuran
TSI	p-Toluenesulfonyl isocyanate

---

**Reaction parameters and characterization techniques**

---

ACE	Active end chain
AM	Active monomer
AROP	Anionic ring-opening polymerization
ATR-FTIR	Attenuated Total Reflection Fourier Transform Infrared Spectroscopy
COL	Cyclic oligomer
CROCOP	Cationic ring-opening copolymerization
CROP	Cationic ring-opening polymerization
DSC	Differential Scanning Calorimetry
dTG	Derivative Thermo-Gravimetric analysis
H	Humidity content
HPLC	High-Performance Liquid Chromatography
L wt. %	Lignin content in weight given as a percentage
MON	Monomer
MON wt. %	Monomer content in weight given as a percentage
MR	Molar ratio
MR BF <sub>3</sub> /OH-L	Molar ratio between boron trifluoride etherate and monomer
MR DMEA/BF <sub>3</sub>	Molar ratio between N,N-Dimethylethylamine, and boron trifluoride etherate
MR OH:MON:THF	Average molar ratio of monomer and THF per OH group
MR THF/MON	Average molar ratio between tetrahydrofuran and monomer

---

MWD	Molecular weight distribution
OH#	Hydroxyl number
PDI	Polydispersity index
Q <sub>s</sub>	Specific flow rate
ROP	Ring-opening polymerization
SEC	Size Exclusion Chromatography
S/G	Syringyl and guaiacyl ratio
T	Temperature
T <sub>5%</sub>	Temperature associated with a 5 % weight loss of the sample
T <sub>50%</sub>	Temperature associated with a 50 % weight loss of the sample
TGA	Thermo-Gravimetric Analysis
THF wt. %	Tetrahydrofuran content in weight given in percentage
$\overline{M}_w$	Average molecular weight

**Units**

---

g	gram
h	hour
kg	kilogram
kPa	kilopascal
m <sup>3</sup>	cubic meter
min	minute
mL	milliliter
L	liter
n <sub>OH-L</sub>	mol of lignin hydroxyl groups
t	tonne
°C	degree centigrade





---

# TABLE OF CONTENTS

<b>I. ACKNOWLEDGEMENTS</b>	<b>i</b>
<b>II. MOTIVATION AND OBJECTIVES</b>	<b>iii</b>
<b>III. LIST OF ABBREVIATIONS</b>	<b>vii</b>
<b>CHAPTER 1 - INTRODUCTION</b>	<b>1</b>
1.1 Overview	3
1.2 Biomass as a source for sustainable applications	5
1.3 Lignocellulosic biomass	8
1.3.1 <i>Inorganic matter</i>	8
1.3.2 <i>Extractives</i>	9
1.3.3 <i>Cellulose</i>	9
1.3.4 <i>Hemicellulose</i>	10
1.3.5 <i>Lignin</i>	11
1.3.6 <i>Potential routes for lignin valorization</i>	16
1.4 Aim and outline of the thesis	27
1.5 References	29
<b>CHAPTER 2 - LIGNIN SELECTION FOR OBTAINING LIGNIN-BASED POLYOLS</b>	<b>41</b>
2.1 Background	43
2.1.1 <i>Lignin sources</i>	43
2.1.2 <i>Technical lignins</i>	46
2.1.3 <i>Lignin solubility</i>	54
2.2 Objective	55
2.3 Methodology	55
2.3.1 <i>Materials</i>	55
2.3.2 <i>Characterization</i>	56
2.4 Results and discussion	57

2.4.1	<i>Lignin selection</i>	57
2.4.2	<i>Lignin characterization</i>	59
2.5	Conclusions	66
2.6	References	67
<b>CHAPTER 3 - LIGNIN-BASED POLYOLS BY CATIONIC RING-OPENING POLYMERIZATION</b>		<b>75</b>
3.1	Background	77
3.1.1	<i>Cationic ring-opening polymerization mechanism</i>	80
3.2	Objectives	86
3.3	Methodology	87
3.3.1	<i>Materials</i>	87
3.3.2	<i>Synthesis of LBPs</i>	87
3.3.3	<i>Characterization of LBPs</i>	89
3.4	Results and discussion	89
3.4.1	<i>Reaction parameter evaluation</i>	89
3.4.2	<i>LBP proposed mechanism</i>	112
3.4.3	<i>Other lignin sources</i>	115
3.4.4	<i>LBP potential applications</i>	124
3.5	Conclusions	136
3.6	References	139
<b>CHAPTER 4 - LIGNIN-BASED POLYOLS WITH CONTROLLED MICROSTRUCTURE</b>		<b>149</b>
4.1	Background	151
4.2	Objective	154
4.3	Methodology	155
4.3.1	<i>Materials</i>	155
4.3.2	<i>Synthesis of the LBPs</i>	155
4.3.3	<i>Characterization of LBPs</i>	156
4.4	Results and discussion	157
4.4.1	<i>Influence of the nature of the oxirane</i>	157

---

4.4.2	<i>Hyperbranched LBPs</i>	170
4.4.3	<i>Terpolymers and tetrapolymers</i>	173
4.5	Conclusions	184
4.6	References	186
<b>CHAPTER 5 - CONCLUSIONS, FUTURE WORK, AND PUBLISHED RESEARCH</b>		<b>191</b>
5.1	Conclusions	193
5.2	Future work	196
5.3	Published research	197
<b>LIST OF FIGURES</b>		<b>199</b>
<b>LIST OF TABLES</b>		<b>203</b>
<b>LIST OF SCHEMES</b>		<b>206</b>
<b>APPENDIX I - PROCEDURES FOR LIGNIN AND LIGNIN-BASED POLYOLS CHARACTERIZATION</b>		<b>207</b>
	Moisture content determination	209
	Lignin ash content determination	210
	Acid-insoluble lignin and carbohydrate content of lignin determination	211
	Acid-soluble lignin determination	214
	Lignin purity determination	215
	Pyrolysis-Gas Chromatography/Mass Spectrometry analysis	215
	Lignin solubility determination	216
	Differential Scanning Calorimetry analysis	216
	Molecular weight analysis	217
	Lignin and LBP functional groups determination	218
	Lignin-based polyol composition determination	218
	Monomer conversion and unreacted monomer determination	220
	Hydroxyl number determination	221

Thermo-Gravimetric Analysis	222
References	222

# CHAPTER 1

## INTRODUCTION

---



## 1.1 Overview

Nowadays, society is highly dependent on fossil resources, not only to produce energy but also for the production of many daily-use products, such as plastics, oils, detergents, asphalt, and fertilizers, among others [1.1]. The term “fossil fuel” encompasses non-renewable energy sources such as coal, natural gas, crude oil, and derived products. Fossil resources are carbon-based sources originated millions of years ago from plants and animals. In 2018, fossil resources supplied 84.7 % of the total energy, and it is expected that the primary energy demand is going to increase by 50-60 % in 2030, mainly due to population growth and the desire for better living standards around the world [1.2]. However, the use of fossil resources in recent years has begun to shrink in developed countries in favor of renewable and sustainable sources (**Figure 1.1**).

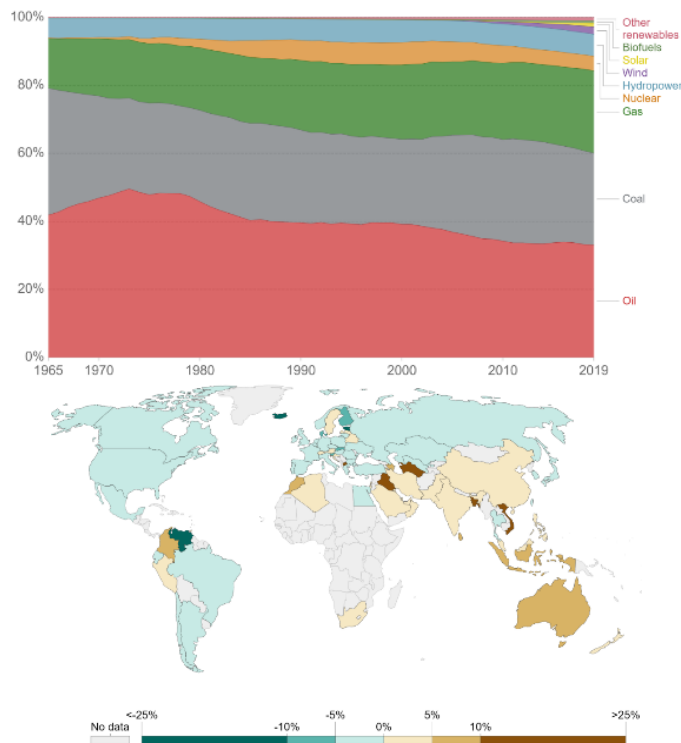


**Figure 1.1** Energy consumption timeline by source (up) and annual percentage change in fossil consumption in 2019 (down) (data obtained from: '<https://ourworldindata.org/energy>').

Along with human history, polymers, both natural and synthetic, have played a pivotal role simplifying every facet of our lives and contributing ambiguously to modern civilization. Since the Second World War, the employment of polymers has grown exponentially in production, market, and applications. Polymers are broadly applied in food packages, textiles, automobiles, and electronics, penetrating almost every aspect of daily life. Since the production of polymers began to be counted in 1950 (two million metric tons in that year), the global annual plastic production has grown almost exponentially. Polyols global market represented approximately USD 26.2 billion in 2019 with an estimation of a market value of USD 34.4 billion in 2024. And they are essential in the manufacturing of some indispensable materials as polyurethanes, polycarbonates, and polyesters [1.3]. In accordance with this data, the global annual production has increased year over year, despite of almost half of the fabrication was done during the last decades [1.4].

Currently, most of the polymers we use daily are manufactured employing fossil-based feedstocks [1.5]. The polymer manufacturing, including the obtaining of the required precursor monomers, is considered one of the most significant contributions to greenhouse gas emissions and public health concerns [1.6]. Furthermore, when these polymers are disposed of at the end of their life cycle, large amounts of plastic waste are generated. As of 2015, over 6.3 billion metric tons of plastic waste were generated, of which ~9 % was recycled, and ~12 % was incinerated to recover energy. The remainder is regrettably discarded and mostly goes into the environment [1.6].

The depletion of fossil resources and its market instability, the rising environmental awareness, and health concerns in both industry and society, are strongly pushing the scientific community to look for bio-based alternatives such as the production of bio-polymers. The great



challenge of bio-polymers is that they should have a similar final price and comparable or superior quality in the final products as their fossil counterparts [1.7, 1.8]. Although it is a fact that nowadays, the bio-based monomers and bio-based materials cannot compete from a cost perspective with their petrochemical counterparts, the future success of the industry will depend on the development of these sustainable polymers. In the long term, it is expected that the fluctuation of the cost of fossil resources combined with the government policies along public awareness will encourage the growth of the renewable/bio-based industry [1.1].






## 1.2 Biomass as a source for sustainable applications

Our planet stores an enormous amount of available biomass in different areas, from forests to oceans, which is an advantage because it is universally accessible. Biomass is a complex heterogeneous combination of mainly organic matter, and to a lesser extent, inorganic matter [1.9]. The organic material comes from vegetables or animals, including crops and wastes, forest residues, animal wastes, municipal and industrial wastes, among others (**Table 1.1**).

The continuous biological activity of the Earth provides not only the human survival but also a variety of complementary substances and materials that have been exploited by humanity since its beginning. Over the centuries, the sophistication of the use of natural resources has increased, e.g., from the use of wood as an energy source and building material to paper manufacturing. At the beginning of the 19<sup>th</sup> century, the exploitation of renewable resources to prepare products of greater applicability was very prominent. Illustrative examples are the employment of natural rubber, cellulose acetate, vegetable dyes, and

drying oils. However, everything was left in the background with the massive exploitation, first of coal and then of oil, and the exponential growth of the commodities production, intermediate products, and polymers based on these compounds. Due to the problems associated with oil discussed above, the need to return to the exploitation of renewable resources has strongly emerged. However, to return to the use of biomass as a source of energy and materials, an intensive exploitation of the available resources is totally necessary following a more rational and complete strategy to be able to compete with the oil market.

**Table 1.1** Biomass classification according to their biological diversity, source, and origin [1.10].

BIOMASS GROUP	SUB-GROUP, VARIETIES, AND SPECIES
 WOODY BIOMASS	Coniferous or deciduous; angiospermous or gymnosperms; softwoods or hardwoods; stems, branches, foliage, bark, chips, lumps, and pellets.
 HERBACEOUS/AGRICULTURAL BIOMASS	Grasses and flowers, straws, fruits, shells, pipes, grains, seeds, coir, bagasse, and pulps.
 AQUATIC BIOMASS	Marine or freshwater algae; macroalgae or microalgae; and seaweed.
 ANIMAL BIOMASS WASTE	Bones, meat-bone meal, chicken litter, and manures.
 MUNICIPAL/INDUSTRIAL WASTE BIOMASS	Municipal solid waste, sewage sludge, paper-pulp sludge, waste papers, paperboard waste, chipboard, fibreboard, and wood pallets.

Under this topic, bio-based polymers have the potential to reduce the environmental impact of commercial plastics by offering significant performance and economic benefits over petrochemical-derived

macromolecules. According to European Bioplastics, the association representing the interests of the thriving bioplastics industry in Europe, plastic material is defined as a bioplastic if it is either biobased, biodegradable, or features both properties [1.11]. Bioplastic products have two significant advantages compared to their fossil-based counterparts: they save fossil resources employing biomass, which regenerates (annually), and they provide the unique potential of carbon neutrality. However, most of the currently available bio-based polymers are hampered by inadequate thermomechanical properties, low economic feasibility, and low-level scalability compared to their fossil-based counterparts. Therefore, bio-based materials must overcome these limitations to be more competitive in the marketplace [1.12]. Scientific research has mainly focused on the replacement of fossil raw materials by renewable alternatives and the development of bio-materials suitable for recycling or biodegradation. There are already well-established bio-based products on the market, such as bio-poly(ethylene terephthalate) (bio-PET), bio-polyethylene (bio-PE), poly(lactic acid) (PLA), and polybutylene adipate terephthalate (PBAT) [1.13, 1.14]. However, the total production of bio-based polymers represented only 2 % of the 360 million metric tons of polymers produced in 2019 (**Figure 1.2**) [1.13].

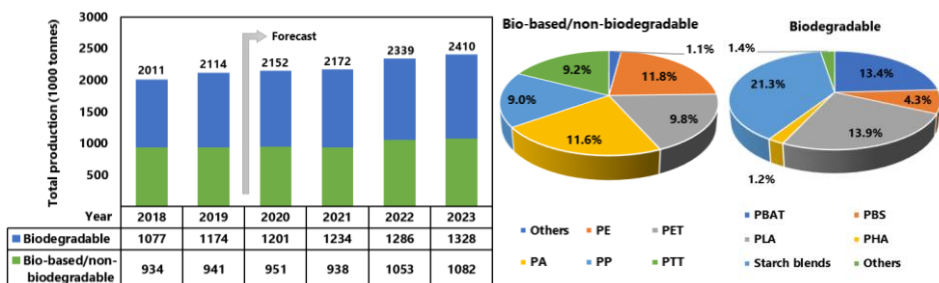


**Figure 1.2** Global production capacity of bioplastics (left) and global production capacity in 2019 (right), (adapted from <https://www.european-bioplastics.org>). Polyethylene (PE), polypropylene (PP), polyethylene terephthalate (PET), polyamides (PA), polytrimethylene terephthalate (PTT), polylactic acid (PLA), polyhydroxyalkanoates (PHA), polybutylene succinate (PBS), and polybutylene adipate terephthalate (PBAT).

The commercial application of bioderived polymers can benefit from improvements in environmental performance (as well as supporting policy or legislation). However, favorable economics and material properties at least equal to conventional materials are also required, including thermal resistance, mechanical strength, processability, and compatibility [1.15]. In this context, lignocellulosic biomass is a promising feedstock for the production of more sustainable and economic monomers and polymers and, at the same time, with the potential to provide improvements in their final performance.

### 1.3 Lignocellulosic biomass

Lignocellulose is the main component in the plant cells. It is a complex material consisting mainly of structural elements such as polymeric carbohydrates (cellulose and hemicelluloses) and an aromatic polymer structure (lignin), along with different extractives and inorganic materials. The composition of the lignocellulosic biomass depends greatly from the biomass source, growth conditions, geographical location, age, and plant tissue. In general, its composition is formed by a cellulose content of 40-50 wt. %, hemicellulose content of 15-35 wt. %, lignin content of 15-40 wt. % along with other minor components: proteins (3-10 wt. %), lipids (1.5 wt. %), and extractives (10.5 wt. %) [1.16, 1.17].

#### 1.3.1 Inorganic matter

The inorganic material content in biomass depends primarily on the type of raw material and environmental factors. They are absorbed from the soil and fixed in the cell wall. The common elements are calcium, sodium, potassium, magnesium, phosphorus, silicon, aluminum, nitrogen, sulfur, and iron [1.18].

### 1.3.2 Extractives

Extractives are the main non-structural components of lignocellulosic biomass. Although it is not a critical fraction of the structure of lignocellulosic matter, its existence is necessary for the growth of the plants. Furthermore, extractives protect the plant from various stress situations, such as pests or extreme weather conditions. This fraction is a mixture of compounds that can be extracted by different solvents, such as water or organic solvents. Major compounds considered as extractives are flavonoids, tannins, lignans, fatty acids, phenols, terpenes, low molecular weight carbohydrates, resins, and waxes, among others [1.19].

Obtaining extracts from biomass has always been ignored, mainly due to the low content of most of the raw materials. However, in recent years, because of the increased interest in the use of natural products, its study and valorization have increased considerably. The latest studies have revealed that this fraction is rich in compounds with different capacities as antioxidant, antifungal, antibacterial, anticarcinogenic, anti-inflammatory. This wide variety of properties makes the extractives a promising source in various industries such as agri-food, pharmaceutical, and cosmetics [1.20].

### 1.3.3 Cellulose

Cellulose is the most abundant polysaccharide and the most abundant polymer that can be found in nature. It is a linear polymer with high molecular weight formed by monomeric units of D-glucose linked by  $\beta$ -1,4-glucoside bonds, with a maximum of 15,000 monomeric units. Each glucose unit rotates  $180^\circ$  concerning its neighbors in the cellulose chain, forming the cellobiose (**Figure 1.3**). The union of different branches of cellobiose creates the cellulose structure. Finally, these cellulose chains

make a specific network between them, building bigger structures called microfibrils (**Figure 1.3**). This structure is formed by hydrogen bonds and van-der-Waals forces, which generated a solid interaction between cellulose crystal chains.

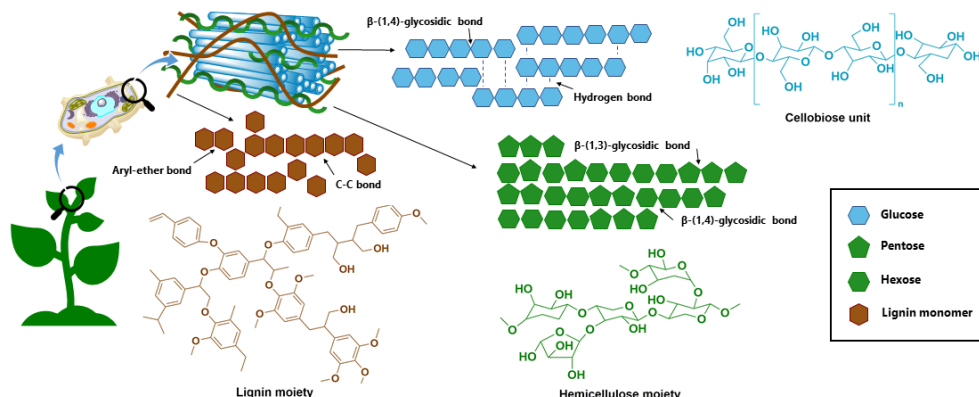


**Figure 1.3** Main compounds of the lignocellulosic biomass.

The cell walls that form the plant tissue are constituted by interlinkages of these microfibrils along with the hemicellulose and the lignin. This structure gives to the plant strength and protects it from microbial attack. The complexity of this structure makes it very difficult to extract these compounds separately, so fragmentation treatments are necessary to obtain them. In the industry, cellulose has been used mainly in paper manufacturing, although in the last decades, its number of applications has increased significantly. Currently, cellulose is used to produce different materials such as nanocrystals, films, fibers, membranes, and as a source of glucose as precursors for a wide variety of products, mainly bioethanol [1.21].

### 1.3.4 Hemicellulose

Hemicelluloses are an amorphous and heterogeneous group of branched polysaccharides. It is constituted mainly by pentoses (xylose and

arabinose), hexoses (mannose, glucose, and galactose), uronic acids (glucuronic and galacturonic acids), and acetylated sugars joined covalently assembling long chains [1.22]. In accordance with how they are joined, hemicellulose can be divided into three main groups: mannans, xylans, and xyloglucans.

The primary function of hemicellulose is to stabilize the cell wall by interacting with cellulose and lignin through hydrogen and covalent bonds, respectively. The hemicellulose content and structure vary depending on the plant [1.18], comprising approximately 15-35% of the lignocellulosic material. In softwoods, sugars derived from mannan are the most abundant, while sugars derived from xylan are predominant in hardwoods, annuals, and cereals. Hemicelluloses are applied in different areas such as food, medicine, or chemical industry, due to their good capacities of biodegradability, biocompatibility, and bioactivity [1.22, 1.23].

### 1.3.5 Lignin

Lignin is the most abundant natural polymer, after cellulose, and the first one with an aromatic structure. The word lignin is derived from the word lignum, which means wood. In 1838, Payen was the first to recognize the presence of lignin in wood, referring to it as “encrusting material” embedding cellulose [1.24]. Later, in 1865, Schulze defined this “encrusting material” as lignin [1.25]. Lignin is found in the cell wall of cellulose fibers performing different functions. The main functions are to provide structural support against oxidative stresses and microbial attacks, participate in water transportation, and increase the resistance to drought and extreme temperatures [1.26, 1.27]. The lignin content and type depend on its source: hardwood (angiosperms), softwoods (gymnosperm), and grasses. The average lignin content in hardwood and

softwood biomass is about 20-40 wt. % while grasses have less than 15 wt. %, although these values may be altered according to the location and growing environment, species diversity, and longevity [1.28].

Lignin is composed of three different derivatives of the cinnamyl alcohol precursor: *p*-coumaryl alcohol, coniferyl alcohol, and sinapyl alcohol (**Figure 1.4**). The monolignols are phenyl-propane units with a hydroxyl group in the  $C_\gamma$  position, an unsaturation between  $C_\alpha$  and  $C_\beta$  and with different degree of methoxylation at positions  $C_3$  and  $C_5$  of the ring. The abundance ratio of these monolignols depends on the species. When these monolignols are incorporated into the lignin structure, the resulting units are called guaiacyl (G), syringyl (S), and *p*-hydroxyphenyl (H), respectively (**Figure 1.4**).

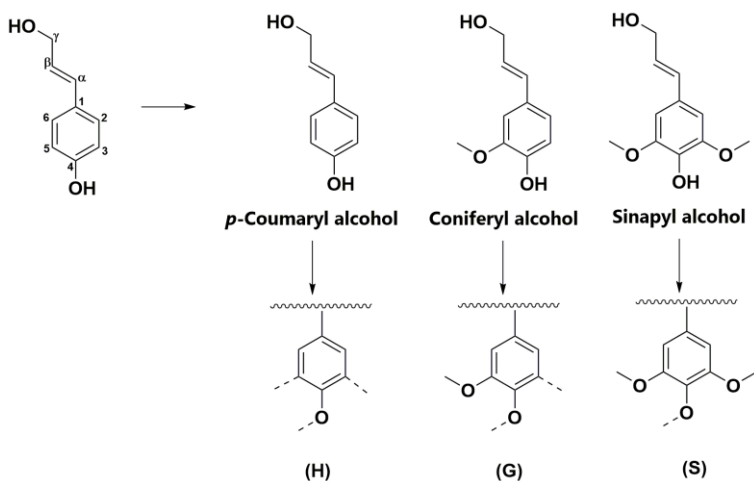


**Figure 1.4** Lignin monolignols precursors.

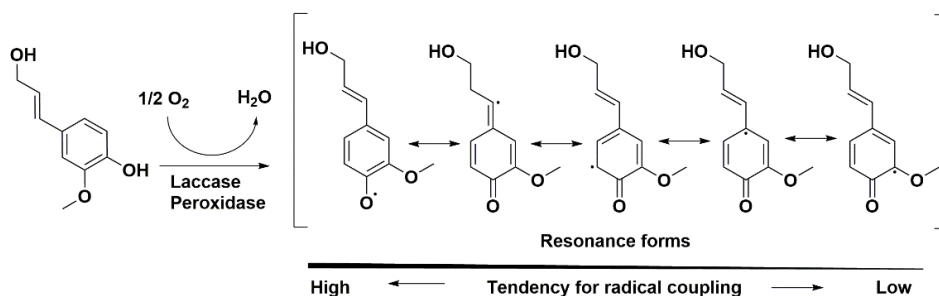
In **Table 1.2**, it is observed that the softwood lignin generally has a very high coniferyl alcohol monolignol content. In contrast, hardwood lignin has a mixture of coniferyl alcohol and sinapyl alcohol monolignols, and grass lignin has a combination of all the three aromatic units.



**Table 1.2** Monolignol distribution in different types of lignin [1.37-1.39].

Monolignols	Broadleaf Wood	Conifer Wood	Grass
	<i>Hardwoods</i>	<i>Softwoods</i>	
Sinapyl alcohol (S) (%)	50 – 75	0 – 1	25 – 50
Coniferyl alcohol (G) (%)	25 – 50	80 – 95	25 – 50
<i>p</i> -Coumaryl alcohol (H) (%)	Traces	0.5 – 3.4	10 – 25
S/G	5 – 1	0.05 – 0	1 – 0.5

The combination by polymerization of these three monolignols in different proportions through different carbon-oxygen and carbon-carbon bonds results into the heterogeneous structure of lignin [1.29]. This phenomenon occurs through the oxidative radicalization of the phenol units. First, the phenol monolignol is oxidized, forming a relatively stable phenolic radical due to the delocalization of the unpaired electron in the 4-hydroxyphenyl-propanoid structure. The oxidation reaction is usually catalyzed by peroxidases and laccases (**Figure 1.5**) [1.30]. Subsequently, pairs of monomer radicals can be coupled by a covalent bond forming a (dehydro)dimer through different linkages.

**Figure 1.5** Enzymatic formation of resonance monolignol radicals.

The type and abundance of each linkage depend on the radical stability in each position into the monolignol. The linkages can be grouped in ether linkages (e.g.,  $\alpha$ -O-4, 5-O-4, and  $\beta$ -O-4) and condensed linkages (e.g., 5-5, b-b, b-5, and b-1 linkages) (**Figure 1.6**) [1.31, 1.32].

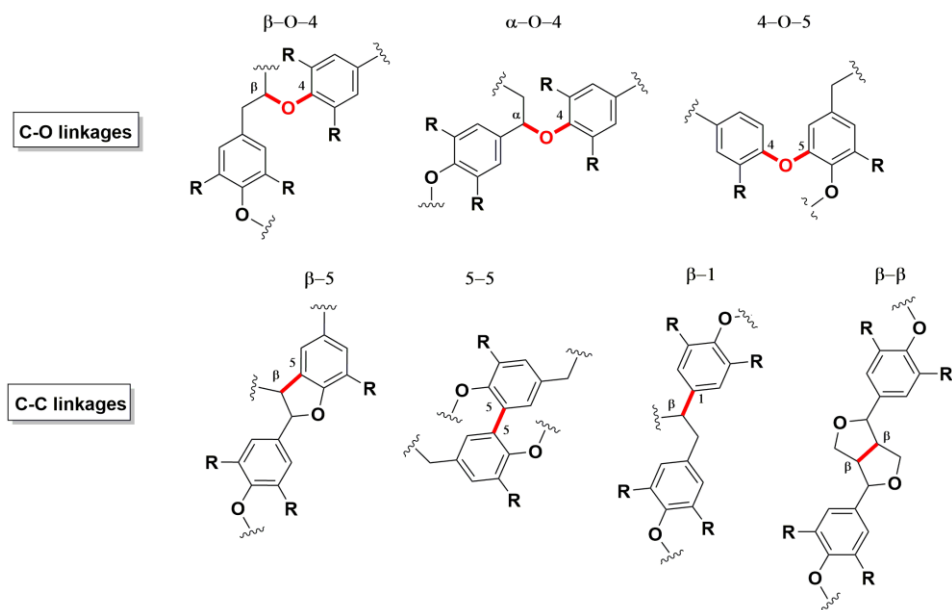


**Figure 1.6** Mayor linkages formed in the lignin formation.

Once the dimer is formed, it needs to be dehydrogenated again to form a radical and to be able to couple with another monomer by endwise coupling to obtain a polymer structure [1.33]. Lignin can be isolated from a wide range of plant biomass sources, including, among others, timber, grass, and bamboo [1.34]. The percentage of each type of linkage formed in the lignin depends on the plant species and the growing environment [1.35, 1.36].

**Table 1.3** indicates that hardwoods are predominantly made up of  $\beta$ -O-4 linkages. Around 40–60 % of the total intermolecular linkages in the structure of lignin are ether bonds, being the  $\beta$ -O-4 bond the predominant ether linkage, while softwoods have a more uniform distribution among the  $\beta$  linkages.

The wide range of combinations of the monolignols through the different linkages generates the final lignin structure. Unfortunately, the

overwhelming complexity of lignin formation is not fully defined yet. However, the structure proposed by Alder in 1977 (**Figure 1.7**) it is generally accepted [1.25]. In this representation, lignin is shown as a three-dimensional aromatic structure with different functional groups. These primary functional groups include hydroxyl, methoxyl, carbonyl, and carboxyl moieties in various amounts depending on its botanic origin [1.41].

**Table 1.3** Percentage of linkages in softwood and hardwood lignins [1.34, 1.35, 1.40].

Linkage type	Softwood (%)	Hardwood (%)
$\beta$ -O-4	45-50	60
5-5	9-25	4-5
$\beta$ -5	9-12	6
4-O-5	4-8	6-7
$\beta$ -1	7-10	7-8
$\beta$ - $\beta$	2-3	3
$\alpha$ -O-4	6-8	6-8

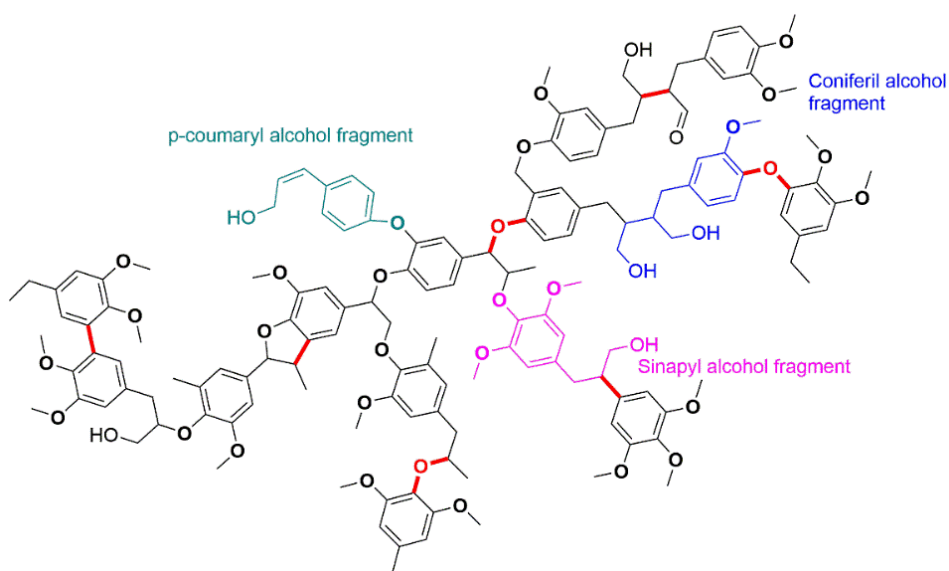


**Figure 1.7** Proposed lignin structure [1.25].

The history of lignin was attached for hundreds of years as an undesired by-product in the pulping process and cellulosic ethanol plants [1.33]. Less than 1 % of all lignin is recovered and sold as an added-value material, whereas the rest is used for energy recovery in pulp mills due to it is considered until now as a non-added-value by-product [1.42, 1.43]. The interest in the lignin valorization is an increasing topic promoted by the scientific society and society in general, motivated by environmental concerns and constant fluctuations of the petroleum market (**Figure 1.8**).

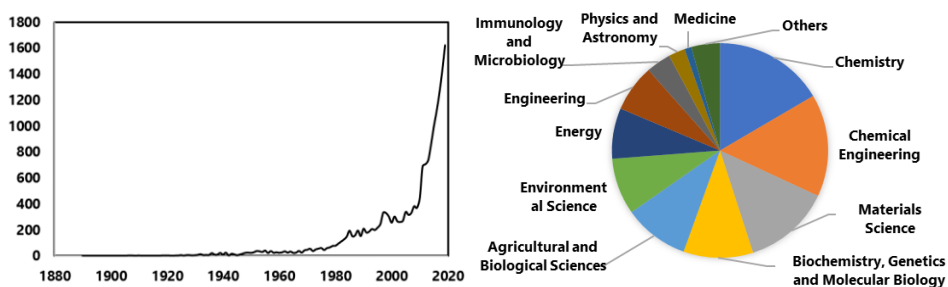


**Figure 1.8** Number of research publications (left) and sorted by subject area (right) filtered with “lignin” as a keyword in the title (data obtained from Web Of Science).

The availability of lignin in the biosphere exceeds 300 billion tons, with a growth rate of about 20 billion tons each year [1.44]. With this rate of natural production, lignin should be considered as a potential candidate to replace fossil-based products due to its relatively low cost, availability, and inherent properties due to the aromatic structure.

### 1.3.6 Potential routes for lignin valorization

In the last decades, due to the depletion of fossil resources, the necessity of reducing the waste production and increasing the market from pulp and paper industries, and the rising awareness of environmental issues have promoted a growing interest in the utilization of lignin as a feedstock for the synthesis of bio-aromatic chemicals and bio-based polymeric materials.

The availability and the presence of various functional groups in the lignin make it a potential candidate for its exploitation (**Table 1.4**), from the synthesis of bio-aromatic chemicals (such as vanillin and phenols) to bio-based polymeric materials (resins and polymers) [1.43-1.45].

**Table 1.4** Main applications for lignin.

<b>Group</b>	<b>Volume</b>	<b>Value</b>	<b>Application example</b>
Power-fuel-syngas	High	Low	Energy production
Aromatics	Low	High	Aromatics, Vanillin, Phenol, BTX
Macromolecules	Medium	Medium	Adhesives, Carbon fibers, polymers

Lignin has undergone a wide range of both fundamental and applied studies, and therefore, the development of conversion technologies could provide greater added value to lignin. The ways of lignin exploitation can be grouped into three categories:

- (1) Lignin depolymerization to use it as a source of aromatic compounds and energy.
- (2) Lignin functionalization by creating new active chemical sites.
- (3) Chemical modification mainly through its hydroxyl groups to obtain lignin-based polyols and its subsequent use as an intermediate to synthesize materials.

- **Lignin depolymerization**

The structure of lignin can be a valuable source of chemicals, particularly of phenolic compounds. The breakdown of lignin into phenolic or monolignol products is an energy-intensive process, which is part of the reason why lignin is currently more valuable as fuel than as raw material. However, depolymerization of lignin with selective bond cleavage is

nowadays the best approach to transform an amorphous aromatic structure into aromatic added-value chemicals.

The main fragmentation technologies can be classified into thermochemical processes and biological processes. However, the latter is still under development at laboratory scale, and they are not as efficient as the thermochemical processes [1.46]. The main thermochemical methods studied for lignin depolymerization are pyrolysis, gasification, hydrogenation, oxidation, and liquefaction. **Figure 1.9** illustrates the typical conditions and types of catalysts used in these processes.

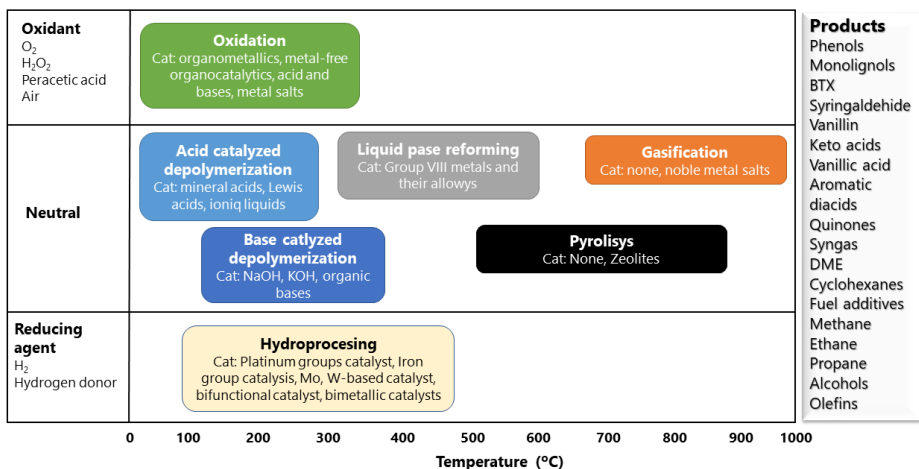


**Figure 1.9** Lignin fractionation diagram to obtain added-value compounds and energy, (adapted from [1.37]).

Pyrolysis is the most studied method for lignin depolymerization, where the thermal decomposition of lignin is performed in absence of oxygen at 200-700 °C. The degradation generates pyrolysis oils, monophenols, solids, and gases, mainly CO, CO<sub>2</sub>, CH<sub>4</sub>. If the pyrolysis is made faster (flash pyrolysis), no wastes are generated, and the liquid obtained in the process, called bio-oil, can be used for liquid fuel production.

Gasification transforms biomass at higher temperatures than pyrolysis (800-900 °C) by partial oxidation into O<sub>2</sub> and CO mainly for fuel, gas, and electricity purposes. The main objective of the lignin gasification is the production of Syngas.

Lignin oxidation involves a heating process in the presence of oxidants. The reaction conditions, solvent, and catalyst selection are the main factors in the yield and final composition of the products obtained [1.35].

The lignin hydroprocessing is a promising route to transform lignin into phenolic-derivates compounds such as vanillin, vanillic acid, acetovanillone, syringaldehyde, syringic acid, and acetosyringone.

The liquefaction of the lignin consists of thermo-chemical conversion through simultaneous solvolysis and depolymerization to get hydroxyl-rich liquid products. The high pressures and temperatures produce low molecular weight phenolic compounds, such as vanillin, cresols, catechols, and guaiacol. These -OH groups have less steric hindrance than the original lignin -OH groups, and consequently, they are more reactive. The liquefied lignin is employed in the preparation of polyesters, polyurethanes, and epoxy resins [1.47-1.49].

There are many possible alternatives for lignin conversion into added-value aromatic products or agrochemicals, polymers, and high-performance materials. However, all these processes depend on the improvements and developments in the fields of product separation and catalysis performance [1.50]. Complete lignin depolymerization or fragmentation is an energy-negative process aimed at undoing what nature has done during biosynthesis.

- **Lignin functionalization**

Methods to use lignin as a source to synthesize new materials without any degradation would not only be useful but also would be energy-effective and environmentally friendly. The employment of lignin with any modification is widely studied since lignin is a relatively cheap material. The use of lignin as an additive could contribute to the development of partially or fully biodegradable materials with new or improved properties, such as antioxidant activity, thermal stabilizer, flame retardant, and hydrophobic agent [1.51, 1.52].

In this context, the direct application of lignin as adsorbent, precursors for carbon materials, and polymer blends is investigated [1.53]. However, lignin has several disadvantages, such as a high molecular weight distribution with steric hindrance effects, low solubility in typical industrial organic solvents, and low reactivity. Therefore, the incorporation of lignin without being modified, although in low quantities, results in a deficient performance of the produced materials [1.54-1.57].

Many efforts to introduce lignin in the final materials are focused on increasing the low percentage of lignin that can be incorporated, avoiding structural failures, losing functionality, or handling problems in the processes through the lignin modification [1.58]. These modifications consist of increasing the reactivity of the hydroxyl groups or changing the nature of the active chemical sites, but always with the aim of synthesizing new efficient and more reactive macromonomers. The most developed processes are shown in **Figure 1.10**.



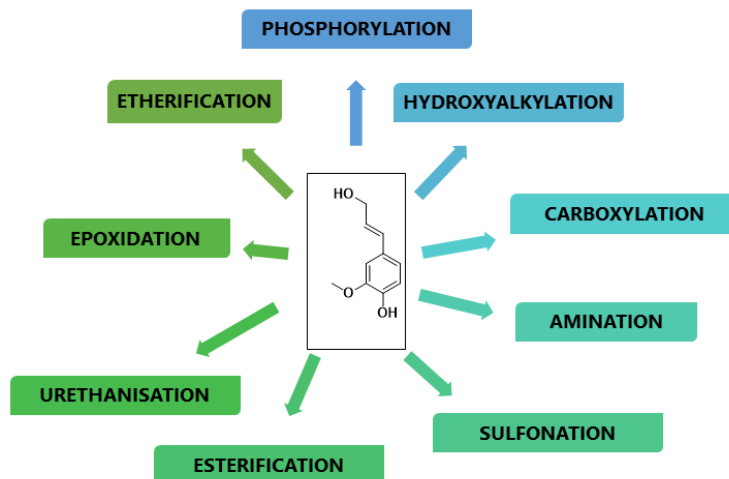


**Figure 1.10** Lignin modification main approaches.

The phosphorylation of lignin has been studied to develop more environmentally friendly flame retardants to reduce the production of toxic fumes and vapors during combustion and hinder the combustibility of the polymers [1.59, 1.60].

The hydroxyalkylation is one of the most widely used methods to produce lignin derivatives with higher -OH groups with applications in wood adhesives [1.61, 1.62], fillers in rubber composites [1.63], and more recently, lignin nanoparticles [1.64]. Another alternative approach is the lignin carboxylation. This modification is a useful technique to introduce carboxylic groups into lignin as an intermediate for various end applications such as bio-based drug delivery products [1.65, 1.66], and dispersants [1.67].

In order to increase the lignin solubility in water treatment applications, the lignin amination has been extensively studied to generate cationic surfactants and coagulants (mainly based on Mannich reaction with amine and formaldehyde) [1.68-1.70], as slow-release fertilizers [1.71, 1.72], and metal adsorbents [1.73]. The lignin sulfonation has found a

wide range of industrial applications, such as the production of cation-exchange resin from lignin [1.74], in water-based oil drilling [1.75], and as a cement dispersant [1.76].

The processes to modify the lignin through its hydroxyl groups are very interesting and have been widely studied. The lignin esterification has been commonly used to reduce the hydrophilicity and the capacity of being solvated by substituting the alcohol groups with ester groups, which makes it favorable to be used for composite materials [1.77-1.79]. Furthermore, the esterification provides one of the most convenient approaches to modify the lignin to enhance its solubility for structural analysis [1.80].

Lignin epoxidation relies on introducing a highly reactive group, such as an epoxy group into the lignin structure. Epoxy lignins are a widely used intermediate in the synthesis of epoxy resins and membranes [1.81-1.84].

Lignin urethanization has as its primary objective the synthesis of lignin-based polyurethanes. Polyurethanes are synthesized by the polyaddition reaction of diisocyanates and polyols with terminal hydroxyl groups, forming polyurethane groups in the polymer backbone. Lignin-based polyurethanes offer the potential of preparing a wide variety of products such as low-temperature elastomers, high tensile adhesives, flexible and rigid foams depending on their final applications. However, the direct interaction between lignin and isocyanates results in most of the lignin remaining as insoluble residue, making further exploitation impractical at industrial scale [1.85].

- Lignin-based polyols

The synthesis of low-cost polyols from abundant and renewable biomass sources has created industrial interest. In the last decades, numerous studies have focused on the development of lignin-based polymers. The aim is to introduce polymeric chains through the hydroxyl lignin groups, resulting in a star-branched copolymer with a lignin core.

Two types of polymerization reactions have been carried out to produce lignin-based polymers. The first one involves the radical polymerization of vinyl monomers. The second one consists of the ring-opening polymerization (ROP) of different monomers, initiated by hydroxyl groups of lignin. Three types of ROP have been described in the literature:  $\epsilon$ -caprolactone, lactide, and propylene oxide (**Figure 1.11**).

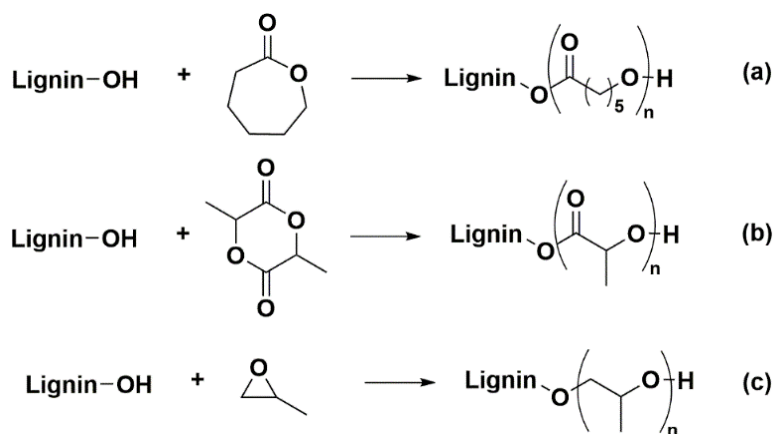


**Figure 1.11** Ring-opening polymerization of a)  $\epsilon$ -caprolactone, b) lactide, and c) propylene oxide [1.65].

Different lignin polymers were synthesized such as lignin-*g*-poly(acrylic acid) [1.86], lignin-*g*-polystyrene [1.87], and lignin-*g*-poly(vinyl acetate) (PVAc) [1.88]. Free radical polymerization initiated by lignin does not provide good control of the grafting reaction. In addition to create the lignin radicals, the presence of free radicals from the initiator may also

cause the homopolymerization of the vinyl monomers and the lignin polymerization by radical coupling, limiting the efficacy of the reaction [1.88].

Polymerization by  $\epsilon$ -caprolactone results in lignin-g-polycaprolactone (PCL) type polymers. The association with biodegradable aliphatic polymers such as polycaprolactone (PCL) has attracted much attention because of the biological degradation of the corresponding blends. The ratio of monomer to initiator groups employed determines the degree of polymerization for these polyols. These reactions can be carried out in an organic solvent such as toluene or bulk using stannous octanoate ( $\text{SnOct}_2$ ) as a catalyst [1.91].

Recently, ROP has also been used to synthesize lignin-poly(lactic acid) (PLA) copolymers [1.92]. The lignin reacts in bulk with lactide (LA) in the presence of an organo-catalyst such as 1,5,7-triazabicyclo[4.4.0]dec-5-ene (TBD). The thermal properties of lignin-g-PLA copolymers depend on the lignin and the PLA composition. These copolymers can also be mixed with the conventional PLA, resulting in a homogeneous material with increased mechanical properties and UV-blocking capacity, thus improving their potential use in packaging and in composite materials.

The most developed lignin modification route and the one with the most outstanding industrial interest is the oxyalkylation of the lignin with oxygen-containing heterocycles by ring-opening polymerization (ROP), and more specifically with the propylene oxide [1.85]. The interest of this route is that the hydroxyl groups of the lignin are converted into ether groups when they react with the cyclic compounds. In response, another terminal hydroxyl group is formed due to the opening of the ring containing the oxygen group resulting in a polymerization reaction giving new macropolyols [1.89]. In this type of synthesis, the lignin undergoes a

substantial change in properties, converting the solid lignin into a polyol with very interesting properties for industrial purposes, especially for the polyurethane industry [1.90].

In this context, biomass oxypropylation has been researched intensively over the last decades using different natural polymeric substrates containing hydroxyl groups such as sugar beet pulp [1.93], cellulose [1.94], chitin and chitosan [1.95], cork [1.96], lignin [1.97], starch [1.98], and tannins [1.99]. Among the biomass susceptible to being oxypropylated, lignin oxypropylation was the most studied source to obtain bio-based polyols.

The reaction of PO with lignin -OH groups leads to the formation of a liquid lignin polyol, called oxypropylated lignin. Fully oxypropylated lignin has the advantage of containing mainly more reactive aliphatic hydroxyl groups. All -OH groups, including the aromatics and aliphatics, have been replaced by secondary aliphatic hydroxyl groups at the end of the chains. The -OH groups are putting away from the bulky lignin structure, reducing the steric hindrance hugely and increasing their reactivity, making lignin-based polyols a more suitable macromolecule as intermediate for final applications.

The development of oxypropylated lignin macromolecules for the synthesis of polyurethanes was developed at the beginning of 1980 by Glasser et al. [1.100]. The lignin oxypropylation pathway by anionic ring-opening polymerization (AROP) is detailed in **Figure 1.12**. The reaction starts with its activation by a strong Brønsted base, which generates the corresponding oxyanions that function as the starting site of the oxirane propagation reaction. The C-O bond of the propylene oxide does not begin to break until the carbon is attacked by the nucleophile. The nucleophile is more likely to attack the less substituted carbon because it is less

sterically hindered. Both ethylene oxide (EO) and propylene oxide (PO) respond efficiently to this type of polymerization. However, it is more common to use PO because EO could make uncontrolled hazardous exothermic reactions [1.101]. Once the oxyanion of the lignin is formed, it is capable of opening the propylene oxide and begin its own homopropagation until it is consumed. Termination occurs when the alkoxide ion picks up a proton from the solvent or from an added acid.

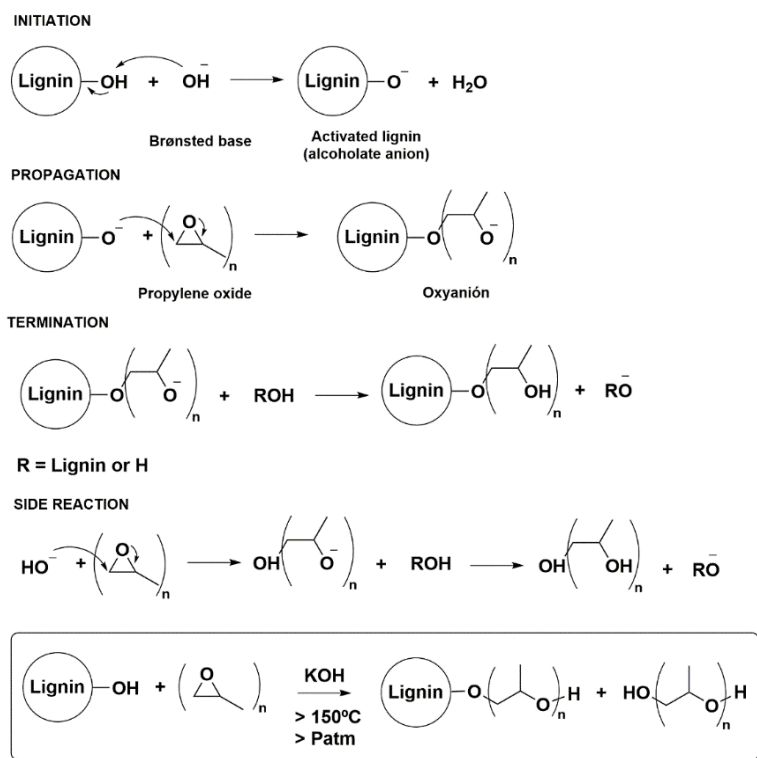


**Figure 1.12** Lignin oxypropylation by anionic ring-opening polymerization.

However, this route presents significant disadvantages concerning the aggressive conditions employed in the process. AROP requires harsh reaction conditions and base-catalyzed carried out at 150-330 °C and 6-40 bar [1.102-1.104]. These operating conditions may result in the formation of side products such as homopolymers in large amounts (up to 70 %) [1.104], insoluble fractions by lignin self-condensation, and bad odor from

the partial lignin depolymerization into phenolic compounds. Furthermore, the reaction requires special equipment able to ensure safety against explosions and reaction conditions, increasing considerably the costs associated with the production.

The oxypropylation of lignin has been studied in detail to obtain lignin-based polyols as an intermediate mainly for the synthesis of polyurethanes. Nevertheless, the operating conditions related to the energy consumption and cost equipment, along with the drawbacks mentioned before, make this process economically less attractive against the well-established commercial polyols hampering any industrial application [1.104].

## 1.4 Aim and outline of the thesis

Lignin is an excellent candidate to be employed as a raw material to develop new bio-based added-value products or key intermediates in polymer synthesis. However, the direct use of lignin as a bio-polyol to obtain bio-based materials is still hampered by its inherent low reactivity, mainly associated with the steric effects limiting the accessibility to its active -OH groups.

In this thesis, an alternative route to prepare improved lignin-based polyols (LBPs) is proposed. The synthesis and characterization of a new family of lignin-based polyols by cationic ring-opening polymerization (CROP) of oxiranes in presence of lignin is described. This route is expected to avoid the disadvantages associated with current production routes, such as the formation of by-products and the energy costs. The reactions parameters are studied and discussed in terms of the LBPs characterization and the microstructure obtained.

With the aim of making this pathway more attractive at an industrial level, a research of this route will be carried out to obtain lignin-based polyols with other lignin sources and with different monomers. With the most interesting polyols obtained, their use in various final applications will be studied, using them as final products or as intermediate macromolecules for the synthesis of other materials.



## 1.5 References

- [1.1] D. K. Schneiderman and M. A. Hillmyer, “50th Anniversary Perspective: There Is a Great Future in Sustainable Polymers,” *Macromolecules*, vol. 50, no. 10, pp. 3733–3749, 2017.
- [1.2] J. G. Speight, “Refinery of the Future,” in *The Refinery of the Future*, no. 1, Elsevier Inc, 2011, pp. 315–340.
- [1.3] “European Bioplastics” <https://www.european-Bioplastics.org/market/> (accessed Jul. 12, 2020).
- [1.4] R. Geyer, “Production, use, and fate of synthetic polymers,” in *Plastic Waste and Recycling*, Elsevier, pp. 13–32, 2020
- [1.5] V. K. Thakur, M. K. Thakur, P. Raghavan, and M. R. Kessler, “Progress in green polymer composites from lignin for multifunctional applications: A review,” *ACS Sustain. Chem. Eng.*, vol. 2, no. 5, pp. 1072–1092, 2014.
- [1.6] R. Geyer, J. R. Jambeck, and K. L. Law, “Production, use, and fate of all plastics ever made,” *Sci. Adv.*, vol. 3, no. 7, p. e1700782, 2017.
- [1.7] O. Faruk and M. Sain, *Lignin in Polymer Composites*. 2015.
- [1.8] O. Gómez-Jiménez-Aberasturi and J. R. Ochoa-Gómez, “New approaches to producing polyols from biomass,” *J. Chem. Technol. Biotechnol.*, vol. 92, no. 4, pp. 705–711, 2017.
- [1.9] S. V. Vassilev, D. Baxter, L. K. Andersen, C. G. Vassileva, and T. J. Morgan, “An overview of the organic and inorganic phase composition of biomass,” *Fuel*, vol. 94, pp. 1–33, 2012.
- [1.10] S. V. Vassilev, D. Baxter, L. K. Andersen, and C. G. Vassileva, “An overview of the chemical composition of biomass,” *Fuel*, vol. 89, no. 5, pp. 913–933, 2010.

- [1.11] “Bioplastics–European Bioplastics e.V.” <https://www.european-bioplastics.org/bioplastics/> (accessed Aug. 09, 2020).
- [1.12] R. M. O’Dea, J. A. Willie, and T. H. Epps, “100th Anniversary of Macromolecular Science Viewpoint: Polymers from Lignocellulosic Biomass. Current Challenges and Future Opportunities,” *ACS Macro Lett.*, pp. 476–493, 2020.
- [1.13] F. Aeschelmann and M. Carus, “Biobased building blocks and polymers in the world: Capacities, production, and applications-status quo and trends towards 2020,” *Ind. Biotechnol.*, vol. 11, no. 3, pp. 154–159, 2015.
- [1.14] S. Spierling, C. Röttger, V. Venkatachalam, M. Mudersbach, C. Herrmann, and H. J. Endres, “Bio-based Plastics - A Building Block for the Circular Economy?,” *Procedia CIRP*, vol. 69, pp. 573–578, 2018.
- [1.15] Y. Zhu, C. Romain, and C. K. Williams, “Sustainable polymers from renewable resources,” *Nature*, vol. 540, no. 7633, pp. 354–362, 2016.
- [1.16] F. G. Calvo-Flores, J. A. Dobado, J. Isac-García, and F. J. Martín-Martínez, *Lignin and Lignans as Renewable Raw Materials: Chemistry, Technology and Applications*. Chichester, UK: John Wiley & Sons, Ltd, 2015.
- [1.17] J. Sameni, S. Krigstin, D. Dos Santos Rosa, A. Leao, and M. Sain, “Thermal Characteristics of Lignin Residue from Industrial Processes,” *BioResources*, vol. 9, no. 1, pp. 725–737, 2013.
- [1.18] A. Tursi, “A review on biomass: Importance, chemistry, classification, and conversion,” *Biofuel Res. J.*, vol. 6, no. 2, pp. 962–979, 2019.
- [1.19] K. R. Oleson and D. T. Schwartz, “Extractives in Douglas-fir forestry residue and considerations for biofuel production,” *Phytochem. Rev.*, vol. 15, no. 5, pp. 985–1008, 2016.

- [1.20] A. N. Panche, A. D. Diwan, and S. R. Chandra, “Flavonoids: An overview,” *J. Nutr. Sci.*, vol. 5, 2016.
- [1.21] L. Rocha Meneses, M. Raud, K. Orupold, and T. Kikas, “Second-generation bioethanol production: A review of strategies for waste valorisation,” *Agron. Res.*, vol. 15, no. 3, pp. 830–847, 2017.
- [1.22] J. Zhang, D. Cai, Y. Qin, D. Liu, and X. Zhao, “High value-added monomer chemicals and functional bio-based materials derived from polymeric components of lignocellulose by organosolv fractionation,” *Biofuels, Bioprod. Biorefining*, vol. 14, no. 2, pp. 371–401, 2020.
- [1.23] I. Dávila, B. Gullón, J. L. Alonso, J. Labidi, and P. Gullón, “Vine shoots as new source for the manufacture of prebiotic oligosaccharides,” *Carbohydr. Polym.*, vol. 207, no. November 2018, pp. 34–43, 2019.
- [1.24] A. Payen, “Mémoire sur la composition du tissu propre des plantes et du ligneux.,” *Comptes Rendus L’ Académie Des Sci. Ser. III-Sciences La Vie-Life Sci.*, vol. 7, pp. 1052–1054, 1838.
- [1.25] E. Adler, “Wood Science anci Technology,” *Wood Sci. Technol.*, vol. 11, pp. 169–218, 1977.
- [1.26] Q. Liu, L. Luo, and L. Zheng, “Lignins: Biosynthesis and biological functions in plants,” *Int. J. Mol. Sci.*, vol. 19, no. 2, 2018.
- [1.27] J. C. M. S. Moura, C. A. V. Bonine, J. de Oliveira Fernandes Viana, M. C. Dornelas, and P. Mazzafera, “Abiotic and biotic stresses and changes in the lignin content and composition in plants,” *J. Integr. Plant Biol.*, vol. 52, no. 4, pp. 360–376, 2010.
- [1.28] F. B. De La Cruz, “Fate and Reactivity of Lignin in Municipal Solid Waste (MSW) Landfill.,” 2014.
- [1.29] Y. Li *et al.*, “An ideal lignin facilitates full biomass utilization,” *Sci. Adv.*, vol. 4, no. 9, 2018.

- [1.30] R. Rinaldi *et al.*, “Paving the Way for Lignin Valorisation: Recent Advances in Bioengineering, Biorefining and Catalysis,” *Angew. Chemie - Int. Ed.*, vol. 55, no. 29, pp. 8164–8215, 2016.
- [1.31] F. G. Calvo-Flores and J. A. Dobado, “Lignin as renewable raw material,” *ChemSusChem*, vol. 3, no. 11, pp. 1227–1235, 2010.
- [1.32] J. Zakzeski, P. C. A. Bruijninx, A. L. Jongerius, and B. M. Weckhuysen, “The catalytic valorization of lignin for the production of renewable chemicals,” *Chem. Rev.*, vol. 110, no. 6, pp. 3552–3599, 2010.
- [1.33] R. Vanholme, B. Demedts, K. Morreel, J. Ralph, and W. Boerjan, “Lignin biosynthesis and structure,” *Plant Physiol.*, vol. 153, no. 3, pp. 895–905, 2010.
- [1.34] G. Gellerstedt and G. Henriksson, “Lignins: Major Sources, Structure and Properties,” in *Monomers, Polymers and Composites from Renewable Resources*, Elsevier, 2008, pp. 201–224.
- [1.35] J. Barros, H. Serk, I. Granlund, and E. Pesquet, “The cell biology of lignification in higher plants,” *Ann. Bot.*, vol. 115, no. 7, pp. 1053–1074, 2015.
- [1.36] M. P. Pandey and C. S. Kim, “Lignin Depolymerization and Conversion: A Review of Thermochemical Methods,” *Chem. Eng. Technol.*, vol. 34, no. 1, pp. 29–41, 2011.
- [1.37] C. Li, X. Zhao, A. Wang, G. W. Huber, and T. Zhang, “Catalytic Transformation of Lignin for the Production of Chemicals and Fuels,” *Chem. Rev.*, vol. 115, no. 21, pp. 11559–11624, 2015.
- [1.38] A. Eraghi Kazzaz, Z. Hosseinpour Feizi, and P. Fatehi, “Grafting strategies for hydroxy groups of lignin for producing materials,” *Green Chem.*, vol. 21, no. 21, pp. 5714–5752, 2019.

- [1.39] R. J. Sammons, D. P. Harper, N. Labbé, J. J. Bozell, T. Elder, and T. G. Rials, "Characterization of organosolv lignins using thermal and FT-IR spectroscopic analysis," *BioResources*, vol. 8, no. 2, pp. 2752–2767, 2013.
- [1.40] F. S. Chakar and A. J. Ragauskas, "Review of current and future softwood kraft lignin process chemistry," *Ind. Crops Prod.*, vol. 20, no. 2, pp. 131–141, 2004.
- [1.41] X. Erdocia, R. Prado, M. Á. Corcuera, and J. Labidi, "Effect of different organosolv treatments on the structure and properties of olive tree pruning lignin," *J. Ind. Eng. Chem.*, vol. 20, no. 3, pp. 1103–1108, 2014.
- [1.42] A. Vishtal and A. Kraslawski, "Challenges in industrial applications of technical lignins," *BioResources*, vol. 6, no. 3, pp. 3547–3568, 2011.
- [1.43] A. Eraghi Kazzaz and P. Fatehi, "Technical lignin and its potential modification routes: A mini-review," *Ind. Crops Prod.*
- [1.44] M. Alekhina, O. Ershova, A. Ebert, S. Heikkinen, and H. Sixta, "Softwood kraft lignin for value-added applications: Fractionation and structural characterization," *Ind. Crops Prod.*, vol. 66, pp. 220–228, 2015.
- [1.45] R. Behling, S. Valange, and G. Chatel, "Heterogeneous catalytic oxidation for lignin valorization into valuable chemicals: What results? What limitations? What trends?," *Green Chem.*, vol. 18, no. 7, pp. 1839–1854, 2016.
- [1.46] H. Lange, S. Decina, and C. Crestini, "Oxidative upgrade of lignin - Recent routes reviewed," *Eur. Polym. J.*, vol. 49, no. 6, pp. 1151–1173, 2013.
- [1.47] A. Jablonskis, A. Arshanitsa, and G. Telysheva, "Solvent pre-treatment of lignin for obtaining of low viscosity lignopolyols by

- oxypropylation for synthesis of polyurethanes,” *IOP Conf. Ser. Mater. Sci. Eng.*, vol. 111, no. 1, p. 012007, 2016.
- [1.48] J. Bernardini, P. Cinelli, I. Anguillesi, M. B. Coltelli, and A. Lazzeri, “Flexible polyurethane foams green production employing lignin or oxypropylated lignin,” *Eur. Polym. J.*, vol. 64, pp. 147–156, 2015.
- [1.49] T. V. Lourençon *et al.*, “Phenol-formaldehyde resins with suitable bonding strength synthesized from ‘less-reactive’ hardwood lignin fractions,” *Holzforschung*, vol. 74, no. 2, pp. 175–183, 2020.
- [1.50] Z. Strassberger, S. Tanase, and G. Rothenberg, “The pros and cons of lignin valorisation in an integrated biorefinery,” *RSC Adv.*, vol. 4, no. 48, pp. 25310–25318, 2014.
- [1.51] C. Pouteau, P. Dole, B. Cathala, L. Averous, and N. Boquillon, “Antioxidant properties of lignin in polypropylene,” *Polym. Degrad. Stab.*, vol. 81, no. 1, pp. 9–18, 2003.
- [1.52] P. Alexy, B. Košíková, and G. Podstránska, “The effect of blending lignin with polyethylene and polypropylene on physical properties,” *Polymer (Guildf)*, vol. 41, no. 13, pp. 4901–4908, 2000.
- [1.53] D. Kun and B. Pukánszky, “Polymer/lignin blends: Interactions, properties, applications,” *Eur. Polym. J.*, vol. 93, no. April 2017, pp. 618–641, 2017.
- [1.54] A. Duval and M. Lawoko, “A review on lignin-based polymeric, micro- and nano-structured materials,” *React. Funct. Polym.*, vol. 85, pp. 78–96, 2014.
- [1.55] S. Laurichesse and L. Avérous, “Chemical modification of lignins: Towards biobased polymers,” *Prog. Polym. Sci.*, vol. 39, no. 7, pp. 1266–1290, 2014.
- [1.56] A. Jablonskis, A. Arshanitsa, A. Arnautov, G. Telysheva, and D.

- Evtuguin, "Evaluation of Ligno Boost™ softwood kraft lignin epoxidation as an approach for its application in cured epoxy resins," *Ind. Crops Prod.*, vol. 112, no. April 2017, pp. 225–235, 2018.
- [1.57] K. R. Kurple, "Lignin Based Polyols," 6,025,452, 2000.
- [1.58] C. Xu and F. Ferdosian, *Conversion of Lignin into Bio-Based Chemicals and Materials*. 2017.
- [1.59] B. Prieur *et al.*, "Phosphorylation of lignin: characterization and investigation of the thermal decomposition," *RSC Adv.*, vol. 7, no. 27, pp. 16866–16877, 2017.
- [1.60] H. Yang, B. Yu, X. Xu, S. Bourbigot, H. Wang, and P. Song, "Lignin-derived bio-based flame retardants toward high-performance sustainable polymeric materials," *Green Chem.*, pp. 2129–2161, 2020.
- [1.61] N. E. El Mansouri, A. Pizzi, and J. Salvado, "Lignin-based polycondensation resins for wood adhesives," *J. Appl. Polym. Sci.*, vol. 103, no. 3, pp. 1690–1699, 2007.
- [1.62] F. Ferdosian, Z. Pan, G. Gao, and B. Zhao, "Bio-based adhesives and evaluation for wood composites application," *Polymers (Basel)*, vol. 9, no. 2, 2017.
- [1.63] N. Mohamad Aini, N. Othman, M. Hussin, K. Sahakaro, and N. Hayeemasae, "Hydroxymethylation-Modified Lignin and Its Effectiveness as a Filler in Rubber Composites," *Processes*, vol. 7, no. 5, p. 315, 2019.
- [1.64] I. A. Gilca, R. E. Ghitescu, A. C. Puitel, and V. I. Popa, "Preparation of lignin nanoparticles by chemical modification," *Iran. Polym. J. (English Ed.)*, vol. 23, no. 5, pp. 355–363, 2014.
- [1.65] M. Pishnamazi, H. Hafizi, S. Shirazian, M. Culebras, G. M. Walker, and M. N. Collins, "Design of controlled release system for

- paracetamol based on modified lignin,” *Polymers (Basel)*, vol. 11, no. 6, pp. 1–10, 2019.
- [1.66] P. Figueiredo *et al.*, “Functionalization of carboxylated lignin nanoparticles for targeted and pH-responsive delivery of anticancer drugs,” *Nanomedicine*, vol. 12, no. 21, pp. 2581–2596, 2017.
- [1.67] M. K. Konduri, F. Kong, and P. Fatehi, “Production of carboxymethylated lignin and its application as a dispersant,” *Eur. Polym. J.*, vol. 70, pp. 371–383, 2015.
- [1.68] F. Kong, K. Parhiala, S. Wang, and P. Fatehi, “Preparation of cationic softwood kraft lignin and its application in dye removal,” *Eur. Polym. J.*, vol. 67, pp. 335–345, 2015.
- [1.69] X. Du, J. Li, and M. E. Lindström, “Modification of industrial softwood kraft lignin using Mannich reaction with and without phenolation pretreatment,” *Ind. Crops Prod.*, vol. 52, pp. 729–735, 2014.
- [1.70] R. Li *et al.*, “Amine-Cross-Linked Lignin-Based Polymer: Modification, Characterization, and Flocculating Performance in Humic Acid Coagulation,” *ACS Sustain. Chem. Eng.*, vol. 3, no. 12, pp. 3253–3261, 2015.
- [1.71] F. Ramírez, V. González, M. Crespo, D. Meier, O. Faix, and V. Zúñiga, “Amoxidized kraft lignin as a slow-release fertilizer tested on *Sorghum vulgare*,” *Bioresour. Technol.*, vol. 61, no. 1, pp. 43–46, 1997.
- [1.72] J. Chen, X. Fan, L. Zhang, X. Chen, S. Sun, and R. C. Sun, “Research Progress in Lignin-Based Slow/Controlled Release Fertilizer,” *ChemSusChem*, pp. 1–12, 2020.
- [1.73] X. Liu, H. Zhu, C. Qin, J. Zhou, J. R. Zhao, and S. Wang, “Adsorption of heavy metal ion from aqueous single metal solution by aminated epoxy-lignin,” *BioResources*, vol. 8, no. 2, pp. 2257–2269, 2013.



- [1.74] S. Kamel, "Preparation of Cation-Exchange Resin from Lignin," *Int. J. Polym. Mater.*, vol. 55, no. 4, pp. 283–291, 2005.
- [1.75] R. Zhang *et al.*, "The application of ferric chloride-lignin sulfonate as shale inhibitor in water-based drilling fluid," *Molecules*, vol. 24, no. 23, pp. 1–8, 2019.
- [1.76] X. Ouyang, L. Ke, X. Qiu, Y. Guo, and Y. Pang, "Sulfonation of alkali lignin and its potential use in dispersant for cement," *J. Dispers. Sci. Technol.*, vol. 30, no. 1, pp. 1–6, 2009.
- [1.77] K. A. Y. Koivu, H. Sadeghifar, P. A. Nousiainen, D. S. Argyropoulos, and J. Sipilä, "Effect of Fatty Acid Esterification on the Thermal Properties of Softwood Kraft Lignin," *ACS Sustain. Chem. Eng.*, vol. 4, no. 10, pp. 5238–5247, 2016.
- [1.78] X. Zhao *et al.*, "Esterification mechanism of lignin with different catalysts based on lignin model compounds by mechanical activation-assisted solid-phase synthesis," *RSC Adv.*, vol. 7, no. 83, pp. 52382–52390, 2017.
- [1.79] L. Y. Liu, Q. Hua, and S. Rennekar, "A simple route to synthesize esterified lignin derivatives," *Green Chem.*, vol. 21, no. 13, pp. 3682–3692, 2019.
- [1.80] J. Sameni, S. Krigstin, and M. Sain, "Solubility of Lignin and Acetylated Lignin in Organic Solvents," *BioResources*, vol. 12, no. 1, pp. 1548–1565, 2017.
- [1.81] N. E. El Mansouri, Q. Yuan, and F. Huang, "Synthesis and characterization of kraft lignin-based epoxy resins," *BioResources*, vol. 6, no. 3, pp. 2492–2503, 2011.
- [1.82] Y. Zhang *et al.*, "Preparation and characterization of chemical grouting

- derived from lignin epoxy resin,” *Eur. Polym. J.*, vol. 118, no. April, pp. 290–305, 2019.
- [1.83] C. Gioia, G. Lo Re, M. Lawoko, and L. Berglund, “Tunable Thermosetting Epoxies Based on Fractionated and Well-Characterized Lignins,” *J. Am. Chem. Soc.*, vol. 140, no. 11, pp. 4054–4061, 2018.
- [1.84] X. Zhang, J. Benavente, and R. Garcia-Valls, “Lignin-based membranes for electrolyte transference,” *J. Power Sources*, vol. 145, no. 2, pp. 292–297, 2005.
- [1.85] L. N. Mozheiko, M. F. Gromova, L. A. Bakalo, and V. N. Sergeyeva, “Polyurethanes prepared from oxypropylated lignin,” *Polym. Sci. U.S.S.R.*, vol. 23, no. 1, pp. 141–149, 1981.
- [1.86] D. Z. Ye, X. C. Jiang, C. Xia, L. Liu, and X. Zhang, “Graft polymers of eucalyptus lignosulfonate calcium with acrylic acid: Synthesis and characterization,” *Carbohydr. Polym.*, vol. 89, no. 3, pp. 876–882, 2012.
- [1.87] J. J. Meister and M. J. Chen, “Graft 1-Phenylethylene Copolymers of Lignin. 1. Synthesis and Proof of Copolymerization,” *Macromolecules*, vol. 24, no. 26, pp. 6843–6848, 1991.
- [1.88] S. S. Panesar, S. Jacob, M. Misra, and A. K. Mohanty, “Functionalization of lignin: Fundamental studies on aqueous graft copolymerization with vinyl acetate,” *Ind. Crops Prod.*, vol. 46, pp. 191–196, 2013.
- [1.89] V. P. Saraf and W. G. Glasser, “Engineering plastics from lignin. III. Structure property relationships in solution cast polyurethane films,” *J. Appl. Polym. Sci.*, vol. 29, no. 5, pp. 1831–1841, 1984.
- [1.90] C. A. Cateto, M. F. Barreiro, C. Ottati, M. Lopretti, A. E. Rodrigues, and M. N. Belgacem, “Lignin-based rigid polyurethane foams with improved biodegradation,” *J. Cell. Plast.*, vol. 50, pp. 81–95, 2014.

- [1.91] S. Laurichesse and L. Avérous, “Synthesis, thermal properties, rheological and mechanical behaviors of lignins-grafted-poly( $\epsilon$ -caprolactone),” *Polymer*, vol. 54, no. 15, pp. 3882–3890, 2013.
- [1.92] Y. L. Chung *et al.*, “A renewable lignin-lactide copolymer and application in biobased composites,” *ACS Sustain. Chem. Eng.*, vol. 1, no. 10, pp. 1231–1238, 2013.
- [1.93] C. Pavier and A. Gandini, “Oxypropylation of sugar beet pulp. 1. Optimisation of the reaction,” *Ind. Crops Prod.*, vol. 12, no. 1, pp. 1–8, 2000.
- [1.94] A. J. de Menezes, D. Pasquini, A. A. da S. Curvelo, and A. Gandini, “Self-reinforced composites obtained by the partial oxypropylation of cellulose fibers. 1. Characterization of the materials obtained with different types of fibers,” *Carbohydr. Polym.*, vol. 76, no. 3, pp. 437–442, 2009.
- [1.95] S. Fernandes, C. S. R. Freire, C. P. Neto, and A. Gandini, “The bulk oxypropylation of chitin and chitosan and the characterization of the ensuing polyols,” *Green Chem.*, vol. 10, no. 1, pp. 93–97, 2008.
- [1.96] M. Evtiouguina *et al.*, “The oxypropylation of cork residues: Preliminary results,” *Bioresour. Technol.*, vol. 73, no. 2, pp. 187–189, 2000.
- [1.97] L. C. -F. Wu and W. G. Glasser, “Engineering plastics from lignin. I. Synthesis of hydroxypropyl lignin,” *J. Appl. Polym. Sci.*, vol. 29, no. 4, pp. 1111–1123, 1984.
- [1.98] M. Yoshioka, Y. Nishio, D. Saito, H. Ohashi, M. Hashimoto, and N. Shiraishi, “Synthesis of biopolyols by mild oxypropylation of liquefied starch and its application to polyurethane rigid foams,” *J. Appl. Polym. Sci.*, vol. 130, no. 1, pp. 622–630, 2013.
- [1.99] A. Arbenz and L. Avérous, “Synthesis and characterization of fully

- biobased aromatic polyols - Oxybutylation of condensed tannins towards new macromolecular architectures,” *RSC Adv.*, vol. 4, no. 106, pp. 61564–61572, 2014.
- [1.100] W. G. Glasser, V. P. Saraf, and W. H. Newman, “Hydroxy Propylated Lignin-Isocyanate Combinations as Bonding Agents for Wood and Cellulosic Fibers,” *J. Adhes.*, vol. 14, no. 3–4, pp. 233–255, 1982.
- [1.101] M. N. Belgacem and A. Gandini, *Monomers , Polymers and Composites*. 2008.
- [1.102] B. Berrima, G. Mortha, S. Boufi, E. El Aloui, and M. Naceur Belgacem, “Oxypropylation of Soda Lignin: Characterization and Application in Polyurethane Foams Production,” *Cellul. Chem. Technol. Cellul. Chem. Technol.*, vol. 50, no. 9, pp. 941–950, 2016.
- [1.103] H. Nadji, C. Bruzzèse, M. N. Belgacem, A. Benaboura, and A. Gandini, “Oxypropylation of Lignins and Preparation of Rigid Polyurethane Foams from the Ensuing Polyols,” *Macromol. Mater. Eng.*, vol. 290, no. 10, pp. 1009–1016, 2005.
- [1.104] C. A. Cateto, M. F. Barreiro, A. E. Rodrigues, and M. N. Belgacem, “Optimization Study of Lignin Oxypropylation in View of the Preparation of Polyurethane Rigid Foams,” *Ind. Eng. Chem. Res.*, vol. 48, no. 5, pp. 2583–2589, 2009.

## **CHAPTER 2**

# **LIGNIN SELECTION FOR OBTAINING LIGNIN-BASED POLYOLS**

---



## 2.1 Background

### 2.1.1 Lignin sources

Lignin is one of the main components of lignocellulosic biomass, being the second most abundant biopolymer on the terrestrial surface after cellulose, and the first with an aromatic structure [2.1]. Lignin is formed by photosynthesis reaction like the other biomass components, and its natural annual production has been estimated in the range of  $5\text{-}36 \cdot 10^8$  tons [2.2].

Lignin has a non-uniform distribution in the medium of the lamella and on the primary and secondary cell walls depending on the plant species and cell type [2.3]. The average lignin content in hardwood (angiosperms) and softwood (gymnosperm) biomass is about 15-40 wt. % while herbs have less than 15 wt. % of lignin content [2.4]. Depending on the location and growing environment, species diversity, and its longevity, this association may be altered (**Table 2.1**) [2.5].

Lignin protects cell wall polysaccharides from microbial degradation, increasing resistance to decomposition. It is also one of the most critical limiting factors in the conversion of plant biomass to pulp or biofuels. The history of lignin was attached for hundreds of years as an undesired by-product in the pulping process and cellulosic ethanol plants. Until now, around 70 million tons per year of lignin is produced, of which 98 % was concentrated and burned together with other waste wood components in the pulp liquor to produce steam, electricity, and inorganic chemicals for internal factory use [2.9]. The excess generated is used as a low-added-value product in applications such as tire filling, concrete, and asphalt [2.10, 2.11].

**Table 2.1** Lignin content in different biomass [2.2, 2.6-2.8].

<i>Hardwood (Gymnosperms)</i>		<i>Softwood (Angiosperms)</i>		<i>Grasses</i>	
<b>Common name</b>	<b>L (wt. %)</b>	<b>Common name</b>	<b>L (wt. %)</b>	<b>Common name</b>	<b>L (wt. %)</b>
Norway spruce	39	Black wattle	21	Corn	15
Monterey pine	27	Silver birch	20	Cotton	1
Scots pine	28	Bluegum eucalyptus	22	Flax	3
Pinus Sylvestris	27	Rose Eucalyptus	25	Hemp	6
Douglas fir	29	European aspen	19	Jute	13
Eastern hemlock	31	Kenaf	12	Wheat	15

L (wt. %) = Lignin content in weight given as a percentage.

Many efforts are being concentrated to take advantage of the lignin generated as a by-product (with lower production costs) and to give it an added-value by generating more competitive lignin-based products. In line with the exploitation of waste products, the biorefinery concept was developed as an attempt to make full exploitation of the biomass. The biorefinery is defined as a sustainable process for the transformation of biomass into a range of commercially available products and energy [2.12].

Analogous to refineries, the biorefinery attempts to obtain from biomass all types of products, from fuels and energy production, chemicals employed as intermediates in other applications, to end-use products. However, due to the heterogeneity of the biomass, the process needs more steps of transformation and separation. Currently, several types of biorefineries can be encompassed depending on the development approach: (1) platforms (lignins, sugars, oils, syngas, biogas); (2) products (biodiesel, bioethanol, electricity, and heat, biomaterials, polymers); (3) feedstock (oil, sugar, starch, lignocellulosic crops, marine biomass); and (4) processes (thermochemical, biochemical, chemical, mechanical processes) (**Figure 2.1**) [2.13].



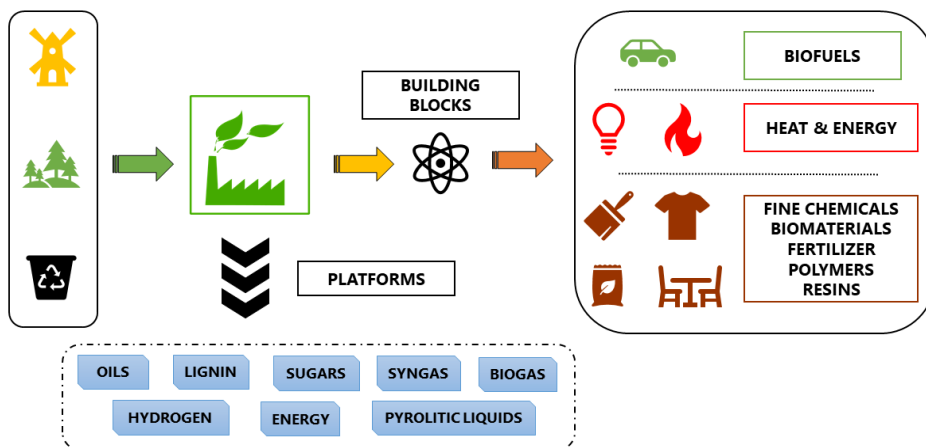


**Figure 2.1** Scheme of the biorefinery concept.

The biorefinery concept, in accordance with the green chemistry approach, avoids the production of low-value waste and recycles the solvents used to extract all the components from biomass. Bearing in mind this concept, it should be noted that lignin can no longer be considered as a waste. Consequently, it should be regarded as a raw material with an enormous potential for the synthesis of value-added products.

Concerning the subject mentioned above, the sources to obtain lignin are: 1) lignin from original wood sources, 2) the pulp and paper industry, 3) sugar cane bagasse derived from bioethanol production, and 4) agricultural residues [2.14]. Obtaining lignin directly from biomass for use in the manufacture of bioproducts is economically unfeasible. However, every year, an abundance of post-harvest agro-biomass is generated and often wasted that can be approached. These agro-wastes can be considered a source of valuable products such as lignin due to their high availability and low or no cost and environmentally low impact compared to energy crops [2.14]. For example, the worldwide production of the sugarcane bagasse fiber is about 540 million metric tons per year

[2.15], so it can be considered a promising source of lignin. However, the obtention from agro-waste biomass must be integrated along the development of commercially viable technologies to make the process profitable. Adopting the biorefinery concept (circular economy approach) into the lignin exploitation is a strategic point to make the process cost-effective.

### 2.1.2 Technical lignins

Lignin can be isolated from the lignocellulosic biomass by different chemical, physical, and biological treatments [2.16]. In all commercial pulping processes, including the hydrolysis of wood for biofuel production, lignin is structurally altered compared to the native lignin. These processes are characterized by the type of reagents used, energy consumption, and the final properties that the lignin acquires. Therefore, each process gives a name to the type of technical lignin obtained. The most common technical lignins include lignosulfonates (isolated from sulfite pulping), kraft lignins (isolated from black liquor from kraft pulping), organosolv lignins (isolated from organosolv pulping), soda lignins (isolated from sodium pulping), and hydrolysis lignin obtained from the residues after enzymatic treatment of biomass.

- **Kraft lignin**

Kraft pulping was first introduced in 1879 and has become the most dominant technology used in the pulping industry [2.17]. The kraft process is potentially the largest source of lignin feedstock. Only in the United States, the total capacity of dry wood pulp was 54 280 million tons in the last five years [2.18].

The kraft pulping process is extensively employed in the production of cellulose fibers. This process is a chemical pulping where lignin is

degraded in a sulfate (kraft) cooking process and dissolved to separate the pure cellulose from the lignocellulosic material. Kraft lignin is isolated from biomass in the presence of sodium hydroxide and sodium sulfide solution at high temperature (165-175 °C) and pressure for 1-2 h [2.11, 2.19, 2.20]. The ether linkages are broken, and lignin fragments are dissolved in the solvent, forming black liquor. Around 95 % of the lignin present in wood is dissolved in the aqueous solution [2.21]. The weak black liquor is concentrated to give heavy black liquor and is used mainly in the recovery boilers for heat and power generation in the kraft pulping mills. However, the amount of produced lignin exceeds the quantity needed for the energy supply-demand. For this reason, most of the technical lignin is generated in kraft pulp processes [2.17].

Kraft lignin is hydrophobic at neutral pH and contains less than 4 % of sulfur lignin groups, which gives the special sulfur characteristic odor. Kraft lignin has some remarkable properties compared to other types of lignin, such as a higher content of phenolic hydroxide groups generated from the cleavage of  $\beta$ -aryl linkages during the pulping process [2.22].

- **Sulfite lignin**

The sulfite process was the predominant pulping process from the late 19<sup>th</sup> century to the early 20<sup>th</sup> century. Lignosulfonate has been used extensively in the industry, with the total annual production of one million tons sold in the market with a price range of 180-500 US\$/t [2.23, 2.24]. The sulfite lignin, sulfonated lignin, or lignosulfonates was obtained by reaction of the lignocellulosic biomass at different pH ranges with sulfurous acid or a sulfite salt containing magnesium, calcium, sodium, or ammonium [2.25, 2.26]. Generally, sulfite pulping processes involve the breaking of ether bonds along with the loss of methoxyl groups, the introduction of sulfonated groups in the C<sub>α</sub>-positions, and the

formation of carbon-carbon bonds [2.2]. Sulfite liquor is mainly composed of lignosulfonate, acetic acid, hemicellulose sugars, inorganic and small amounts of derivatives from sugar dehydration [2.18]. Lignosulfonates are produced in relatively large quantities, around 1 million tons per year as dry solids [2.27].

Due to the wide range of conditions under which sulfite pulp production can occur, the lignosulfonate structures obtained vary considerably [2.28]. Besides, the sulfonated lignin has a broad molecular weight distribution, which often contains up to 30 wt. % of impurities, ash, or remaining carbohydrates. The incorporation of sulfonic acid groups (3-8 wt. %) linked to its aliphatic part, make it soluble in water and giving it the ability to emulsify and binding properties [2.29].

- **Soda lignin**

The soda process is the oldest pulping method. In this process, sodium hydroxide is employed at high temperature and pressure. The feedstock is digested at 140-170 °C with 13-16 wt. % of sodium hydroxide (pH 11-13). Although the soda process it is an economic process (has a price range of 200–300 US\$/t) [2.30], it is not very selective because it also acts on carbohydrates and extracts, dissolving them together with the desired lignin [2.31].

In this process, anthraquinone is often employed to cleave the  $\beta$ -O-4 linkages to increase the delignification process [2.32]. The resulted lignin separated from black liquor with  $\text{Na}_2\text{CO}_3$  is called soda lignin. The  $\alpha$ -ether bonds are cleaved in this process. Until the organosolv process development, the soda process was used as the main lignin source for material development since the structure of the lignin was not modified due to the absence of sulfur functionality.

- **Organosolv lignin**

In the organosolv pulping process, different mixtures of organic solvents and water are used as a cooking medium at different temperatures from 140 to 220 °C [2.33]. The most used solvents employed in combination with water that are: acetic acid, ethanol, formic acid, and peroxyacids [2.34]. The lignin is fragmented and dissolved in an organic solvent, and the hemicellulose is depolymerized into soluble saccharides, resulting in insoluble cellulose in the medium. In the process, the most broken linkages are the ether linkages by hydrolytic cleavage, making the fragments solvent-soluble. It is a suitable process for the treatment of annual plants and hardwoods.

Different routes are being developed to bring this process to an industrial scale: Alcell®, Acetosolv®, ASAM®, FormicoFib®, and Organocell® in the presence of water mixtures with different organic solvents, including the solvents as mentioned above or their mixtures [2.29].

The organosolv lignin molecular weight is lower than other technical lignins, and it was considered very pure lignin since the ash formation and the carbohydrates content is very low. The use of organic solvents increases the cost of processing, but the advantages mentioned previously make this route the most suitable to produce high added-value chemicals [2.35, 2.36].

- **Hydrolyzed lignin**

Since the recognition of the impact of greenhouse gases in the 2000s, efforts are being made to replace fossil fuels with renewable fuels progressively. In less than ten years, sugarcane ethanol has adopted a significant role in transportation fuel [2.37]. The conversion of lignocellulosic material to ethanol requires three steps: (1) pre-treatment

to separate hemicellulose and lignin from cellulose, (2) hydrolysis of cellulose to obtain fermentable sugars, and (3) fermentation to convert sugars into ethanol [2.7]. The hydrolyzed lignin is generated as a by-product of the residual biomass that must be discarded from crops. The global yield of waste from these feedstocks was estimated between 10 and 50 billion tons per year, making the hydrolyzable lignin an ideal lignin feedstock.

Hydrolyzed lignin is characterized by a high molecular weight structure with strong steric hindrance. It contains typically sugar impurities, so it is not as reactive as organosolv or kraft lignin in chemical applications, and therefore, it is often used as fuel [2.38, 2.39]. Overall, hydrolyzed lignin would be more suitable for generating smaller molecules, such as vanillin, rather than larger polymers.

- **Lignin market**

In **Table 2.2**, the current state of production of the different technical lignins is detailed. The most established technical lignins, with the highest production and commercially accessible, are kraft lignin and lignosulfonates. Lignin soda and organosolv lignin are gaining more and more market share. However, they are still in pilot-scale production, but they are expected to increase their production due to the growing applications in which they are employed. Hydrolyzed lignins are starting to be produced because of the rise of the biorefinery concept. However, due to their low lignin quality, they are still far from being commercially viable.

**Table 2.2** Major industrial producers of various types of lignin, (adapted from [2.24]).

<i>Lignin type</i>	<i>Production (t/year)</i>	<i>Quality</i>	<i>Scale</i>	<i>Main companies</i>
Lignosulfonates	1055	High medium	Commercial	Lignotech Borregaard Tembec Nippon Papers
Kraft lignin	183	High	Commercial	Domtar Ingevity Stora Enso Westrock
Soda lignin	10	High	Pilot	Green Value
Organosolv lignin	13	High	Pilot	Inbicon
Hydrolyzed lignin	-	Low	Pilot	SEKAB Changhae Ethanol Co.

In **Table 2.3**, the main characteristics of the technical lignins are collected. The properties of lignin vary greatly depending on the source of lignin, the used extraction method, and the secondary treatments applied to isolate the lignin.

**Table 2.4** details several studies carried out for the use of different lignins for different applications. As detailed, each type of lignin has its possible final applications depending on the properties of the isolated lignin. Therefore, it is demonstrated that there is not one lignin better than another. Every kind of technical lignin has a market segment according to its properties, purity, and production cost.

**Table 2.3** Chemical composition and properties of the technical lignins [2.11, 2.16].

<b>Technical lignin</b>	<b>Kraft lignin</b>	<b>Lignosulfonate</b>	<b>Soda lignin</b>	<b>Organosolv lignin</b>	<b>Hydrolyzed lignin</b>
Purity	High	Low	Medium-high	Very high	Medium
Ash content (wt. %)	0.5-3.0	4.0-8.0	0.7-2.3	1.7	1.0-3.0
Moisture content (wt. %)	3.0-6.0	5.8	2.5-5.0	7.5	4.0-9.0
Carbohydrates (wt. %)	1.0-2.3	0	1.5-3.0	1.0-3.0	10.0-22.4
Acid soluble lignin (wt. %)	1-4.9	0	1.0-11	1.9	2.9
H content (wt. %)	5.8	3.7	5.9	5.9	6.2
C content (wt. %)	62.8	47.9	61.9	61.1	47.4
Nitrogen content (wt. %)	0.9	0.2	0.2-1.0	0-0.3	0.5-1.4
Sulphur content (wt. %)	1.0-3.0	3.5-8.0	0	0	0-1.0
$\overline{M}_w$ (g/mol)	1500-5000 up to 25000	1000-50000 up to 150000	1000-3000 up to 15000	500-5000	5000-10000
PDI	2.5-3.5	4.2-7.0	2.5-3.5	1.5	4.0-11.0
$T_g$ (°C)	108-165	127-164	150-155	89-97	75-90
Main applications	Dispersants	Dispersants	Soil conditioner	Aromatic polyols	Carbon fibers
	Carbon fibers	Agricultural chemicals	Release agent	Resins	Vanillin
	Emulsifiers	Blinders	Contaminant absorbent	Carbon fibers	Phenol derivatives
	Blinders	Pigments	Fire retardant	Phenol derivatives	Antioxidants



**Table 2.4** Grafting reactions conducted with different technical lignins, (adapted from [2.30]).

<b>Grafting reactions conducted on liginosulfonate</b>		
<b>Reaction Type</b>	<b>Lignin source</b>	<b>Application</b>
Hydroxymethylation	Hardwood Softwood	Thermal stability
Carboxyethylation	Not defined	Foaming ability
Sulfomethylation	Softwood	Adhesive
Amination	Softwood	Adsorbent
<b>Grafting reactions conducted on hydrolyzed lignin</b>		
<b>Reaction Type</b>	<b>Lignin source</b>	<b>Application</b>
Phosphorylation	Not defined	Fire retardant
Phenolation	Wheat straw	Adhesive
Sulfomethylation	Cornstalk	Dispersion for graphite and concrete paste
Amination	Cornstalk Softwood	Flocculant for azo dyes Kaolin, sulfate, and humic acid removal
<b>Grafting reactions conducted on soda lignin</b>		
<b>Reaction Type</b>	<b>Lignin source</b>	<b>Application</b>
Oxyalkylation	Grass Wheat straw	Polyurethane foams Substitute for polyols
Esterification	Mixed of grass Wheat straw	Polymer blends Dispersant
Phosphorylation	Not defined	Metal ion adsorption
Phenolation	Not defined	Resins
Methylation	Sarkanda grass Wheat straw	Improve storage stability
Amination	Softwood/Bagasse	Adsorbent for heavy metals
Epoxidation	Softwood	Resin
<b>Grafting reactions conducted on soda lignin</b>		
<b>Reaction Type</b>	<b>Lignin source</b>	<b>Application</b>
Phosphorylation	Not defined	Flame retardant for polybutylene succinate
Phenolation	Hardwood	Resin
Carboxymethylation	Sugarcane bagasse Hardwood	Stabilizer of crude bitumen and ceramic industries Heavy metal adsorption
Epoxidation	Hardwood	Epoxy resin
Oxyalkylation	Hardwood	Polyurethane foam Substitute for polyols
Esterification	Hardwood Softwood Wheat straw	Polymer blends Dispersant Lignin-based carbons
Amination	Hardwood	Additive for plasticizing Adsorbent for sulfate, kaolin, humic acid

### 2.1.3 Lignin solubility

The use of lignin in the synthesis of bio-based products may be favored with a suitable extraction method and its subsequent modification. However, lignin has many disadvantages, such as high molecular weight distribution, steric hindrance effects, and low reactivity [2.40]. Furthermore, when lignin is applied as an intermediate or incorporated for the synthesis of bio-based products, one of the significant drawbacks is the low solubility in the most common organic solvents used, promoting processing failures and meager reaction yields [2.41-2.43]. Therefore, several publications have been devoted to determine the lignin solubility and its possible modification pathways to increase this feature.

The best way to solubilize any type of lignin, regardless of its origin, structure, or extraction method, is in a basic aqueous medium since, at neutral pH, it is practically insoluble [2.44]. Sameni et al. conducted extensive work analyzing different types of lignins with various organic solvents [2.45]. They concluded that the best organic solvents to solubilize lignin were pyridine and dimethyl sulfoxide, followed by tetrahydrofuran, dioxane, acetone, and methanol. The worst solvents were diethyl ether, neutral water, chloroform, and dichloromethane. Concerning to the lignin structure, lignins with lower molecular weight, as expected, were more soluble. It was found that the acetylation of the lignin increased its solubility in all tested solvents except for water, alcohols, and ethers [2.46-2.48]. Acetylation is a well-established technique to increase lignin solubility in organic solvents for lignin characterization, when organic solvents are required by modifying lignin through its hydroxyl groups [2.49].

Since as stated in **Chapter 1**, the main objective of this thesis work is to obtain lignin-based polyols (LBPs) by cationic ring-opening

polymerization (CROP). Even if the most plausible solvent choice would be in basic aqueous media, it is not suitable for CROP since the reaction media would neutralize the action of the acid catalyst making not viable this novel proposed approach to obtain lignin-based polyols. Thus, the typical solvents employed as reaction media in CROP reaction are usually organic aprotic solvents such as dichloromethane [2.50-2.54], dichloroethane [2.55], and tetrahydrofuran [2.56, 2.57], or a mix of them [2.58, 2.59].

## 2.2 Objective

The objective of this chapter is to determine the best lignin sources to be employed in the synthesis of lignin-based polyols by CROP, considering their solubility in organic aprotic solvents. To this purpose, the first partial objective will be to select different types of lignin and determine their solubility in those suitable aprotic organic solvents for the CROP without any other modification. The solvents chosen for this purpose were dichloromethane (DMC) and tetrahydrofuran (THF). To better understand the modification that lignin may undergo in the polymerization process, a more exhaustive characterization of the selected lignin will be carried out.

## 2.3 Methodology

### 2.3.1 Materials

Different lignin sources and different isolation methods were used to determine which one was the most suitable for the synthesis of lignin-based polyols. Poplar hydrolysis lignin was obtained in Tecalia. An organosolv lignin obtained from a mixture of different woods was kindly

supplied by the Netherlands Organization for Applied Scientific Research (TNO). Beech organosolv lignin was kindly provided by Fraunhofer. Elm kraft, eucalyptus kraft, poplar kraft, eucalyptus hydrolysis, pine hydrolysis, soda olive were kindly supplied by the National Institute of Agricultural and Food Research and Technology (INIA).

### 2.3.2 Characterization

The moisture content and the solubility of all lignin samples were determined according to the procedures in **Appendix I**.

The lignin selected as the best one to conduct the polymerization reaction was fully characterized. The structural analysis of the lignin was characterized by Attenuated Total Reflection Fourier Transform Infrared Spectroscopy (ATR-FTIR) analysis and by Pyrolysis-Gas Chromatography/Mass Spectrometry (Py-GC/MS). The molecular weight distribution (MWD), the average molecular weight ( $\overline{M_w}$ ), and the polydispersity index (PDI), were determined by Size Exclusion Chromatography (SEC). The hydroxyl number (OH#) was determined by potentiometric titration. The acid-insoluble lignin (AIL) was determined gravimetrically by an acid lignin hydrolysis, and the acid-soluble lignin (ASL) was determined by a spectrophotometer (UV absorption at 205 nm). Sugar content was determined by a High-Performance Liquid Chromatography (HPLC). The thermal degradation and ash content of the lignin was determined by Thermo-Gravimetric Analysis (TGA) and the glass transition temperature by Differential Scanning Calorimetry (DSC). All these characterizations are described in **Appendix I**.

## 2.4 Results and discussion

### 2.4.1 Lignin selection

The different lignins (**Figure 2.2**) detailed in the methodology section were dried before the solubility test in organic solvents. The lignin moisture content (H) is reported in **Table 2.5**.

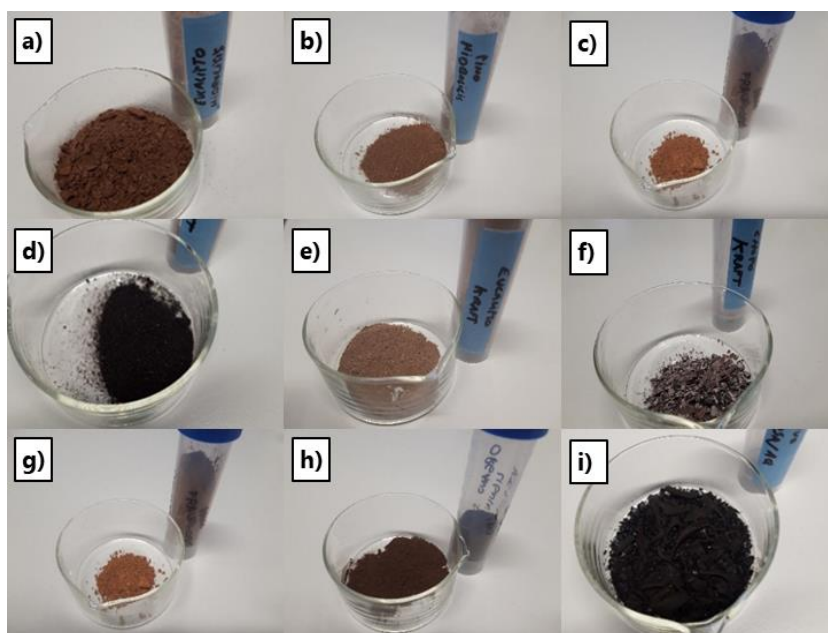


**Figure 2.2** Picture of the different lignin employed: a) Eucalyptus-HL, b) Pine-HL, c) Poplar-HL, d) Elm-KL, e) Eucalyptus-KL, f) Poplar-KL, g) Beech-OL, i) Mix-OL, and j) Olive-SL.

All lignins have low moisture content, being slightly higher than those obtained by hydrolysis. These results are in accordance with the moisture data detailed in **Table 2.3**. Once the moisture was determined, the lignins were dissolved in two different organic solvents used commonly in CROP, dichloromethane (DCM) and tetrahydrofuran (THF). The results are detailed in **Figure 2.3**.

**Table 2.5** Moisture content of different technical lignins.

Sample	Biomass	Type of lignin	H (wt. %)
Eucalyptus-HL	Eucalyptus	Hydrolysis lignin	2.46
Pine-HL	Pine	Hydrolysis lignin	4.92
Poplar-HL	Poplar	Hydrolysis lignin	5.70
Elm-KL	Elm	Kraft lignin	3.39
Eucalyptus-KL	Eucalyptus	Kraft lignin	2.14
Poplar-KL	Poplar	Kraft lignin	1.99
Beech-OL	Beech	Organosolv lignin	1.41
Mix-OL	Mixture of trees	Organosolv lignin	1.30
Olive-SL	Olive	Soda lignin	3.44

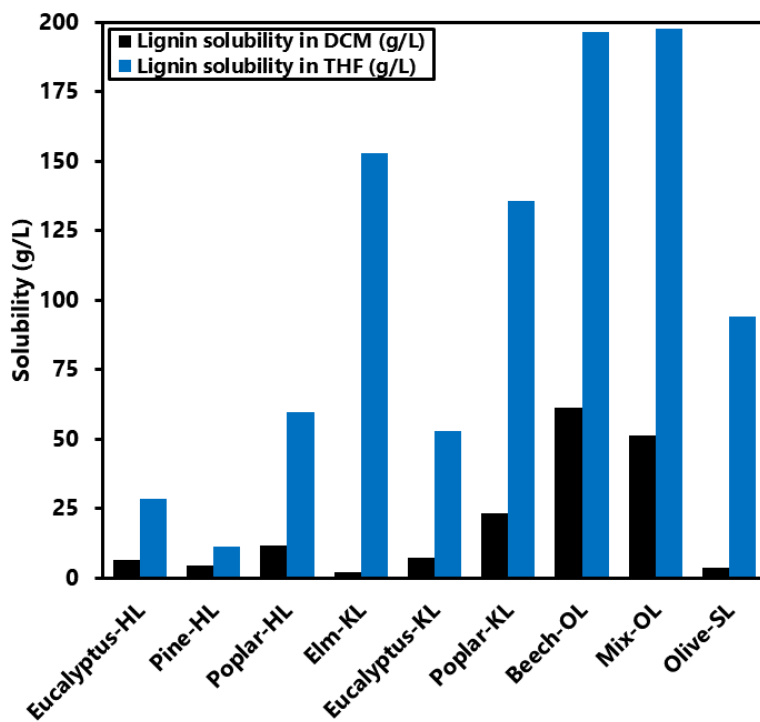


**Figure 2.3** Lignin solubility in different organic solvents.

In general, all lignins are more soluble in THF than in DCM. The studied lignins showed little or negligible solubility in DCM, as it is reported in several studies [2.45-2.48]. The most soluble are the organosolv lignins, followed only by poplar kraft lignin. On the other hand, elm and eucalyptus kraft lignins, as well as hydrolysis lignins and soda lignin, are almost insoluble in the used solvents.

In THF, the most soluble lignins are again the organosolv lignins. It can be considered that the solubility is total since solutions were prepared with a concentration of 200 g/L. Kraft lignins also show good solubility except for the eucalyptus kraft lignin. As in DCM, the hydrolysis lignins have low solubility. However, soda lignin, which is insoluble in DCM, is partially solubilized in THF.

The use of insoluble lignin in the polymerization reaction could make the overall control of the reaction parameters, the reproducibility, and the final polyol microstructure quite difficult. With this lignin solubility study, it has been shown that organosolv lignins (Mix-OL and Beech-OL) are the most suitable for reactions where the reaction medium is an organic solvent. Between the two organosolv lignins, the lignin from the tree mixture (Mix-OL) is selected for the lignin polymerization study because it is easier to handle than the Beech-OL.

#### 2.4.2 Lignin characterization

The selected organosolv lignin for the polymerization study from a mixture of woods obtained by an organosolv treatment (Mix-OL) was fully characterized by different procedures and techniques described in **Appendix I**.

- **Lignin composition and functional groups**

The chemical composition of the lignin is shown in **Table 2.6**. The Mix-OL has a high purity lignin content of 98.16 wt. % (Klason lignin and acid-soluble lignin) with low carbohydrate content of 0.359 wt. % (glucan and hemicellulose), in large part, derived from hemicelluloses. The lignin ash content is in accordance with other types of lignins [2.60]. These lignin properties are in line with the technical organosolv lignins detailed in **Table 2.3**.

**Table 2.6** Chemical composition of the Mix-OL.

<b>Mix-OL chemical composition</b>	
Klason lignin (acid-insoluble lignin) (wt. %)	91.64
Acid-soluble lignin (wt. %)	6.52
Cellulose (wt. %) <sup>a</sup>	0.011
Hemicellulose (wt. %)	0.348
Ash (wt. %)	0.40
OH# (mg KOH/g)	243

wt. % given on dry sample.

The total balance being unidentified products.

<sup>a</sup> Cellulose represented as glucan content.

The lignin was analyzed by Py-GC/MS to determine the phenolic compounds qualitatively considering their abundance (**Table 2.7**). The sample was determined according to the NIST library, although considering that the determined compounds could do not be forming in the original lignin. The compounds are sorted by lignin derivative compounds and carbohydrate-derivative compounds. The formed are sub-classified into guaiacyl derivatives (G), *p*-coumaryl derivatives (H), syringyl derivatives (S), and catechol derivatives (C).



**Table 2.7** Main compounds obtained in the pyrolysis of the Mix-OL (expressed as g/100 g lignin).

Compound name	S/G/H/C	Main fragments (m/z)	Area (%)
Furfural	Carbohydrate	96,95,67	0.76
Phenol	H	94,66,65	0.92
<i>p</i> -cresol	H	107,108,77	1.08
<i>o</i> -guaiacol	G	109,124,81	9.57
<i>m</i> -xylenol	H	107,122,121	0.63
4-methylguaiacol (cresol)	G	138,123,95	9.45
3-methoxy catechol	C	140,125,97	4.67
3-methyl catechol	C	124,78,123	0.64
4-ethylguaiacol	G	137,152,122	4.32
Vinyl guaiacol	G	150/135/77/107	4.01
Syringol	S	154,139,111	17.12
3,4-dimethoxyphenol	S	154,139,111	2.73
<i>p</i> - propylguaiacol	G	137,166,122	0.93
Vanillin	G	151,152,109	1.36
<i>cis</i> -isoeugenol	G	164,149,77	0.90
4-methyl syringol	S	168, 153, 125	18.38
4-ethyl syringol	S	167,182,77	4.20
4-vinylsyringol	S	180,165,137	4.64
4-allylsyringol	S	194,91,119	1.51
Syringaldehyde	S	167,196,168	1.37
4-Allylsyringol	S	194,91,119	3.79
<i>n</i> -hexadecanoic acid	FA	73,99,57	5.14
<i>cis</i> -vaccenic acid	FA	55,69,41	0.60
octadecanoic acid	FA	43,60,73	1.31
Total syringyl derivatives		S (%)	53.73
Total guaiacyl derivatives		G (%)	30.53
Total fatty acids derivatives		FA (%)	7.05
Total catechol derivatives		C (%)	5.31
Total <i>p</i> -coumaryl derivatives		H (%)	2.63
syringyl/guaiacyl ratio		S/G	1.76

As it is detailed in **Table 2.7**, the most abundant products obtained are the syringyl derivates, followed by guaiacyl derivates. The most abundant products are: syringol, guaiacol, 4-methyl syringol, *o*-guaiacol, and cresol. In less quantity can be found fatty acids, catechol derivatives, and *p*-coumaryl derivatives. The catechol derivatives, although it is not one of the three lignin precursors, could be formed in the lignin linkages formation or could be created during the pyrolysis analysis. The syringyl derivates/guaiacyl derivates ratio (S/G) could determinate the lignin nature. A S/G value ratio above one could be considered as indicative of hardwood lignin [2.61]. The Mix-OL S/G ratio is 1.76, which means this comes from a hardwood lignin.

- Lignin structure

The structural analysis of the lignin was characterized by ATR-FTIR. The ATR-FTIR spectra of the Mix-OL is showed in **Figure 2.4** with their corresponding bands and wavelenghts collected in **Table 2.8**.

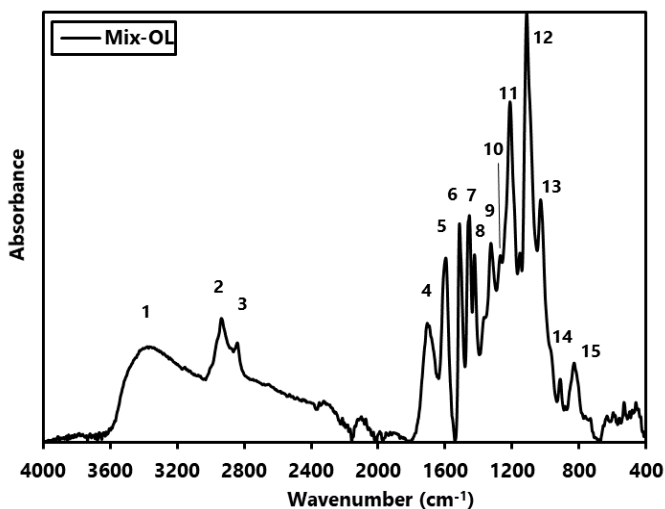


**Figure 2.4** ATR-FTIR spectra of the Mix-OL.

The broad band at 3370  $\text{cm}^{-1}$  corresponds to the stretching of lignin aliphatic and phenolic -OH groups. The bands at 2935  $\text{cm}^{-1}$  and 2840  $\text{cm}^{-1}$  are related to the C-H methyl and methylene groups stretch vibrations. The band at 1454  $\text{cm}^{-1}$  is also associated with the bending deformation of the C-H group. The band at 1700  $\text{cm}^{-1}$  is linked to the C=O stretch of unconjugated ketone, carboxyl, and ester groups. The bands from 1600  $\text{cm}^{-1}$  to 1423  $\text{cm}^{-1}$  belongs to aromatic skeletal stretching and deformation vibrations. The bands at 1325  $\text{cm}^{-1}$  and 1211  $\text{cm}^{-1}$  correspond to aryl ring breathing with C-O and C=O stretching vibrations [2.8]. The highest intense band at 1100  $\text{cm}^{-1}$  corresponds to C-O deformation of the secondary alcohols and aliphatic ethers. The bands detected at 1028  $\text{cm}^{-1}$  and 828  $\text{cm}^{-1}$  correspond with the C-H deformation of syringyl rings. The deformation of the C-H corresponding to the guaiacyl ring appeared at 912  $\text{cm}^{-1}$ .

**Table 2.8** Wavenumber of the lignin Mix-OL ATR-FTIR spectra.

Peak	Wavenumber ( $\text{cm}^{-1}$ )	Peak	Wavenumber ( $\text{cm}^{-1}$ )	Peak	Wavenumber ( $\text{cm}^{-1}$ )
1	3370	6	1513	11	1211
2	2935	7	1454	12	1100
3	2840	8	1423	13	1028
4	1700	9	1326	14	912
5	1600	10	1268	15	828

A quick ratio of the S-type and G-type (S/G) structural units can be obtained using the ATR-FTIR technique comparing the intensity of bands at 1326  $\text{cm}^{-1}$  and 1268  $\text{cm}^{-1}$  [2.62]. In the Mix-OL lignin, the calculated ratio S/G is 1.066. This ratio is indicative of a hardwood lignin source. Furthermore, this value is in accordance with the results obtained in the Py-GS/MS.

The isolated lignin was analyzed by SEC to determine its molecular weight distribution (MWD), its average molecular weight ( $\overline{M}_w$ ), number average ( $\overline{M}_n$ ) and polydispersity index (PDI) ( $\overline{M}_w/\overline{M}_n$ ) collected in **Table 2.9**. The Mix-OL MWD is plotted in **Figure 2.5**.

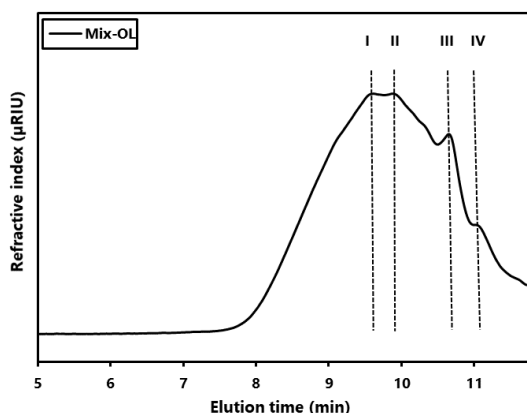


**Figure 2.5** Mix-OL molecular weight distribution profile.

The MWD of lignin revealed that it is not formed by a uniform structure. **Table 2.9** shows the lignin splitting in the most representative peaks. Lignin is formed by a continuous series of peaks that gave it a  $\overline{M}_w$  of 1095 g/mol, with  $\overline{M}_n$  of 472 g/mol resulting in a PDI of 2.32. These results are in accordance with the technical lignins obtained by a standard organosolv process isolation (**Table 3.3**).

**Table 2.9** Molecular weight distribution of Mix-OL lignin.

<i>Mix-OL</i>	$\overline{M}_n(\text{g/mol})$	$\overline{M}_w(\text{g/mol})$	<i>PDI</i>	<i>Area (%)</i>
I	944	1115	1.2	61.0
II	534	537	1.0	12.2
III	357	368	1.0	16.0
IV	118	148	1.3	10.8
all at once	472	1095	2.3	100.0

- Mix-OL thermal profile

Thermogravimetric analysis of the lignin was carried out to determine the thermal stability profile of the Mix-OL. The obtained thermogravimetric curve (TG) weight loss is detailed in **Figure 2.6-a** and its derivative curve (dTG) profile in **Figure 2.6-b**. The first weight loss below 100 °C corresponded to water evaporation, while the second and degradation step between 200 °C and 400 °C was attributed to the degradation of the lignin structural components. Finally, the third weight loss was observed above 400 °C, which corresponded to the oxidation and breakdown of charred residue into low molecular weight gaseous components. The thermal stability of the lignin is measured as the temperature at which the 5 % weight is lost ( $T_{5\%}$ ) which is 249 °C. The lignin lost half of its weight ( $T_{50\%}$ ) at 465 °C.

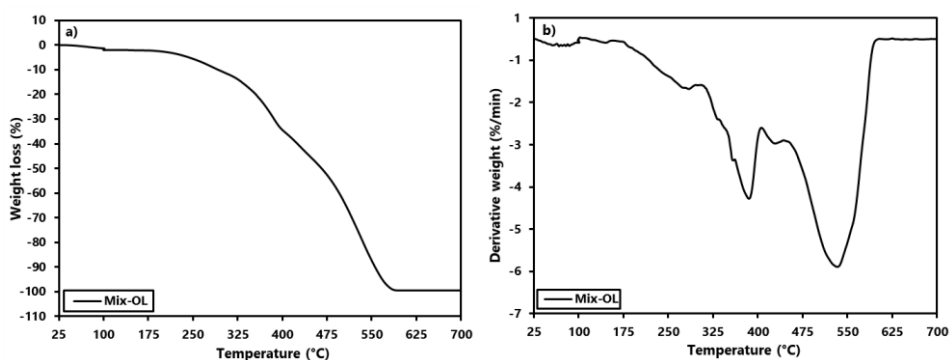


**Figure 2.6** Thermal profile of the Mix-OL: a) TG, b) dTG.

The glass transition temperature ( $T_g$ ) obtained by DSC analysis of the Mix-OL is illustrated in **Figure 2.7**. Mix-OL revealed a  $T_g$  midpoint at 91.06 °C. This value is in the range of the glass transition temperatures for an organosolv lignin (**Table 2.3**). These results are also supplemented with data provided by TNO: Elemental Analysis: C (64.7%), H (5.8%), N (0.2%), S (0.0%), O (29.3%) and hydroxyl content of 4.510 mmol OH/g

(3.330 mmol phenolic OH/g). This value is consistent with the value obtained in the OH# determination (243 mg KOH/g)

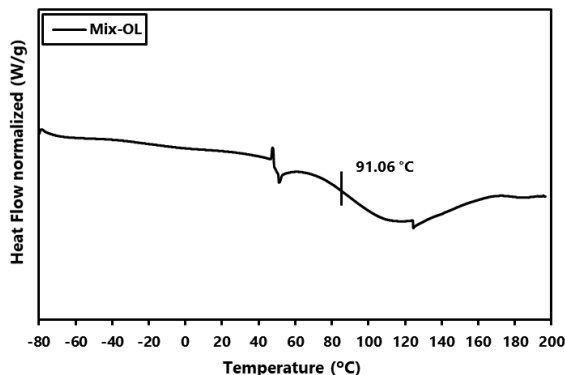


**Figure 2.7** DSC curve of the Mix-OL.

## 2.5 Conclusions

In this chapter, the solubility of different technical lignins (kraft, organosolv, soda, and hydrolyzed) in aprotic organic solvents has been studied. The study was done using dichloromethane (DCM) and tetrahydrofuran (THF) as solvents since they are the most used in the CROP reaction.

It has been shown that lignins generally are not dissolved well in these organic solvents, particularly in DCM. In THF, the lignin solubility was better compared with DCM, being the organosolv lignins the best of all the investigated lignins. The lignin solubility is a critical parameter since low values lead into deficient performance. The selected lignin (Mix-OL) was fully characterized, and the results obtained in the different characterizations conducted were in accordance with the parameters reported in the bibliography for organosolv lignins. Consequently, the Mix-OL was chosen for the next chapters, where polymerizations based on this lignin have been carried out.

## 2.6 References

- [2.1] A. J. Ragauskas et al., “Lignin valorization: Improving lignin processing in the biorefinery,” *Science*, vol. 344, no. 6185, 2014.
- [2.2] G. Gellerstedt and G. Henriksson, “Lignins: Major Sources, Structure and Properties,” in *Monomers, Polymers and Composites from Renewable Resources*, Elsevier, 2008, pp. 201–224.
- [2.3] S. V. Vassilev, D. Baxter, L. K. Andersen, C. G. Vassileva, and T. J. Morgan, “An overview of the organic and inorganic phase composition of biomass,” *Fuel*, vol. 94, pp. 1–33, 2012.
- [2.4] H. Abreu, M. Maria, and J. Reis, “Dual Oxidation Ways Toward Lignin Evolution,” *Brazilian J. For. Environment*, vol. 8, no. único, pp. 207–211, 2001.
- [2.5] F. B. De La Cruz, “Fate and Reactivity of Lignin in Municipal Solid Waste (MSW) Landfill.,” 2014.
- [2.6] F. G. Calvo-Flores, J. A. Dobado, J. Isac-García, and F. J. Martín-Martínez, *Lignin and Lignans as Renewable Raw Materials: Chemistry, Technology and Applications*. Chichester, UK: John Wiley & Sons, Ltd, 2015.
- [2.7] L. Rocha Meneses, M. Raud, K. Orupold, and T. Kikas, “Second-generation bioethanol production: A review of strategies for waste valorisation,” *Agron. Res.*, vol. 15, no. 3, pp. 830–847, 2017.
- [2.8] O. Faruk and M. Sain, *Lignin in Polymer Composites*. 2015.
- [2.9] N. Smolarski, “High-Value Opportunities for Lignin: Unlocking its Potential Lignin potential,” *Frost & Sullivan*, pp. 1–15, 2012.
- [2.10] A. Gandini, “The irruption of polymers from renewable resources on

- the scene of macromolecular science and technology,” *Green Chem.*, vol. 13, no. 5, pp. 1061–1083, 2011.
- [2.11] A. Vishtal and A. Kraslawski, “Challenges in industrial applications of technical lignins,” *BioResources*, vol. 6, no. 3, pp. 3547–3568, 2011.
- [2.12] N. Rombaut, A.-S. Tixier, A. Bily, and F. Chemat, “Green extraction processes of natural products as tools for biorefinery,” *Biofuels, Bioprod. Biorefining*, vol. 8, no. 4, pp. 530–544, 2014.
- [2.13] F. Cherubini et al., “Toward a common classification approach for biorefinery systems,” *Biofuels, Bioprod. Biorefining*, vol. 3, no. 5, pp. 534–546, Sep. 2009.
- [2.14] P. Manara, A. Zabaniotou, C. Vanderghem, and A. Richel, “Lignin extraction from Mediterranean agro-wastes: Impact of pretreatment conditions on lignin chemical structure and thermal degradation behavior,” *Catal. Today*, vol. 223, pp. 25–34, 2014.
- [2.15] T. L. Bezerra and A. J. Ragauskas, “A review of sugarcane bagasse for second-generation bioethanol and biopower production,” *Biofuels, Bioprod. Biorefining*, vol. 10, no. 5, pp. 634–647, 2016.
- [2.16] A. Eraghi Kazzaz and P. Fatehi, “Technical lignin and its potential modification routes: A mini-review,” *Ind. Crops Prod.*
- [2.17] N. Mahmood, Z. Yuan, J. Schmidt, and C. (Charles) Xu, “Production of polyols via direct hydrolysis of kraft lignin: Effect of process parameters,” *Bioresour. Technol.*, vol. 139, no. 2, pp. 13–20, 2013.
- [2.18] T. Li and S. Takkellapati, “The current and emerging sources of technical lignins and their applications,” *Biofuels, Bioprod. Biorefining*, vol. 12, no. 5, pp. 756–787, 2018.
- [2.19] F. S. Chakar and A. J. Ragauskas, “Review of current and future



- softwood kraft lignin process chemistry,” *Ind. Crops Prod.*, vol. 20, no. 2, pp. 131–141, 2004.
- [2.20] C. Wang, S. S. Kelley, and R. A. Venditti, “Lignin-Based Thermoplastic Materials,” *ChemSusChem*, vol. 9, no. 8, pp. 770–783, 2016.
- [2.21] G. Gellerstedt and L. Zhang, “Chemistry of TCF-Bleaching with Oxygen and Hydrogen Peroxide,” in *ACS Symposium Series*, vol. 785, pp. 61–72, 2001.
- [2.22] A. Eraghi Kazzaz, Z. Hosseinpour Feizi, and P. Fatehi, “Grafting strategies for hydroxy groups of lignin for producing materials,” *Green Chem.*, vol. 21, no. 21, pp. 5714–5752, 2019.
- [2.23] A. Tribot et al., “Wood-lignin: Supply, extraction processes and use as bio-based material,” *Eur. Polym. J.*, vol. 112, no. December 2018, pp. 228–240, 2019.
- [2.24] L. A. Zevallos Torres et al., “Lignin as a potential source of high-added value compounds: A review,” *J. Clean. Prod.*, vol. 263, p. 121499, 2020.
- [2.25] S. R. Pereira, D. J. Portugal-Nunes, D. V. Evtuguin, L. S. Serafim, and A. M. R. B. Xavier, “Advances in ethanol production from hardwood spent sulphite liquors,” *Process Biochem.*, vol. 48, no. 2, pp. 272–282, 2013.
- [2.26] T. Li and S. Takkellapati, “The current and emerging sources of technical lignins and their applications,” *Biofuels, Bioprod. Biorefining*, vol. 12, no. 5, pp. 756–787, 2018.
- [2.27] N. E. El Mansouri and J. Salvadó, “Analytical methods for determining functional groups in various technical lignins,” *Ind. Crops Prod.*, vol. 26, no. 2, pp. 116–124, 2007.

- [2.28] T. Aro and P. Fatehi, "Production and Application of Lignosulfonates and Sulfonated Lignin," *ChemSusChem*, vol. 10, no. 9, pp. 1861–1877, 2017.
- [2.29] S. Gillet et al., "Lignin transformations for high value applications: Towards targeted modifications using green chemistry," *Green Chem.*, vol. 19, no. 18, pp. 4200–4233, 2017.
- [2.30] A. Eraghi Kazzaz and P. Fatehi, "Technical lignin and its potential modification routes: A mini-review," *Ind. Crops Prod.*, vol. 154, 2020.
- [2.31] S. G. Karp, A. L. Woiciechowski, V. T. Soccol, and C. R. Soccol, "Pretreatment strategies for delignification of sugarcane bagasse: a review," *Brazilian Arch. Biol. Technol.*, vol. 56, no. 4, pp. 679–689, 2013.
- [2.32] J. Gierer, M. Kjellman, and I. Noren, "Alkaline delignification in the presence of antraquinone/antrahydroquinone," *Holzforchung*, vol. 37, no. 1, pp. 17–22, 1983.
- [2.33] X. Zhao, K. Cheng, and D. Liu, "Organosolv pretreatment of lignocellulosic biomass for enzymatic hydrolysis," *Appl. Microbiol. Biotechnol.*, vol. 82, no. 5, pp. 815–827, 2009.
- [2.34] F. Xu, J. X. Sun, R. Sun, P. Fowler, and M. S. Baird, "Comparative study of organosolv lignins from wheat straw," *Ind. Crops Prod.*, vol. 23, no. 2, pp. 180–193, 2006.
- [2.35] J. Zhang, D. Cai, Y. Qin, D. Liu, and X. Zhao, "High value-added monomer chemicals and functional bio-based materials derived from polymeric components of lignocellulose by organosolv fractionation," *Biofuels, Bioprod. Biorefining*, vol. 14, no. 2, pp. 371–401, 2020.
- [2.36] M. F. Li, S. N. Sun, F. Xu, and R. C. Sun, "Sequential solvent fractionation of heterogeneous bamboo organosolv lignin for value-

- added application,” *Sep. Purif. Technol.*, vol. 101, pp. 18–25, 2012.
- [2.37] C. A. Cardona, J. A. Quintero, and I. C. Paz, “Production of bioethanol from sugarcane bagasse: Status and perspectives,” *Bioresour. Technol.*, vol. 101, no. 13, pp. 4754–4766, 2010.
- [2.38] N. Mahmood, Z. Yuan, J. Schmidt, M. Tymchyshyn, and C. Xu, “Hydrolytic liquefaction of hydrolysis lignin for the preparation of bio-based rigid polyurethane foam,” *Green Chem.*, vol. 18, no. 8, pp. 2385–2398, 2016.
- [2.39] J. K. Sameni, “Physico-Chemical Characterization of Lignin Isolated from Industrial Sources for Advanced Applications,” 2015.
- [2.40] A. Duval and M. Lawoko, “A review on lignin-based polymeric, micro- and nano-structured materials,” *React. Funct. Polym.*, vol. 85, pp. 78–96, 2014.
- [2.41] S. Laurichesse and L. Avérous, “Chemical modification of lignins: Towards biobased polymers,” *Prog. Polym. Sci.*, vol. 39, no. 7, pp. 1266–1290, 2014.
- [2.42] A. Jablonskis, A. Arshanitsa, A. Arnautov, G. Telysheva, and D. Evtuguin, “Evaluation of Ligno Boost™ softwood kraft lignin epoxidation as an approach for its application in cured epoxy resins,” *Ind. Crops Prod.*, vol. 112, no. April 2017, pp. 225–235, 2018.
- [2.43] K. R. Kurple, “Lignin Based Polyols,” 6,025,452, 2000.
- [2.44] E. I. Evstigneev, “Factors affecting lignin solubility,” *Russ. J. Appl. Chem.*, vol. 84, no. 6, pp. 1040–1045, 2011.
- [2.45] J. Sameni, S. Krigstin, and M. Sain, “Solubility of Lignin and Acetylated Lignin in Organic Solvents,” *BioResources*, vol. 12, no. 1, pp. 1548–1565, 2017.

- [2.46] I. Cybulska, G. Brudecki, K. Rosentrater, J. L. Julson, and H. Lei, "Comparative study of organosolv lignin extracted from prairie cordgrass, switchgrass and corn stover," *Bioresour. Technol.*, vol. 118, pp. 30–36, 2012.
- [2.47] J. Quesada-Medina, F. J. López-Cremades, and P. Olivares-Carrillo, "Organosolv extraction of lignin from hydrolyzed almond shells and application of the  $\delta$ -value theory," *Bioresour. Technol.*, vol. 101, no. 21, pp. 8252–8260, 2010.
- [2.48] Y. Ni and Q. Hu, "Alcell® lignin solubility in ethanol–water mixtures," *J. Appl. Polym. Sci.*, vol. 57, no. 12, pp. 1441–1446, Sep. 1995.
- [2.49] A. Tolbert, H. Akinosho, R. Khunsupat, A. K. Naskar, and A. J. Ragauskas, "Characterization and analysis of the molecular weight of lignin for biorefining studies," *Biofuels, Bioprod. Biorefining*, vol. 8, no. 6, pp. 836–856, 2014.
- [2.50] J. Su Kim, J. Ohk Kweon, and S. Tae Noh, "Online monitoring of reaction temperature during cationic ring opening polymerization of epichlorohydrin in presence of BF<sub>3</sub> and 1,4-butanediol," *J. Appl. Polym. Sci.*, vol. 131, no. 4, pp. 1–9, 2014.
- [2.51] D. Guanaes, E. Bittencourt, M. N. Eberlin, and A. A. Sabino, "Influence of polymerization conditions on the molecular weight and polydispersity of polyepichlorohydrin," *Eur. Polym. J.*, vol. 43, no. 5, pp. 2141–2148, 2007.
- [2.52] A. U. Francis, S. Venkatachalam, M. Kanakavel, P. V. Ravindran, and K. N. Ninan, "Structural characterization of hydroxyl terminated polyepichlorohydrin obtained using boron trifluoride etherate and stannic chloride as initiators," *Eur. Polym. J.*, vol. 39, no. 4, pp. 831–841, 2003.

- [2.53] A. T. Royappa, "On the copolymerization of epichlorohydrin and glycidol," *J. Appl. Polym. Sci.*, vol. 65, no. 10, pp. 1897–1904, 1997.
- [2.54] M. Wojtania, P. Kubisa, and S. Penczek, "Polymerization of propylene oxide by activated monomer mechanism. Suppression of macrocyclics formation," *Makromol. Chemie. Macromol. Symp.*, vol. 6, no. 1, pp. 201–206, 1986.
- [2.55] J. Sciamareli, S. N. Cassu, and K. Iha, "Water influence in poly(epichlorohydrin) synthesis: An intermediate to energetic propellants," *J. Aerosp. Technol. Manag.*, vol. 4, no. 1, pp. 41–44, 2012.
- [2.56] Y. M. Mohan and K. M. Raju, "Synthesis and Characterization of GAP-THF Copolymers," *Int. J. Polym. Mater.*, vol. 55, no. 3, pp. 203–217, 2006.
- [2.57] T. Hövetborn, M. Hölscher, H. Keul, and H. Höcker, "Poly(ethylene oxide-co-tetrahydrofuran) and poly(propylene oxide-co-tetrahydrofuran): Synthesis and thermal degradation," *Rev. Roum. Chim.*, vol. 51, no. 7–8, pp. 781–793, 2006.
- [2.58] H. Deng, Z. Shen, L. Li, H. Yin, and J. Chen, "Real-time monitoring of ring-opening polymerization of tetrahydrofuran via in situ Fourier Transform Infrared Spectroscopy," *J. Appl. Polym. Sci.*, vol. 131, no. 15, pp. 40503–40509, 2014.
- [2.59] S. L. Malhotra and L. P. Blanchard, "Cationic Copolymerization of Propylene Oxide with Tetrahydrofuran. X. Variation of Reactivity Ratios with Different Reaction Parameters," *J. Macromol. Sci. Part A - Chem.*, vol. 9, no. 8, pp. 1485–1521, 1975.
- [2.60] J. Sameni, S. Krigstin, D. Dos Santos Rosa, A. Leao, and M. Sain, "Thermal Characteristics of Lignin Residue from Industrial Processes," *BioResources*, vol. 9, no. 1, pp. 725–737, 2013.

- [2.61] R. J. Sammons, D. P. Harper, N. Labbé, J. J. Bozell, T. Elder, and T. G. Rials, "Characterization of organosolv lignins using thermal and FT-IR spectroscopic analysis," *BioResources*, vol. 8, no. 2, pp. 2752–2767, 2013.
- [2.62] O. Faix, "Classification of Lignins from Different Botanical Origins by FT-IR Spectroscopy," *Holzforschung*, vol. 45, no. s1, pp. 21–28, 1991.

# CHAPTER 3

## LIGNIN-BASED POLYOLS BY CATIONIC RING-OPENING POLYMERIZATION

---

Confidential chapter

# CHAPTER 4

## LIGNIN-BASED POLYOLS WITH CONTROLLED MICROSTRUCTURE

---





## 4.1 Background

Polymers based on cyclic ethers are a versatile and easily accessible class of polymers. These linear polymers are chemically inert and can be obtained in a wide range of molecular weights with low glass transition temperatures. These qualities make their employment very extensive in many applications. For example, poly(ethylene oxide) (PEO), a water-soluble and non-toxic polyol, is used in pharmaceutical applications and it is also widely used as an additive for food and cosmetic products. Poly(propylene oxide) (PPO), on the other hand, is relatively hydrophobic and is used in many polyurethane formulations. Poly(1,2-butylene oxide) (PBO) is a less widespread material but it has found commercial application as an oil-soluble lubricant.

PEO, PPO, and PBO are produced on a large industrial scale from their respective readily available oxirane monomers [4.1]. However, these commercial polyether diols cannot be obtained by cationic ring-opening polymerization (CROP) because of the uncontrollable and undesired formation of side products that are formed in the reaction, mainly cyclic oligomers compounds (COLs), especially when high molecular weight polyols are desired [4.2]. However, as it was explained in **Chapter 3**, in the presence of alcohols, the propagation mechanism changes from the active chain end (ACE) mechanism to an active monomer (AM) mechanism.

This change in the propagation mechanism leads to the obtention of linear polyether diols with a medium average molecular weight diminishing the undesired side reactions obtaining very interesting polyols. Several studies have been carried out reported in the literature illustrating the possibilities offered by the CROP route. Some of these studies are listed

in **Table 4.1**. As it is observed, mainly four different oxiranes are employed as monomers for the obtention of polyols by CROP: ethylene oxide (EO), propylene oxide (PO), epichlorohydrin (ECH), and glycidol (GLY).

The possibilities offered by EO, PO, and BO polymers have already been mentioned above. The interest in the polymerization of ECH and GLY is based on the remarkable properties of the respectively obtained polyols. Polyepichlorohydrin (PECH) polyols are important functional polyols with reactive pendant  $\text{CH}_2\text{-Cl}$  groups that can be used as intermediate by nucleophile substitution of these groups. PECH has been used in applications such as energetic polymeric binders [4.3], side-chain liquid crystalline polymers [4.4], and solid propellants [4.5, 4.6]. On the other hand, polyglycidol (PGL) can be found in many applications such as the formulation of drug carriers and in the preparation of the implant [4.7].

Concerning the solvents employed in CROP, the most used are dichloromethane (DMC), dichloroethane (DCE), and tetrahydrofuran (THF). The DMC and DCE are “inert” solvents in the CROP process. However, the THF, as explained in previous chapters, depending on the reaction conditions it can be incorporated as a co-monomer by cationic ring-opening copolymerization (CROCOP) with the oxirane into the final polyether.

**Table 4.1** Typical initiators, monomers (oxiranes), co-monomers, catalyst and solvents employed in the CROP and CROCOP reaction.

Reaction	Initiator	Monomer	Co-monomer	Catalyst	Solvent	Reference
CROP	Methanol	PO	-	HBF <sub>4</sub> ·Et <sub>2</sub> O	DCM	[4.8]
CROP	1,6-Hexanediol	PO	-	HBF <sub>4</sub> ·Et <sub>2</sub> O	DCM	[4.9]
CROP	1,6-Hexanediol	ECH	-	HBF <sub>4</sub> ·Et <sub>2</sub> O	DCM	[4.10]
CROP	Ethylene Glycol	ECH	-	BF <sub>3</sub> ·Et <sub>2</sub> O	-	[4.11]
CROP	Methanol	GLY	-	BF <sub>3</sub> ·Et <sub>2</sub> O CF <sub>3</sub> COOH	DCM	[4.12]
CROP	Ethylene Glycol Glycerol	ECH	-	BF <sub>3</sub> ·Et <sub>2</sub> O	DCM	[4.13]
CROP	1,4-Butanediol	ECH	-	BF <sub>3</sub> ·Et <sub>2</sub> O	DCM	[4.14]
CROCOP	1,2-Propanediol	PO	THF	BF <sub>3</sub> ·Et <sub>2</sub> O	DCE	[4.15]
CROCOP	Polyethylene glycol Polypropylene glycol	PO BO	THF	BF <sub>3</sub> ·Et <sub>2</sub> O	DCE	[4.16]
CROCOP	1,2,3-Propanetriol	PO	THF	BF <sub>3</sub> ·Et <sub>2</sub> O	DCE	[4.17]
CROCOP	Ethylene Glycol	SO PO	SO PO	BF <sub>3</sub> ·Et <sub>2</sub> O	DCE	[4.18]
CROCOP	Ethylene Glycol	ECH	THF DIOXANE	HBF <sub>4</sub> ·Et <sub>2</sub> O	-	[4.19]
CROCOP	Ethylene Glycol	EO	THF	HBF <sub>4</sub> ·Et <sub>2</sub> O	-	[4.20]
CROCOP	Ethylene Glycol	ECH	THF	BF <sub>3</sub> ·Et <sub>2</sub> O	-	[4.21]

- : Not employed.

Styrene oxide (SO), Tetrafluoroboric acid etherate (HBF<sub>4</sub>·Et<sub>2</sub>O), Boron trifluoride etherate (BF<sub>3</sub>·Et<sub>2</sub>O), Trifluoroacetic acid (CF<sub>3</sub>COOH).

In **Chapter 3**, it was already demonstrated the potential to obtain lignin-based polyols (LBPs) by CROCOP of BO and THF in the presence of lignin in the role of initiator through its hydroxyl groups (-OH). It was also demonstrated as well in previous chapters that the modification of reaction parameters such as the catalyst amount, the specific flow rate of the oxirane addition, the oxirane amount, the lignin concentration, and the reaction temperature allow obtaining LBPs with different microstructures. And consequently, LBPs with different physical, chemical, and thermal properties can be obtained by modifying the reaction parameters to adjust the properties of the LBPs for specific applications. Taking into account the acquired knowledge in the synthesis of LBPs varying the previously mentioned parameters, it looks plausible that the nature of the employed oxirane will lead to a new series of LBPs with controlled properties and consequently broaden the application of the LBPs obtained by this new CROP approach.

## 4.2 Objective

In this chapter, the main goal is to study the influence of the nature of the employed oxirane or the combination of two or more oxiranes in the synthesis of LBPs by CROP. This approach could lead to obtain LBPs with different microstructures and outstanding physical/chemical and thermal properties. The synthesis will be accompanied by a detailed study of the properties of LBPs through a series of characterization techniques to establish a relation between the nature of the oxiranes and the final LBP properties.

## 4.3 Methodology

### 4.3.1 Materials

Propylene oxide (PO, 99.5%), butylene oxide (BO, 99%), epichlorohydrin (ECH, 99%), glycidol (GLY, 96%), 1,2-Epoxy-5-hexene (EE, 98%), 1,2-Epoxyhexane (HO, 97%), boron trifluoride etherate ( $\text{BF}_3 \cdot \text{Et}_2\text{O}$ , 48%), were purchased from Acros Organics. Tetrahydrofuran (THF, 99%) was purchased from Scharlau. Cyclohexene oxide (CO, 98+%), 1,2-Epoxyoctane (OO, 97%), and Styrene oxide (SO, 98+%) were purchased from Alfa Aesar. N,N-Dimethylethylamine (DMEA, 99%) was purchased from Sigma-Aldrich. All materials were used directly without further purification unless otherwise noted.

The lignin employed in this chapter is the lignin selected in the previous **Chapter 2** (Mix-OL). The complete characterization of the Mix-OL is also detailed in this chapter.

### 4.3.2 Synthesis of the LBPs

The reactions were carried out employing the set-up illustrated in the Methodology section of **Chapter 3** (**Figure 3.1**). The system consisted of a jacketed glass reactor of 100 mL connected to a thermostatic bath, a mechanical stirrer, and a syringe pump to add the selected monomer (oxirane) continuously through the syringe under atmospheric pressure. The desired concentration of dried Mix-OL in THF ( $[\text{L}]$ , g/L) was placed in the reactor. The catalyst was added at a concentration given by the molar ratio between the catalyst and the lignin hydroxyl groups (MR  $\text{BF}_3/\text{OH-L}$ ) under agitation. Subsequently, the target amount of the selected monomer in relation to the moles of lignin hydroxyl groups (MR  $\text{MON}/\text{OH-L}$ ) was added continuously using a syringe pump. For the

polymerizations of two or more monomers in the synthesis of LBPs the addition was done consecutively. The specific flow rate ( $Q_s$ ) was adjusted as a function of the volume of the monomer to be added in relation to the lignin hydroxyl groups moles and time ( $\text{mL}/\text{NOH}\cdot\text{L}\cdot\text{h}$ ). Once the addition was completed, the reaction was kept for 1 h under agitation to ensure the total monomer conversion. The reaction was then quenched with an excess of DMEA in a molar ratio of 1.66 with the catalyst (MR DMEA/ $\text{BF}_3$ ), and the solvent and the excess of DMEA were removed by a rotary evaporator until a constant weight was achieved. The remaining product is the desired LBP.

#### 4.3.3 Characterization of LBPs

Different and complementary characterization techniques were used to study the prepared LBPs, as described in **Appendix I**. The composition of the LBPs was given by the percentage of lignin mass content (L wt. %), monomer mass content (MON wt. %), and THF mass content (THF wt. %). The rate of polymerized THF with respect to the monomer was expressed by the molar ratio of both compounds (MR MON/THF). The average composition of the chains formed in the polymerization with respect to the -OH groups of the lignin was given in molar ratio (MR OH:MON:THF). The structural analysis of the polyols was performed by Attenuated Total Reflection Fourier Transform Infrared Spectroscopy (ATR-FTIR). The Molecular weight distributions (MWD), the weight average molecular weights ( $\overline{M}_w$ ), and the polydispersity indexes (PDI) were determined by Size Exclusion Chromatography (SEC). The hydroxyl number (OH#) of the LBPs was determined by a potentiometric determination, according to ASTM E-1899-02. The thermal properties of the LBPs were analyzed by Differential Scanning Calorimetry analysis (DSC) and Thermo-Gravimetric Analysis (TGA).

## 4.4 Results and discussion

### 4.4.1 Influence of the nature of the oxirane

To gain consistency in this study and to be able to compare the different obtained LBPs, all the preparation was performed at the same reaction conditions keeping the lignin source, lignin concentration, catalyst type, monomer amount, specific flow rate, and solvent constant. The reaction conditions are summarized in **Table 4.2**.

**Table 4.2** Reagents, catalyst, and reaction parameters employed in the synthesis of LBPs with different monomers.

<b>Reagents</b>	
Lignin	Mix-OL
Monomer	PO, BO, HO, OO, CO, SO, EE, ECH, GLY
Solvent	THF
<b>Catalyst</b>	
Catalyst	BF <sub>3</sub> ·Et <sub>2</sub> O
<b>Reaction parameters</b>	
Lignin concentration, [L] (g/L)	110
Catalyst concentration (MR BF <sub>3</sub> /OH-L)	0.125
Monomer added (MR MON/OH-L)	2
Temperature (°C)	25
Specific flow rate (mL/n <sub>OH</sub> -L·h)	36.5

The LBPs were prepared according to the previously established procedure for the polymerization by CROP in the presence of the Mix-OL in **Chapter 3**. **Figure 4.1** illustrates the selected monomers employed as oxiranes in this study to investigate the influence of the final LBP microstructure of the length of the alkyl pendant chain of the employed monomer, PO (1 carbon atom), BO (2 carbon atoms), HO (4 carbon atoms),



and OO (6 carbon atoms). Furthermore, the influence of the substituent on PO (CH<sub>3</sub> carbon) was also studied employing oxiranes with allylic moiety (EE), hydroxyl group (GLY), and chlorine group (ECH). In addition, the influence of one cycloaliphatic monomer (CO) and one monomer with an aromatic substituent (SO) were also tested.

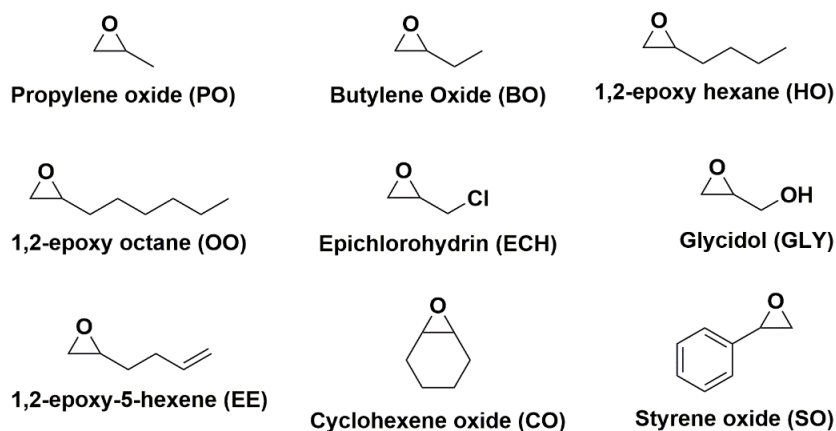


**Figure 4.1** Monomers employed to obtain LBPs with different microstructures.

The influence of the oxirane nature employed as a monomer in the LBPs microstructure is evidenced in **Table 4.3**. In the first four LBPs (LBP-PO, LBP-BO, LBP-HO, LBP-OO), it can be observed how the length of the alkane chain in the oxirane influences the properties of the prepared LBPs. As shown, the lignin content in the LBPs decreases as the length of the alkyl chain in the oxirane increases. As expected, the MON wt. % content increases when an oxirane with higher molecular weight (longer alkyl chain) is employed, and the amount of THF incorporated slightly decreases. In conclusion, the molar ratio between the THF and the oxiranes (MR THF/MON) and regarding with Mix-OL hydroxyl groups (MR OH:MON:THF) do not change significantly independently of the alkyl chain length in the employed oxirane. Concerning the hydroxyl number, this value decreases when in the final LBP the wt. % of lignin content is lower.

**Table 4.3** LBPs properties obtained with different monomers.

<b>LBP composition</b>		<b>LBP-PO</b>	<b>LBP-BO</b>	<b>LBP-HO</b>	<b>LBP-OO</b>	<b>LBP-CO</b>	<b>LBP-SO</b>	<b>LBP-GLY</b>	<b>LBP-ECH</b>	<b>LBP-EE</b>
L (wt. %)		16.5	16.0	14.5	14.4	16.0	47.4	20.3	12.0	11.2
MON (wt. %)		8.7	10.4	13.1	16.5	14.0	51.3	13.5	10.0	10.0
THF (wt. %)		74.8	73.6	72.3	69.1	70.0	1.3	66.2	78.0	78.8
MR THF/MON		7.0	7.1	7.6	7.5	6.8	0.0	5.0	10.0	10.8
MR OH:MON:THF		1:2:14.0	1:2:14.2	1:2:15.2	1:2:15.0	1:2:13.6	1:2:0.0	1:2:10.0	1:2:20.0	1:2:21.6
OH# (mg KOH/g)		77	79	58	57	61	146	217	63	50
<b>LBP molecular weight analysis</b>										
$\overline{M}_w$ (g/mol)		15090	14535	25747	26007	21773	3652	9373	35594	52900
PDI		4.00	3.72	5.52	5.39	4.99	1.80	3.38	7.27	11.78
<b>LBP thermal analysis</b>										
$T_c$ (°C)		-25.79	-24.91	-32.17	-31.88	ND	ND	ND	-28.24	-27.62
$\Delta H_c$ (J/g)		26.49	28.60	28.71	25.9	ND	ND	ND	29.03	27.72
$T_m$ (°C)		9.96	12.08	11.60	11.20	9.01 <sup>a</sup>	ND	7.68 <sup>a</sup>	14.11	14.37
$\Delta H_m$ (J/g)		26.31	27.04	32.09	29.45	21.61 <sup>a</sup>	ND	11.44 <sup>a</sup>	31.72	28.68

ND: Not detected.

<sup>a</sup> Exothermic peak observed just before the melting peak.Reaction conditions: [L] = 110 g/L,  $Q_2$  = 36.5 mL/n<sub>OH-L</sub>, MR BF<sub>3</sub>/OH-L = 0.125, T = 25 °C.

In the LBP-CO, although the CO has a very different structure in comparison with previous ones, the composition obtained in terms of weight of each reactive was very similar. It can be concluded that the ability of the ring strain of the CO did not affect to the copolymerization mechanism.

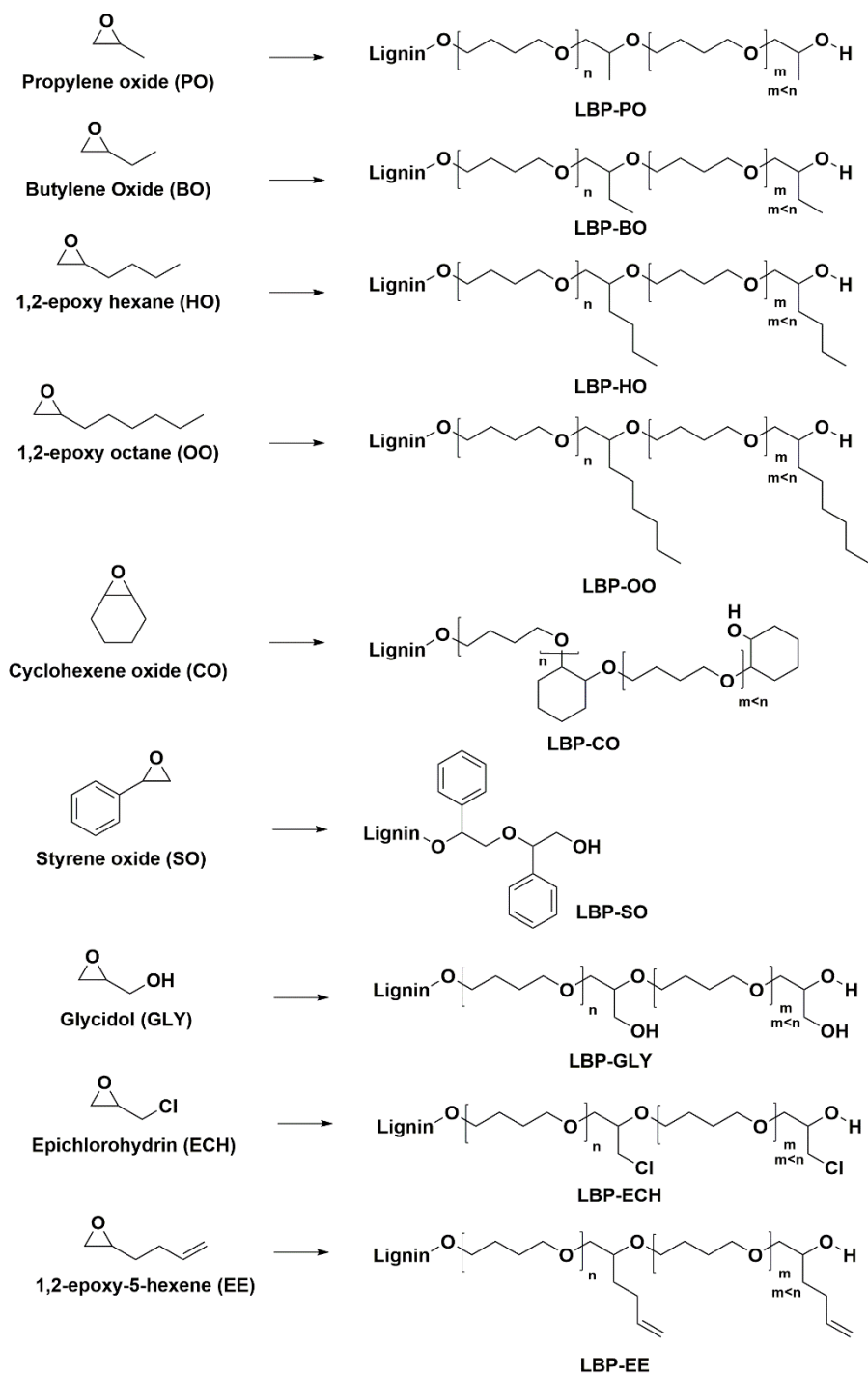
The composition of the LBPs varied significantly when oxiranes with different functional groups in the pendant chain were introduced. Although SO also has a cyclic structure like CO, very different results were obtained in the LBP-SO composition. As detailed in **Table 4.3**, the LBP-SO composition is formed only by lignin and SO. These results are consistent with those published in the literature [4.18]. In fact, THF in the presence of SO and alcohol groups does not undergo in a copolymerization, and the only homopropagation of SO takes place.

Less THF incorporation was also observed in the case of LBP-GLY. A plausible explanation of this phenomenon is proposed based on the CROP of GLY in presence of diols previously discussed by other authors [4.12, 4.22]. The -OH groups of the alcohols are able to open the GLY to yield a polyol by AM mechanism. In each propagation step, two final -OH groups are available to attack another activated GLY molecule. In the presence of THF, the activated GLY is attacked by a THF molecule, starting its homopropagation, as proposed in **Chapter 3**. However, the homopropagation of the THF is lower than with other monomers due to an increase in -OH concentration provided by the glycidol. Consequently, the competition between the -OH groups and the THF homopropagation is tough, and therefore less THF is being polymerized. The less THF incorporation along with the introduction of more -OH units due to the GLY polymerization, increased the OH# (217 mg KOH/g) in values close to the OH# (243 mg KOH/g) of the Mix-OL although the LBP-GLY had a 20.3 wt. % content in lignin.

The LBP-ECH and LBP-EE are very similar polyols in terms of the L wt. %, MON wt. %, and THF wt. % content. The chloride pendant group of the ECH and the unsaturated bond of the EE allowed a longer THF homopropagation. Barzykina et al. reported the THF polymerization catalyzed by  $\text{BF}_3$ -ECH. They found that not more than 1 ECH monomer is incorporated in each polymer molecule and in comparison with the  $\text{BF}_3$ -PO catalytic system, the rate of termination reactions is reduced. This can explain why LBP-ECH has higher THF content [4.23]. The same explanation can be applied for the LBP-EE.

All the obtained LBPs, except LBP-SO, which is solid at room temperature, are highly viscous LBPs. The OH# value of the LBPs was proportional to the lignin content in the final LBP except for the LBP-GLY due to the above-mentioned explanation in the LBP-GLY composition. In accordance with the mechanism proposed in **Chapter 3**, and the LBPs composition detailed in **Table 4.3**, the proposed LBPs structures employing the selected monomers are shown in **Scheme 4.1**.

In **Figure 4.2** all the MWD of the LBPs can be observed. All LBPs have a similar MWD apart from the LBP-SO due to the no incorporation of THF. Except for the LBP-SO, the other LBPs were formed by the main peak of higher molecular weight than the starting lignin with a series of small peaks of lower molecular weight related to the formation of cyclic oligomers (COLs) [4.24].



**Scheme 4.1** Expected LBPs obtained with different monomers.

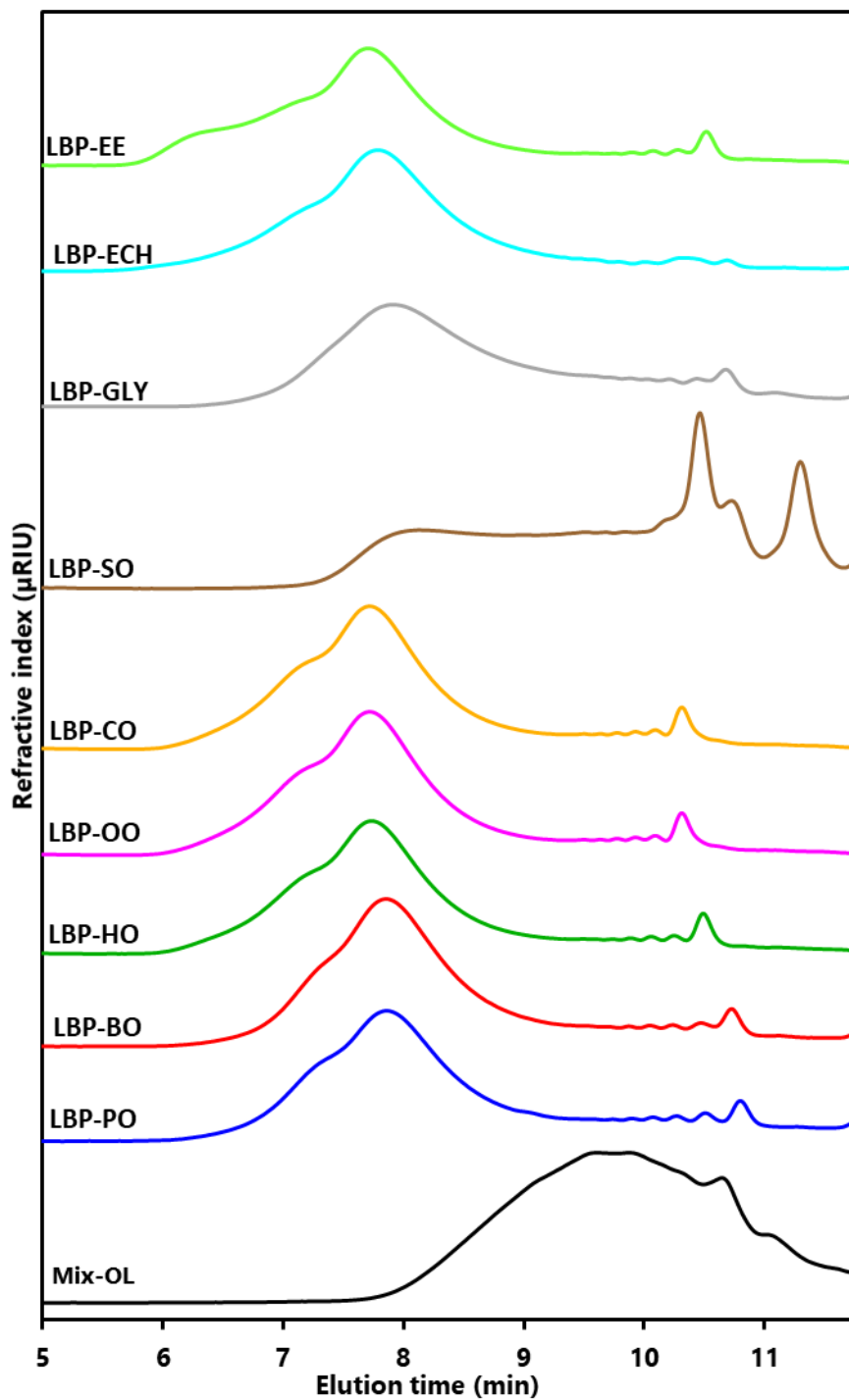


Figure 4.2 Comparative MWD of the LBPs obtained with different monomers.

As expected, all LBPs increased their  $\overline{M}_w$  in comparison with the Mix-OL lignin (**Table 4.3**). The increase in  $\overline{M}_w$  seems to be always associated with a greater PDI and a lower lignin wt. % content. Consequently, the two LBPs with the highest  $\overline{M}_w$  (LBP-ECH and LBP-EE), also have the highest PDI. However, LBP-ECH shows a lower formation of COLs due to the lower tendency of the ECH to form COLs in the copolymerization reaction with THF [4.25]. LBP-GLY and LBP-SO have smaller  $\overline{M}_w$  than the other LBPs. LBP-SO presents some very intense peaks at long elution times. Initially, it can be assumed that they are COLs formed in the reaction. However, without making more precise characterizations, it is not possible to determine their structure. On the other hand, the low  $\overline{M}_w$  of the LBP-GLY was associated with the less incorporation of THF attributed to the increase of -OH groups in the reaction medium as it was previously discussed.

It is worth mentioning that the peaks attributed to COLs shift with the increase of the length of the alkyl pendant chain of the oxirane. This phenomenon can be observed at long elution times, where the peaks associated with the COLs shift to the left in the LBP-PO, LBP-BO, LBP-HO, and LBP-OO in **Figure 4.2**. This behavior is explained on the basis of the typical composition of the COLs formed in the polymerization by CROCOP in the presence of -OH groups. In the literature, it is detailed that the composition of most of the formed COLs have a higher monomer content than THF content [4.26]. Therefore, the COLs molecular weight increases with the increase of the oxirane molecular weight employed.

**Figure 4.3** shows the ATR-FTIR of all LBPs and the starting Mix-OL lignin. The most relevant bands of the Mix-OL are detailed in **Chapter 2**. Concerning the obtained LBPs all share the same pattern.

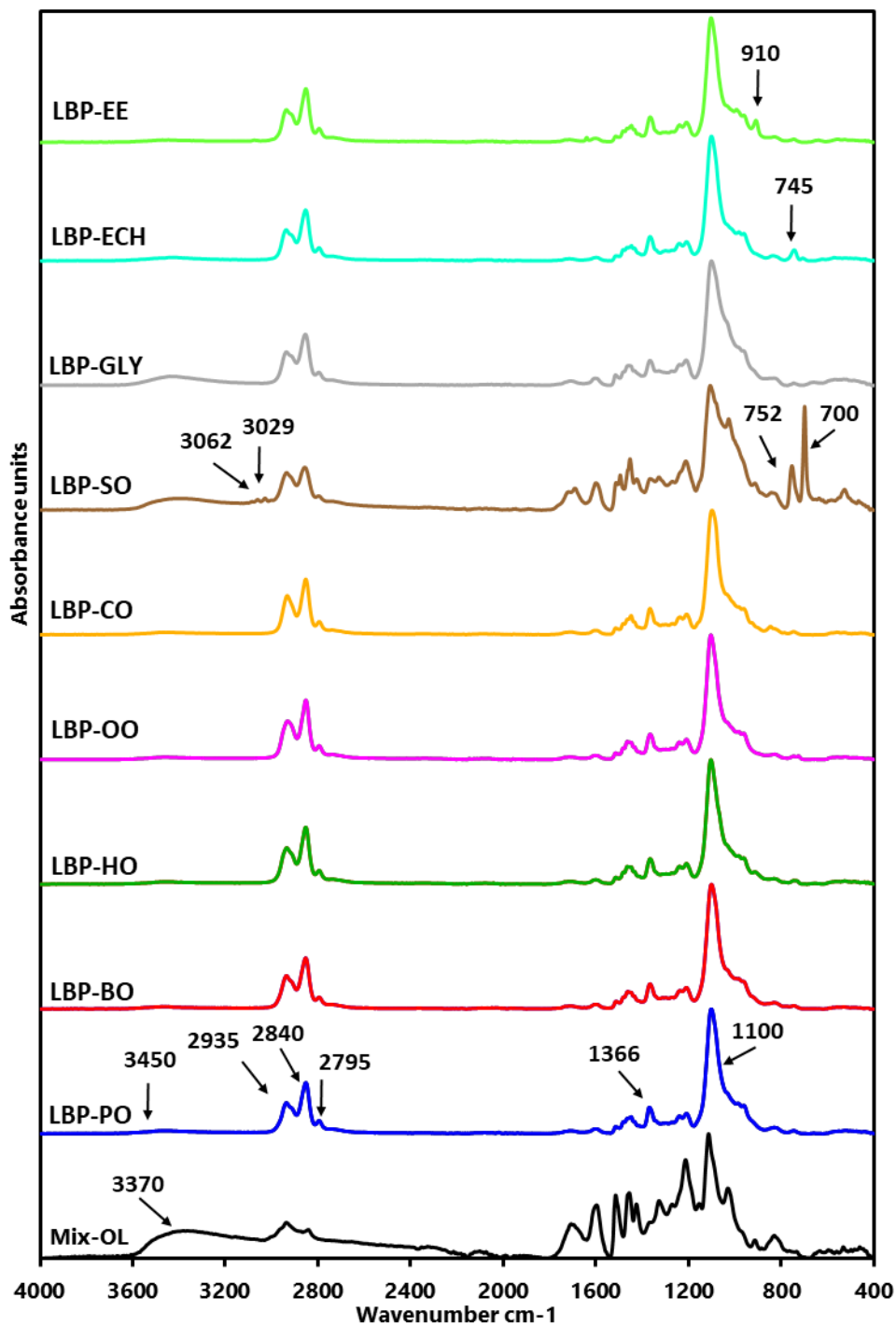


Figure 4.3 Comparative ATR-FTIR spectra of the LBPs obtained with different monomers.



The main changes observed by ATR-FTIR are:

1. The change in the intensity of the -OH stretching band is very significant. This band was converted from a wide band with medium intensity ( $3370\text{ cm}^{-1}$ ) into a smaller and narrower one ( $3450\text{ cm}^{-1}$ ). The decrease in intensity of this band is associated with a lower lignin concentration in the final LBP.
2. The bands at  $2935\text{ cm}^{-1}$ ,  $2840\text{ cm}^{-1}$ , and  $1100\text{ cm}^{-1}$  increased their signal in the obtained LBP. The first two bands are associated with the stretch vibration of  $\text{CH}_3$  and  $\text{CH}_2$  groups, while the last band is associated with the stretching of new C-O-C groups.
3. The two new bands appeared at  $2795\text{ cm}^{-1}$  and  $1366\text{ cm}^{-1}$  are associated with CH and  $\text{CH}_3$  aliphatic band stretching vibrations.
4. The rest of the characteristic bands are associated with the lignin fingerprint in the range from  $1700\text{ cm}^{-1}$  to  $800\text{ cm}^{-1}$ . They lost intensity proportionally, concluding that lignin did not undergo structural changes in the reaction process.

Based on these conclusions, some trends and new bands appeared in some LBPs. The LBP-PO, LBP-BO, LBP-HO, and LBP-OO bands associate with the C-H bands increases in intensity in accordance with the chain length of the oxirane substitute chain. The incorporation of more  $\text{CH}_2$  units in the LBP-CO led to very similar ATR-FTIR spectra to the LBPs discussed previously.

In the LBP-SO, the bands associated with the lignin footprint are more intense than in the other LBPs due to the higher lignin content. In addition, four new bands appear in the ATR-FTIR spectra. Two small bands at  $3062\text{ cm}^{-1}$  and  $3029\text{ cm}^{-1}$  and two of higher intensity at  $752\text{ cm}^{-1}$

and  $700\text{ cm}^{-1}$ . All of them are characteristic bands of the SO, so they are discarded as bands resulting from lignin degradation.

In the LBP-GLY, the stretching band related to the -OH groups is more intense and broader. This phenomenon can be explained due to the incorporation of less THF along the addition of more -OH groups due to the GLY nature.

Both LBP-ECH and LBP-EE present new bands in their respective ATR-FTIR spectra. The LBP-ECH has the same structure as the previous LBPs but with the characteristic stretching band attributed to the C-Cl bond at  $744\text{ cm}^{-1}$ . On the other hand, the LBP-EE has a similar spectra except for the apparition of a new band at  $910\text{ cm}^{-1}$ . This band was associated with the =C-H bending present in the oxirane substitution chain.

The thermal behavior of the LBPs is shown in **Table 4.3**. The nature of the monomer used has a significant influence on the final thermodynamic properties of the LBPs. The longer the chain length of the substituent in the oxirane (LBP-PO < LBP-BO < LBP-HO < LBP-OO) the lower the crystallization temperature and the higher the melting temperature. The enthalpies associated with these two processes also decreased as the chain length increased. It should be noted that there are no observed significant differences between the thermal behavior of LBP-HO and LBP-OO despite of the last one monomer has a longer substituent chain.

As discussed previously, the LBP-CO composition does not differ from the LBPs obtained with different alkyl chain length substituents. However, its thermal behavior was totally different. LBP-CO does not show any enthalpy peak on the cooling ramp. However, it shows an Exothermic peak on the heating ramp just before the melting point. This observation can be attributed to some partial restructuration of the LBP before it

starts melting. The LBP-GLY shows the same behavior, but with less associated enthalpy, maybe related with the less THF incorporation into the LBP. This behavior may explain why the LBP-SO did not show any thermal change.

LBP-ECH and LBP-EE have shown similar LBP composition and MWD. However, these two LBPs have different thermal behavior. The LBP-ECH has a crystallization peak 10 °C lower than the LBP-EE. On the other hand, both LBPs melt at practically the same temperature.

**Figure 4.4** illustrates the influence of the monomer employed in the thermal degradation of the LBP. All LBPs have changed their thermal degradation profile compared to Mix-OL, and all of them have two main weight loss peaks. Except for the LBP-GLY and LBP-SO, the LBPs show a first weight loss at around 360 °C (circa 80 wt. % of the total weight of the LBP) and another at 505 °C. The first one is attributed to the loss of weight from the linear polyether chains formed in the LBPs, and the second one is attributed to the weight loss from the lignin core present in the LBP.

The LBP-GLY has both peaks slightly shifted to the right, which means a bit more thermal stable. This behavior was related to lower incorporation of THF in the final LBP and a more branched and rigid structure due to the increase in -OH groups and their possible interactions between them, increasing the thermal stability of the LBP-GLY.

The LBP-SO has a unique thermal behavior. The first peak of degradation takes place at 283 °C. At this temperature, the other LBPs are still thermally stable. The second degradation peak occurs at 550 °C, a slightly higher temperature than the other LBPs. The percentage of weight loss

in the LBP-SO in each temperature range corresponds to the percentage composition of lignin and SO. Therefore, it is believed that the first degradation peak corresponds to the SO polymerization and the second one to the lignin core of the LBP-SO.

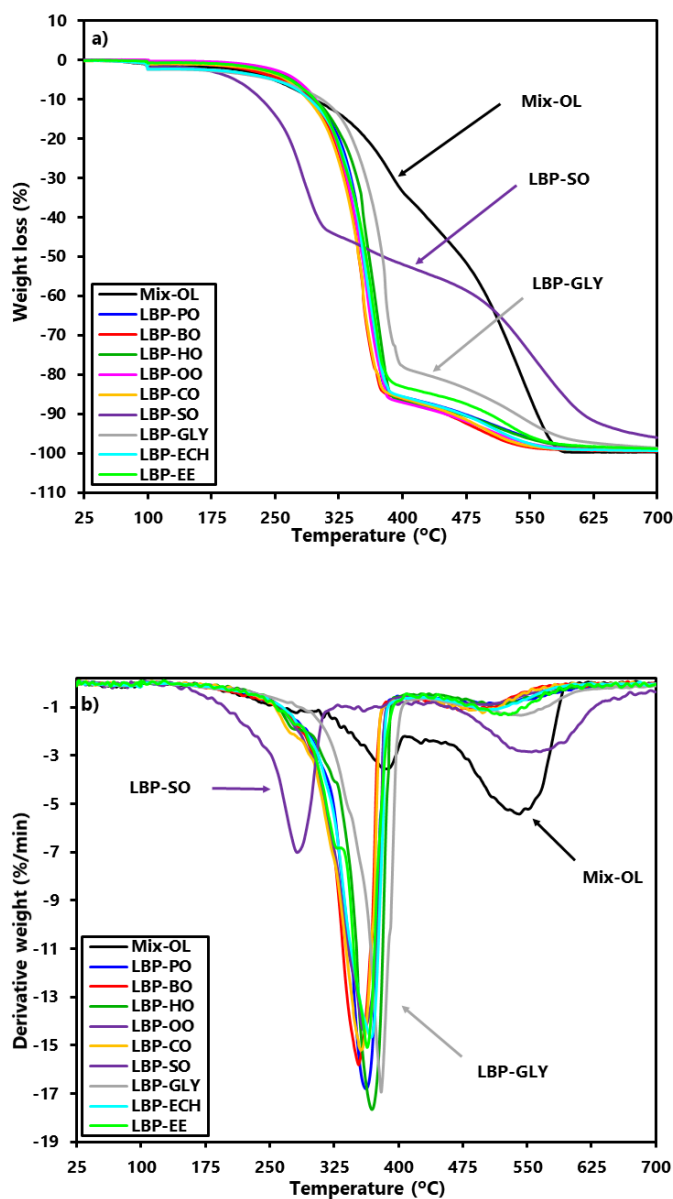


**Figure 4.4** Comparative thermal profile of the LBPs obtained at different monomers: a) TG, b) dTG.

#### 4.4.2 Hyperbranched LBPs

When polyfunctional-hydroxyl initiator or hydroxyl content monomers are employed, the polymerization will lead into branched or star-like polyols [4.27]. Up to now, linear LBPs were obtained using different monomers (**Figure 4.5-a**). To obtain branched LBPs in this section, it is proposed the employment of GLY as an additional -OH group source to get branched polymers with primary and secondary alcohol groups (**Figure 4.5-b**).

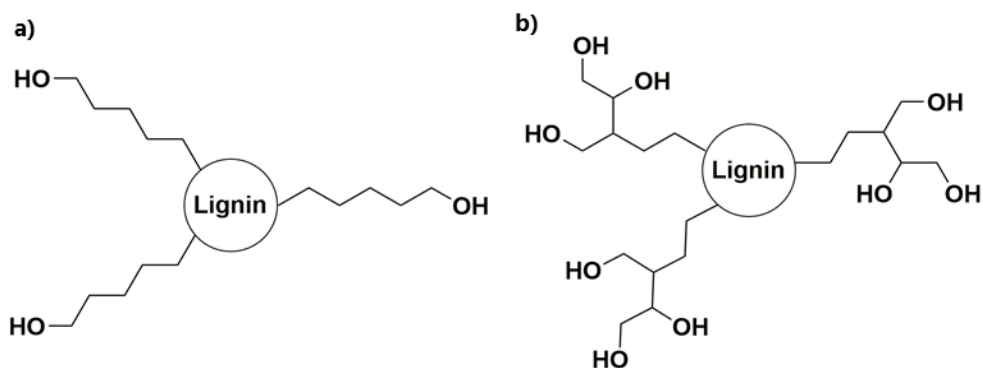


**Figure 4.5** Schematic representation of different LBP types of polymerization: a) linear, b) branching.

Although GLY can be employed to obtain hyperbranched polyols, the GLY incorporation into the chain should be high enough to promote the branching. With less than 2 GLY monomers in a polymerized chain, the branching is not formed, and linear chains are still formed. To study the degree of branching, three LBPs were synthesized using different amounts of GLY under the same reaction conditions:  $[L] = 110 \text{ g/L}$ ,  $Q_s = 73.0 \text{ mL/nOH-L h}$ ,  $MR \text{ BF}_3/\text{OH-L} = 0.125$ ,  $T = 25 \text{ }^\circ\text{C}$ . The results were detailed in **Table 4.4**.

**Table 4.4** LBPs properties obtained with different MR GLY/OH-L.

	<b>LBP-2GLY</b>	<b>LBP-3GLY</b>	<b>LBP-5GLY</b>
	2 MR GLY/OH-L	3 MR GLY/OH-L	5 MR GLY/OH-L
<b>LBP composition</b>			
L (wt. %)	30.1	22.0	14.6
MON (wt. %)	20.5	22.4	25.0
THF (wt. %)	49.4	55.6	60.4
MR THF/GLY	2.5	2.6	2.5
MR OH:GLY:THF	1:2:5.0	1:3:7.8	1:5:12.5
OH# (mg KOH/g)	253	209	157
<b>LBP molecular weight analysis</b>			
$\overline{M}_w$ (g/mol)	2730	8550	11575
PDI	1.45	4.41	4.08
<b>LBP thermal analysis</b>			
$T_c$ (°C)	ND	ND	ND
$\Delta H_c$ (J/g)	ND	ND	ND
$T_m$ (°C)	6.44 <sup>a</sup>	8.85 <sup>a</sup>	ND
$\Delta H_m$ (J/g)	4.84 <sup>a</sup>	4.26 <sup>a</sup>	ND

ND: Not detected.

<sup>a</sup> Exothermic peak observed just before the melting peak.

Reaction conditions: [L] = 110 g/L,  $Q_s$  = 73.0 mL/n<sub>OH-L</sub>·h, MR BF<sub>3</sub>/OH-L, = 0.125, T = 25 °C.

As the MR GLY/OH-L increases, the amount of lignin in the final LBP decreases. In contrast, the amount of GLY and THF increases. It should be noted that the THF homopolymerization regarding to the GLY added (MR THF/GLY) remained constant at 2.5. The regular incorporation of THF along with the decrease in the percentage of lignin content, caused the decrease of the OH# value with the addition of more GLY.

**Figure 4.6-a** provides the ATR-FTIR spectra of the three LBPs. The band at 3450 cm<sup>-1</sup> corresponding to the stretching of the hydroxyl groups decreases with the increase of MR GLY/OH-L due to the incorporation of

THF. Along with this decrease in signal, the bands associated with the lignin fingerprint from  $1700\text{ cm}^{-1}$  to  $800\text{ cm}^{-1}$  also decreases.

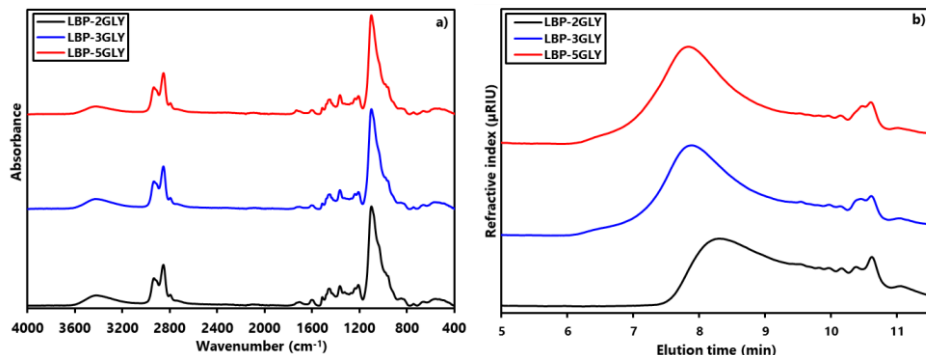


**Figure 4.6** a) Comparative ATR-FTIR spectra of the LBPs obtained with different MR GLY/OH-L. b) Comparative MWD of the LBPs obtained with different MR GLY/OH-L.

This trend is also observed in the MWD profile in **Figure 4.6-b**. When MR GLY/OH-L is increased from 2 to 3 there is a significant increase in the  $\overline{M}_w$  (**Table 4.4**). However, from 3 to 5 MR GLY/OH-L this change is not so relevant. This can be explained by the possible ramification that the LBP can undergo when increasing the amount of the added GLY. Previously it was exposed that it was necessary at least three GLY groups per chain to obtain a branched chain. This affirmation can be justified by observing the PDI obtained from the LBPs. In **Table 4.4** shows how the PDI increased significantly from the LBP-2GLY to the LBP-3GLY. It may be explained due to the formation of the first branched chains in the LBP.

**Figure 4.7-a** illustrates how the first peak weight loss associated with the grafted polyether chains increases with the addition of greater amounts of GLY additions. There is an important difference in thermal behavior between the first two GLY additions. However, with the increased addition of MR GLY/OH-L from 3 to 5, the thermal stability of the LBPs was not modified as it is observed in **Figure 4.7-b**.

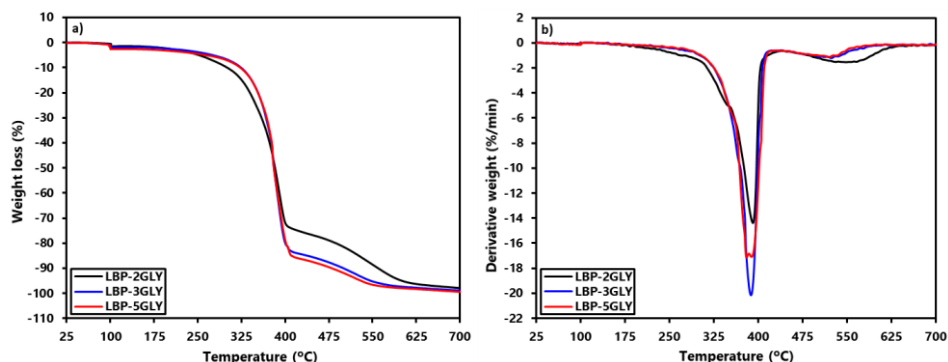


**Figure 4.7** Comparative thermal profile of the LBPs obtained with different MR GLY/OH-L: a) TG, b) dTG.

### 4.4.3 Terpolymers and tetrapolymers

- Terpolymers

The objective of the terpolymerization is to introduce at least three different monomers in the polymerization step to obtain terpolymers. Only a few examples of terpolymerization are described in the literature by CROP [4.18]. However, it is interesting to modify the physical/chemical and thermodynamic properties of final LBPs by introducing a mix of functional monomers into the LBP by CROP.

To explore the feasibility of the proposed CROP reaction to obtain LBP terpolymers (TER-LBPs), two LBPs were synthesized using the oxiranes BO and GLY as monomers in the presence of Mix-OL and THF being the THF the third monomer since it is incorporated into the LBP by copolymerization.

To obtain the desired TER-LBPs, two approaches were employed. The first consisted of the initial addition of the BO and then the GLY denoting the obtained LBP as LBP-BO-GLY. The second approach consisted of adding initially the GLY and then the BO denoting the obtained LBP as LBP-GLY-BO. Both TER-LBPs were characterized and compared with



the LBPs obtained in the same conditions employing only BO (LBP-2BO) or GLY (LBP-2GLY) as monomers. All LBPs were obtained under the same reaction conditions:  $[L] = 110 \text{ g/L}$ ,  $Q_s = 73.0 \text{ mL/n}_{\text{OH-L}} \text{ h}$ ,  $\text{MR BF}_3/\text{OH-L} = 0.125$ ,  $T = 25 \text{ }^\circ\text{C}$ . The compositions of the LBPs are detailed in **Table 4.5** and compared with their LBP copolymers counterparts.

**Table 4.5** CO-LBPs and TER-LBPs properties obtained with different monomer addition.

	<b>LBP-2BO</b>	<b>LBP-BO-GLY</b>	<b>LBP-GLY-BO</b>	<b>LBP-2GLY</b>
<b><i>LBP composition</i></b>				
L (wt. %)	16.6	21.7	27.5	30.1
MON (wt. %)	10.8	14.4	18.3	20.5
THF (wt. %)	72.6	63.9	54.2	49.4
MR THF/MON	6.7	4.5	3.0	2.5
MR OH:MON:THF	1:2:13.4	1:2:9.0	1:2:6.0	1:2:5.0
OH# (mg KOH/g)	76	161	129	253
<b><i>LBP molecular weight analysis</i></b>				
$\overline{M}_w$ (g/mol)	12534	4401	7614	2730
PDI	3.46	1.82	2.78	1.45
<b><i>LBP thermal analysis</i></b>				
$T_c$ ( $^\circ\text{C}$ )	-20.28	-20.60	ND	ND
$\Delta H_c$ (J/g)	35.12	-17.79	ND	ND
$T_m$ ( $^\circ\text{C}$ )	9.68	10.67	6.11 <sup>a</sup>	6.44 <sup>a</sup>
$\Delta H_m$ (J/g)	36.18	26.21	7.12 <sup>a</sup>	4.84 <sup>a</sup>

ND: Not detected.

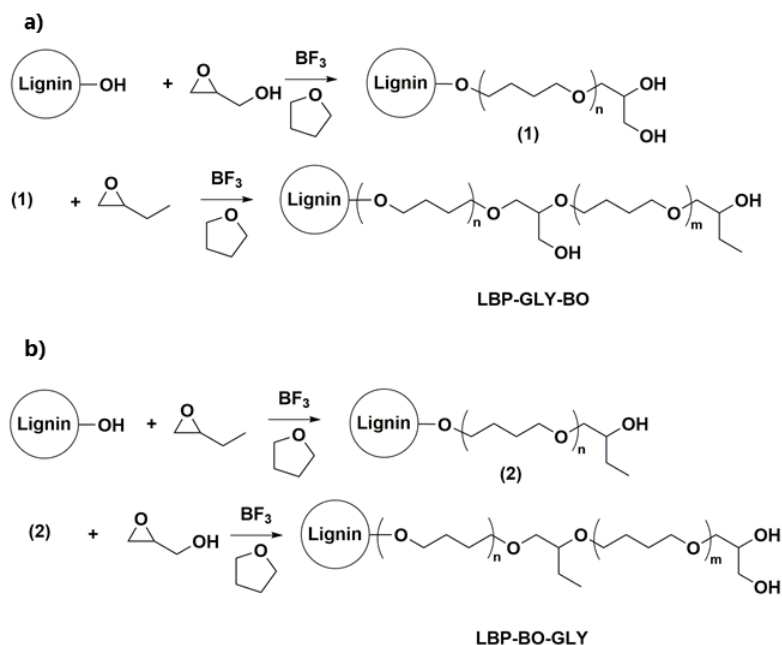
<sup>a</sup> Exothermic peak observed just before the melting peak.

Reaction conditions:  $[L] = 110 \text{ g/L}$ ,  $Q_s = 73.0 \text{ mL/n}_{\text{OH-L}} \text{ h}$ ,  $\text{MR BF}_3/\text{OH-L} = 0.125$ ,  $T = 25 \text{ }^\circ\text{C}$ .

Both TER-LBPs have a lignin wt. % content between the LBP-2BO and LBP-2GLY. In both TER-LBPs, the presence of extra -OH groups due to the addition of GLY increased the competition between the THF homopropagation and the incorporation in the growing chains.

Consequently, both TER-LBPs have higher lignin wt. % content, MR OH:MON:THF, and OH# values than LBP-2BO and lower than LBP-2GLY.

Depending on the oxirane order addition (BO and GLY), two different microstructures are obtained in the TER-LBPs (**Scheme 4.2-a**). If GLY is added first, two hydroxyl groups are formed, both capable to start the propagation of the polymer chain. Therefore, an -OH group will be available in the middle of the formed chain and a final one will be formed due to the opening of the BO (LBP-GLY-BO). However, if BO is added first, a polyether chain grafted to the mix-OL core with two terminal -OH groups is expected (**Scheme 4.2-b**).



**Scheme 4.2** Different TER-LBPs structures according to the sequence of monomer addition.

**Figure 4.8-a** shows the MWD of the TER-LBPs. Both had a lower  $\overline{M}_w$  than LBP-2BO and a higher than LBP-2GLY (**Table 4.5**). The LBP-BO-GLY had a lower  $\overline{M}_w$  than LBP-GLY-BO.

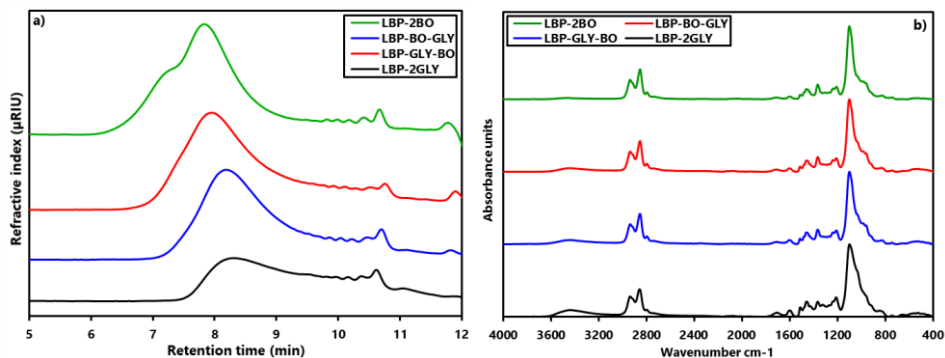


**Figure 4.8** a) Comparative MWD of the CO-LBPs and TER-LBPs. b) Comparative ATR-FTIR spectra of the CO-LBPs and TER-LBPs.

The ATR-FTIR spectra of both TER-LBPs are similar than other LBPs obtained until now (**Figure 4.8-b**). In accordance with their OH# values, the -OH stretching band at 3450 cm<sup>-1</sup> is less intense in LBP-GLY-BO than in the LBP-BO-GLY. On the other hand, the intensity of the stretching of the bands at 2935 cm<sup>-1</sup> and 2840 cm<sup>-1</sup> corresponding to the C-H stretching are lower than the LBP-2BO in both cases.

An interesting aspect of TER-LBPs is their different thermal behavior (**Table 4.5**). The order in which the monomers are added has a significant influence on the crystallization and melting peaks. LBP-BO-GLY with the first addition of BO has higher crystallization and melting peaks than LBP-GLY-BO (**Table 4.5**). Furthermore, these temperatures are very similar to LBP-2BO but with lower enthalpy. Consequently, both TER-LBPs were much more similar to LBP-2BO than to LBP-2GLY, which has not enthalpy changes.

As in the DSC analysis, different behaviors were also observed in the TGA analysis. Taking LBP-2BO and LBP-2GLY as references, in **Figure 4.9-a**, LBP-BO-GLY terpolymer exhibited a behavior closer to LBP-2BO, while LBP-GLY-BO terpolymer was more similar to LBP-2GLY thermal decomposition. This behavior is clearly noted in **Figure 4.9-b**. The LBP-

2BO and LBP-2GLY have a derivative weight loss more similar to the LBP-2BO than LBP-2GLY.

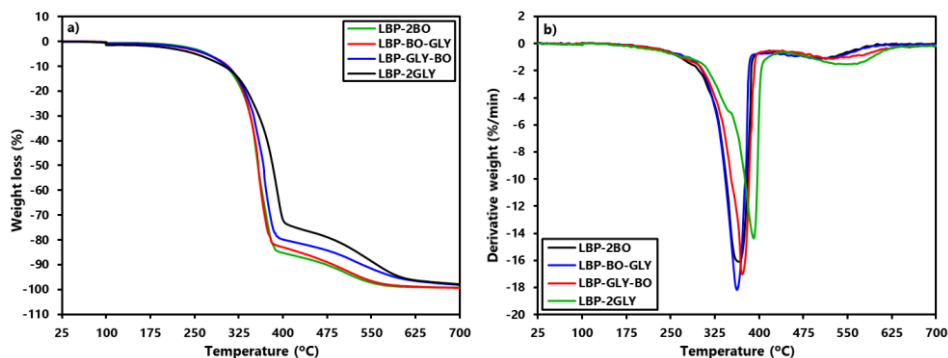


**Figure 4.9** Comparative thermal profile of the CO-LBPs and TER-LBPs: a) TG, b) dTG.

In both cases, the incorporation of different monomers in the synthesis of LBPs allowed the obtention of LBPs with different properties to those obtained with a single type of monomer in the presence of THF.

- **Tetrapolymers**

In the same way that a route has been proposed to obtain TER-LBPs, different monomers could still be added to increase the functionality of the polymerized chain. In the formation of TER-LBPs, it has been observed that the monomer order addition is very important both in the composition of the LBP and in the thermal behavior. Subsequently, it is proposed to obtain a lignin-based tetrapolymer (TETRA-LBP) with different functional groups but keeping a similar structure along the chain.

The first step is to avoid the THF homopolymerization as much as possible to obtain a controlled microstructure. In **Chapter 3** it was observed both the temperature reaction and the -OH concentration had an influence in the THF homopolymerization. When the polymerization of a high amount

of monomer to obtain different microstructures in the LBP chains is desired, the incorporation of the homopropagated THF should be the least as possible. If the length of the THF homopropagated is controlled, not only the lignin content in the LBP, but also the length of the THF between monomers should be similar.

For this purpose, the first monomer addition should be GLY to increase the -OH groups in the LBP and make the competition between the THF homopropagation and the -OH termination higher as it was discussed previously in the obtention of hyperbranched LBPs. In **Table 4.6**, it is studied the THF copolymerization in presence of Mix-OL and GLY at different reaction conditions maintaining the same MR GLY/OH-L = 1 and  $Q_s = 73.0 \text{ mL/n}_{\text{OH-L}} \cdot \text{h}$

**Table 4.6** LBP composition adding GLY as a monomer at different reaction conditions.

<b>Entry</b>	<b>1</b>	<b>2</b>	<b>3</b>	<b>4</b>
[L] (g/L)	110	55	110	164
Temperature (°C)	25.0	Reflux	Reflux	Reflux
<b><i>LBP composition</i></b>				
L (wt. %)	32.1	32.7	47.5	47.8
MON (wt. %)	10.9	11.2	16.2	16.3
THF (wt. %)	57.0	56.1	36.4	35.9
MR THF/MON	5.5	5.3	2.4	2.3
MR OH:MON:THF	1:1:5.5	1:1:5.3	1:1:2.4	1:1:2.3
Reaction conditions: MR GLY/OH-L = 1 and $Q_s = 73.0 \text{ mL/n}_{\text{OH-L}} \cdot \text{h}$ .				

As can be observed in **Table 4.6** from the first two reactions (Entries 1 and 2), temperature plays an essential role in the polymerization of THF as it was discussed in **Chapter 3**. Entry 1 and 2 have almost the same LBP composition, although in Entry 2 a higher THF content was expected due to the lower lignin concentration. Carrying out the reaction under

THF reflux temperature, the higher THF homopolymerization was counterbalanced as it was discussed in the section of the temperature influence in the LBP composition in **Chapter 3**. In both LBPs the amount of polymerized THF was 5 moles of THF per mole of GLY.

Taking the Entry 2 conditions as reference, the amount of Mix-OL was progressively increased to see if the amount of polymerized THF could be reduced. As shown in **Table 4.6**, increasing the initial lignin concentration from 55 g/L to 110 g/L, the amount of polymerized THF is reduced in a half. However, although the lignin concentration is increased in Entry 4, this value remains almost constant. Therefore, the reaction conditions chosen for the formation of a LBP tetrapolymer (TETRA-LBP) were:  $[L] = 110 \text{ g/L}$ ,  $T = T_{\text{reflux}}(\text{THF})$ ,  $Q_s = 73.0 \text{ mL/nOH-L h}$  for the addition of the three monomers.

To carry out the subsequent monomer additions, in addition to GLY monomer, the other two monomers with a boiling point higher than THF were chosen to avoid addition failures. The second monomer added was HO (MR HO/OH-L = 1), which is its opening generates a 4-carbon alkyl chain. And finally, ECH (MR ECH/OH-L = 1) was added to incorporate a new functional group into the chain. With the THF copolymerization, the obtention of TETRA-LBP was expected to obtain. In **Table 4.7**, it is detailed the composition of the LBP in each addition, observing the evolution of the TETRA-LBP.

**Table 4.7** TETRA-LBP properties obtained at different reaction stages.

	<b>1<sup>st</sup> addition</b>	<b>2<sup>nd</sup> addition</b>	<b>3<sup>rd</sup> addition</b>
Type of LBP	Copolymer	Terpolymer	Tetrapolymer
Entry	Mix-OL+GLY	Mix-OL+GLY+HO	Mix-OL+GLY+HO+ECH
<b>LBP composition</b>			
L (wt. %)	47.5	27.8	20.2
Monomer (wt. %)	16.2	22.5	24.7
THF (wt. %)	36.3	49.7	55.1
MR THF/MON	2.4	2.7	2.8
MR (OH:MON:THF)	1:1:4.8	1:2:5.4	1:3:5.6
OH# (mg KOH/g sample)	237	194	143
<b>LBP molecular weight analysis</b>			
$\overline{M}_w$ (g/mol)	NA <sup>a</sup>	3715	4861
PDI	NA <sup>a</sup>	2.08	2.32
<b>LBP thermal analysis</b>			
T <sub>c</sub> (°C)	ND	ND	ND
$\Delta H_c$ (J/g)	ND	ND	ND
T <sub>m</sub> (°C)	6.57 <sup>b</sup>	ND	ND
$\Delta H_m$ (J/g)	9.16 <sup>b</sup>	ND	ND

NA: Not analyzed.

ND: Not detected.

<sup>a</sup> Not soluble in the eluent employed for the characterization.<sup>b</sup> Exothermic peak observed just before the melting peak.Reaction conditions: [L] = 110 g/L, T<sub>reflux</sub> (THF), Q<sub>s</sub> = 73.0 mL/n<sub>OH-L</sub>·h.

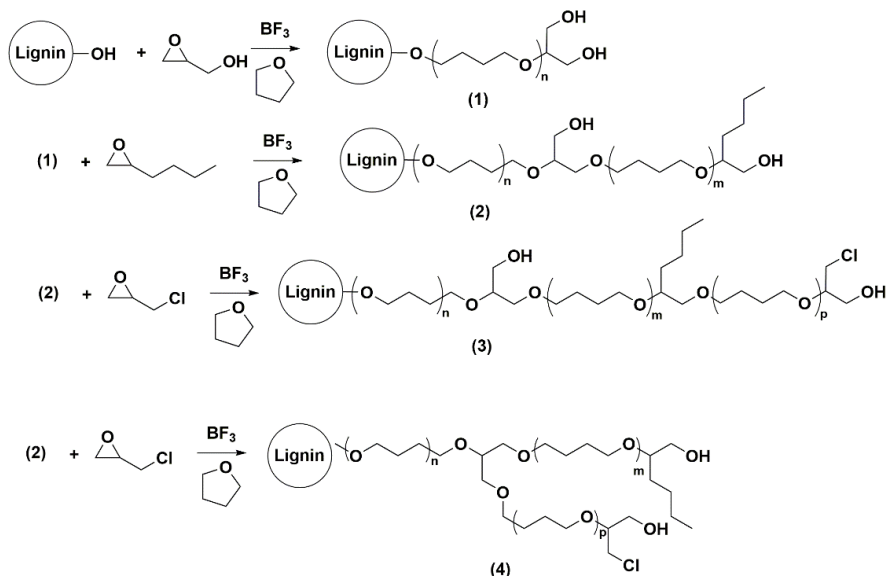
In the first addition, the properties of the copolymer LBP formed by the polymerization of GLY and THF in the presence of the Mix-OL is examined. The copolymer obtained has a LBP composition expected when the reaction is carried out at THF reflux temperature (MR THF/GLY = 2.4). Due to the incorporation of more -OH groups and the low polymerization of THF, the OH# value of the LBP (237 mg KOH/g) is very similar than the starting Mix-OL (243 mg KOH/g).

With the second monomer addition of HO, a TER-LBP was formed. **Table 4.7** details how the L wt. % in the LBP decreases and the MON wt. % and THF wt. % content increases. In this addition it was achieved to maintain the MR THF/MON in constant values between 2-3 moles. Therefore, it is expected that the polymerized chains would have a similar structure. The OH# of this TER-LBP decreases slightly as expected (194 mg KOH/g). Finally, ECH was added as the last monomer to obtain a TETRA-LBP. The TETRA-LBP has a lower L wt. % and higher MON wt. % and THF wt. % content. As in the two previous additions, the MR THF/MON remained constant. Thus, the OH# of the final TETRA-LBP was lower (143 mg KOH/g).

In conclusion, the final TETRA-LBP with controlled polymerization was achieved. The addition of GLY as the first monomer leads the controlled polymerization of the other monomers avoiding a high THF homopolymerization. However, the GLY addition as the first monomer opens the possibility of obtaining two different growing chains as it is illustrated in **Scheme 4.3**.

After the copolymer formation with the addition of GLY (1) and the copolymerization of THF a LBP copolymer is formed. With the following addition of HO, a linear TER-LBP was obtained (2) with two free -OH groups in the chain, one intermediate, and one terminal. With the addition of ECH, two possible routes can be followed. If the opening of the propagation chain generated by ECH is attacked by the terminal -OH, a linear TETRA-LBP is obtained (3). However, if the -OH in the middle of the growing chain is able to attack, a branched growth could be obtained (4).





**Scheme 4.3** Suggested TETRA-LBP final structures.

In **Figure 4.10-a** the structural changes in the polymerization by ATR-FTIR is observed. In the first addition, the typical LBP structure is obtained. The -OH band at  $3450\text{ cm}^{-1}$  is still intense because of the addition of more -OH groups and the high lignin content. With the second addition of HO, this band decreases, and the band associated to the CH linkages at  $2935\text{ cm}^{-1}$ ,  $2840\text{ cm}^{-1}$ , and the C-O band at  $1100\text{ cm}^{-1}$  are enhanced. The addition of the ECH into the LBP to obtain a TETRA-LBP is successfully achieved, as can be observed with the appearance of a new band at  $744\text{ cm}^{-1}$  corresponding to the stretching of the C-Cl group.

In **Figure 4.10-b** illustrates the MWD at different stages of the polymerization. The first addition with GLY (Mix-OL+GLY) could not be measured because the LBP obtained was not soluble in THF. The high lignin content with the hydrogen bonding of the final hydroxyl groups formed an insoluble polyol in the GPC eluent. The intermediate TER-LBP and the final TETRA-LBP has very similar MWD, being the TETRA-LBP slightly bigger.

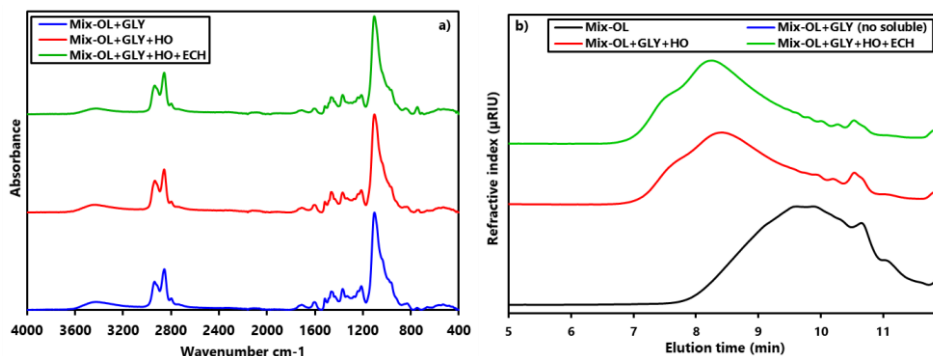


**Figure 4.10** a) Comparative ATR-FTIR spectra of TETRA-LBP at different reaction stages. b) Comparative MWD of TETRA-LBP at different reaction stages.

The  $\overline{M}_w$  evolution of the main peak associated with the TETRA-LBP is detailed in **Table 4.7**. Due to the reaction conditions used avoiding a great homopolymerization of THF, the  $\overline{M}_w$  results in a very small  $\overline{M}_w$  increases with low PDI.

The thermal behavior of the TETRA-LBP observed by DSC is totally different from the rest of the LBPs obtained so far. In **Table 4.7** the data obtained for each monomer addition are shown. With the first addition, a copolymer was obtained by CROP of GLY along with the polymerization of THF. The behavior of this LBP, when it is cooled and heated, is very similar to the LBP-GLY studied in this chapter. However, with the following monomer additions the LBP obtained does not present any melting and crystallization temperatures. This is the first LBP obtained in this thesis that shows this behavior.

The thermogravimetric profile of the TETRA-LBP is illustrated in **Figure 4.11-a**. The addition of each monomer increased the amount of weight loss associated with the polymer chains formed. Furthermore, it is observed that the addition of each monomer does not change the thermal stability of the LBP. In **Figure 4.11-b** is observed how each monomer addition did

not change in excess the temperature of the weight loss, although in each monomer addition these bands were broader.

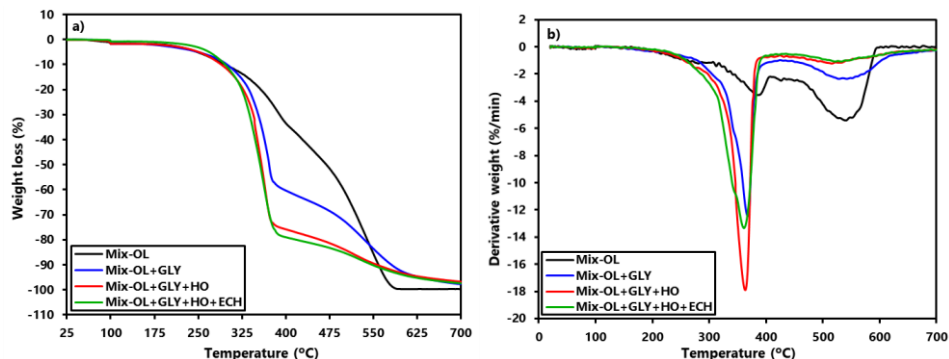


**Figure 4.11** Comparative thermal profile of the TETRA-LBP at different reaction stages: a) TG, b) dTG.

## 4.5 Conclusions

In this chapter, the potential of the CROP route to obtain LBPs (linear and branched) under the same reaction conditions using different oxiranes as monomers has been demonstrated. The employment of different oxiranes changes the microstructure of the LBPs. Under the employed conditions, a family of LBPs with a lignin content in the range between 11.2 and 47.4 wt. % and OH# values from 50 to 217 mg KOH/g and a wide range of average molecular weights from 3652 to 52900 g/mol were obtained. In addition, it has been demonstrated that the TGA profiles of LBPs are affected by the nature of the employed oxiranes.

Furthermore, lignin-based terpolymers (TER-LBP) and tetrapolymers (TETRA-LBP) have been synthesized successfully. It has been shown that by adjusting the reaction parameters, particularly the temperature, regular growth of the chains is obtained, keeping the incorporation of each employed monomer constant.

In summary, a range of possibilities to obtain a plethora of LBPs has been developed. The use of different oxiranes, together with the modification of the reaction parameters, allows to obtain LBPs “a la carte”, increasing the possibilities of these LBPs to be used in several application fields fulfilling the needed requirements.

## 4.6 References

- [4.1] R. Klein and F. R. Wurm, "Aliphatic polyethers: Classical polymers for the 21st century," *Macromol. Rapid Commun.*, vol. 36, no. 12, pp. 1147–1165, 2015.
- [4.2] D. J. Worsfold and A. M. Eastham, "Cationic Polymerization of Ethylene Oxide. II. Boron Trifluoride," *J. Am. Chem. Soc.*, vol. 79, no. 4, pp. 900–902, 1957.
- [4.3] S. Hafner, T. Keicher, and T. M. Klapötke, "Copolymers based on GAP and 1,2-Epoxyhexane as Promising Prepolymers for Energetic Binder Systems," *Propellants, Explos. Pyrotech.*, vol. 43, no. 2, pp. 126–135, 2018.
- [4.4] C. He, C. Zhang, M. Xi, and S. Zhang, "Synthesis and characterization of polyepichlorohydrin-based copolymers with biphenyl groups attached thioether unit," *J. Wuhan Univ. Technol. Mater. Sci. Ed.*, vol. 25, no. 3, pp. 487–491, 2010.
- [4.5] S. Wang *et al.*, "Effects of crosslinking degree and carbon nanotubes as filler on composites based on glycidyl azide polymer and propargyl-terminated polyether for potential solid propellant application," *J. Appl. Polym. Sci.*, vol. 134, no. 39, pp. 1–9, 2017.
- [4.6] A. U. Francis, S. Venkatachalam, M. Kanakavel, P. V. Ravindran, and K. N. Ninan, "Structural characterization of hydroxyl terminated polyepichlorohydrin obtained using boron trifluoride etherate and stannic chloride as initiators," *Eur. Polym. J.*, vol. 39, no. 4, pp. 831–841, 2003.
- [4.7] A. Dworak, S. Slomkowski, T. Basinska, M. Gosecka, W. Walach, and B. Trzebicka, "Polyglycidol-how is it synthesized and what is it used for?," *Polimery/Polymers*, vol. 58, no. 9, pp. 641–649, 2013.

- [4.8] M. Bednarek, P. Kubisa, and S. Penczek, "Polymerization of propylene oxide by activated monomer mechanism - kinetics," *Die Makromol. Chemie*, vol. 15, no. S19891, pp. 49–60, 1989.
- [4.9] M. Wojtania, P. Kubisa, and S. Penczek, "Polymerization of propylene oxide by activated monomer mechanism. Suppression of macrocyclics formation," *Makromol. Chemie. Macromol. Symp.*, vol. 6, no. 1, pp. 201–206, 1986.
- [4.10] T. Biedron, R. Szymanski, P. Kubisa, and S. Penczek, "Kinetics of polymerization by activated monomer mechanism," *Makromol. Chemie. Macromol. Symp.*, vol. 32, no. 1, pp. 155–168, 1990.
- [4.11] T. Biedron, P. Kubisa, and S. Penczek, "Polyepichlorohydrin diols free of cyclics: Synthesis and characterization," *J. Polym. Sci. Part A Polym. Chem.*, vol. 29, no. 5, pp. 619–628, 1991.
- [4.12] A. Dworak, W. Walach, and B. Trzebicka, "Cationic polymerization of glycidol. Polymer structure and polymerization mechanism," *Macromol. Chem. Phys.*, vol. 196, no. 6, pp. 1963–1970, 1995.
- [4.13] D. Guanaes, E. Bittencourt, M. N. Eberlin, and A. A. Sabino, "Influence of polymerization conditions on the molecular weight and polydispersity of polyepichlorohydrin," *Eur. Polym. J.*, vol. 43, no. 5, pp. 2141–2148, 2007.
- [4.14] J. Su Kim, J. Ohk Kweon, and S. Tae Noh, "Online monitoring of reaction temperature during cationic ring opening polymerization of epichlorohydrin in presence of BF<sub>3</sub> and 1,4-butanediol," *J. Appl. Polym. Sci.*, vol. 131, no. 4, pp. 1–9, 2014.
- [4.15] M. D. Bajjal and L. P. Blanchard, "Kinetic aspects of the copolymerization of tetrahydrofuran with propylene oxide. Part II," *J. Polym. Sci. Part C Polym. Symp.*, vol. 23, no. 1, pp. 157–167, 1968.

- [4.16] J. M. Hammond, J. F. Hooper, and W. G. P. Robertson, "Cationic copolymerization of tetrahydrofuran with epoxides. III. Synthesis of block copolymers," *J. Polym. Sci. Part A-1 Polym. Chem.*, vol. 9, no. 2, pp. 295–298, 1971.
- [4.17] L. P. Blanchard, S. Kondo, J. Moinard, J. F. Pierson, and F. Tahiani, "Copolymerization of tetrahydrofuran with propylene oxide. III. 1,2,3-propanetriol as cocatalyst," *J. Polym. Sci. Part A-1 Polym. Chem.*, vol. 10, no. 2, pp. 399–412, 1972.
- [4.18] L. P. Blanchard, A. Aghadjan, and S. L. Malhotra, "Cationic Copolymerization of Styrene Oxide with Propylene Oxide," *J. Macromol. Sci. Part A - Chem.*, vol. 9, no. 2, pp. 299–326, 1975.
- [4.19] M. Bednarek, T. Biedron, P. Kubisa, and S. Penczek, "Activated monomer polymerization of oxiranes. Micro-structure of polymers vs. kinetics and thermodynamics of propagation," *Makromol. Chemie. Macromol. Symp.*, vol. 42–43, no. 1, pp. 475–487, 1991.
- [4.20] M. Bednarek and P. Kubisa, "Cationic copolymerization of tetrahydrofuran with ethylene oxide in the presence of diols: Composition, microstructure, and properties of copolymers," *J. Polym. Sci. Part A Polym. Chem.*, vol. 37, no. 17, pp. 3455–3463, 1999.
- [4.21] Y. M. Mohan and K. M. Raju, "Synthesis and Characterization of GAP-THF Copolymers," *Int. J. Polym. Mater.*, vol. 55, no. 3, pp. 203–217, 2006.
- [4.22] R. Tokar, P. Kubisa, S. Penczek, and A. Dworak, "Cationic polymerization of glycidol: coexistence of the activated monomer and active chain end mechanism," *Macromolecules*, vol. 27, no. 2, pp. 320–322, 1994.

- [4.23] R. A. Barzykina, G. N. Komratov, G. V. Korovina, and S. G. Entelis, "Kinetics of the tetrahydrofuran polymerization on the catalyst system BF<sub>3</sub>-epichlorohydrin," *Polym. Sci. U.S.S.R.*, vol. 20, no. 1, pp. 197–202, 1978.
- [4.24] M. Bednarek and P. Kubisa, "Mechanism of cyclics formation in the cationic copolymerization of tetrahydrofuran with ethylene oxide in the presence of diols," *Macromol. Chem. Phys.*, vol. 200, no. 11, pp. 2443–2447, 1999.
- [4.25] M. Bednarek, P. Kubisa, and S. Penczek, "Kinetic and thermodynamic control in the cationic copolymerization of cyclic ethers," *Macromol. Symp.*, vol. 107, no. 1, pp. 139–148, 1996.
- [4.26] J. M. Hammond, J. F. Hooper, and W. G. P. Robertson, "Cationic copolymerization of tetrahydrofuran with epoxides. II. Characterization and gel-permeation chromatography of by-products formed during polymerization," *J. Polym. Sci. Part A-1 Polym. Chem.*, vol. 9, no. 2, pp. 281–294, 1971.
- [4.27] P. Kubisa, "Hyperbranched polyethers by ring-opening polymerization: Contribution of activated monomer mechanism," *J. Polym. Sci. Part A Polym. Chem.*, vol. 41, no. 4, pp. 457–468, 2003





# CHAPTER 5

## CONCLUSIONS, FUTURE WORK, AND PUBLISHED RESEARCH

---



## 5.1 Conclusions

In this thesis, the principles of a new route to obtain lignin-based polyols (LBPs) under mild conditions has been established. These LBPs are obtained by cationic ring-opening polymerization (CROP) of oxiranes in presence of the lignin in THF.

In **Chapter 2**, the most suitable lignin for CROP was selected. For this purpose, the solubility of lignins obtained from different sources and isolated according to different extraction processes was studied in dichloromethane (DCM) and tetrahydrofuran (THF). All lignins exhibited a poor solubility in DCM. However, most lignins had better solubility in THF, especially the organosolv lignins, which were totally solubilized. The organosolv lignin obtained from different wood sources (Mix-OL) was selected as the best due to its solubility and its handling. This lignin was totally characterized to observe the changes that could suffer in the investigated polymerization process.

In **Chapter 3**, the basis of CROP in the presence of the -OH groups of the lignin was developed. For the polymerization reaction, the selected lignin (Mix-OL) and the best solvent (THF) chosen in the previous chapter were used, adding butylene oxide (BO) as a suitable monomer for polymerization. With the results obtained in the study of the reaction conditions, a polymerization mechanism to obtain lignin polyols by CROP of BO and THF in the presence of Mix-OL -OH groups was proposed. The obtained LBPs varied in composition and their polymerized chain microstructures, with a lignin content from 10.3 % to 34.2 %, with molecular weights from 5517 to 37754 g/mol, and with a hydroxyl number (OH#) from 35 to 127 mg KOH/g.

To evaluate the potential of this new route, two different sources of lignin were used to obtain LBPs. In both cases, LBPs with very similar properties to those obtained with Mix-OL were obtained, even with the use of partially soluble lignins.

To complete the research, two types of applications were selected to test LBPs. The first studied application was the direct use of LBPs as phase change materials (PCMs). This study was based on the thermal properties that LBPs had when they changed state (solid-liquid). The results showed that the higher the ratio of THF to BO introduced in the LBP, and the lower the concentration of lignin, the higher the enthalpies of the processes related to the phase changes. The best result obtained in the studied conditions was 48.05 J/g related to the LBP obtained using the lowest lignin concentration (55 g/L) and monomer amount of MR BO/OH-L = 2. Although this result is low in comparison with other materials used for PCMs, it opens a new unstudied field for the applicability of these LBPs. The second type of application was the use of LBPs as an intermediate for the synthesis of polyurethanes. LBPs were tested by partial addition in the synthesis of rigid polyurethane foams and by partial replacement of a polyol in the synthesis of flexible polyurethane foams. In both cases, they were successfully introduced in the formulation of these polyurethanes adding lignin in their final composition, without any unpleasant odor or residues in the products, and obtaining similar properties to those used as a reference.

Finally, in **Chapter 4**, the family of LBPs was expanded by using different types of oxiranes. For this study, oxiranes with different chain lengths and different functional groups were selected and employed under the same reaction conditions. It was concluded that the type of used oxirane modified the composition, the polymerized chain microstructure, and the thermal properties of the LBPs. A family of LBPs was obtained

with a broad lignin content (11.2 to 47.4 wt. %) and OH# values (50 to 217 mg KOH/g). Therefore, a wide range of average molecular weights was obtained (3652 to 52900 g/mol) as well as different interesting thermal properties in accordance with the employed monomer.

In addition to the linear structures obtained until now, the obtention of branched LBPs was explored by means of the use of monomers containing -OH groups such a glycidol, added in different amounts to observe the branching influence in the LBPs properties. To finish the study, alternative lignin-based terpolymer (TER-LBP) and tetrapolymer (TETRA-LBP) structures were synthesized employing the continuous addition of different oxiranes to demonstrate the possibility of modifying the polymeric chains along the course of the reaction.

These results presented through this work are fairly motivating, providing the need for further research in this new route to valorize the lignin through its incorporation into polymeric materials through well-defined lignin-based polyols.

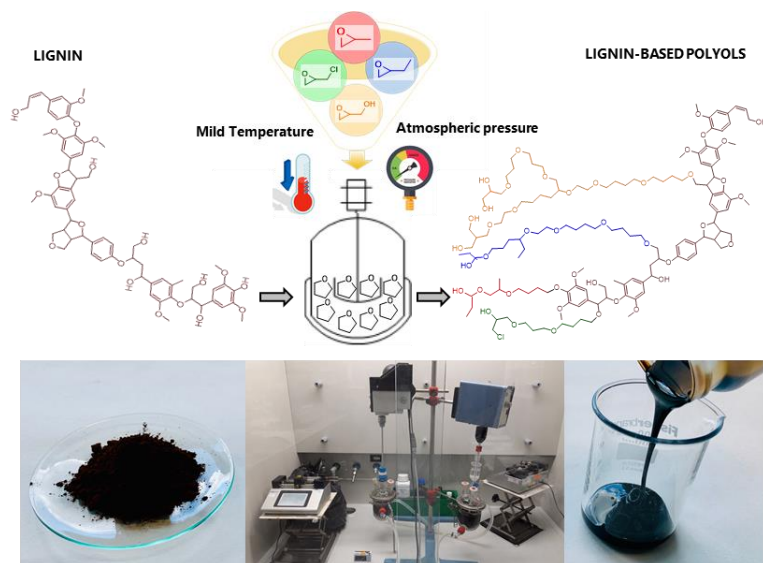


**Figure 5.1** Graphical abstract of the thesis.

## 5.2 Future work

After establishing the basis to obtain lignin-based polyols by cationic ring-opening polymerization, to continue the work in this field, the following lines of research could be approached:

- Further characterization of lignin-based polyols to elucidate the formed structures, for example, by nuclear magnetic resonance spectroscopy.
- Expand the range of lignin sources to be used in CROP to yield LBPs with other technical lignins.
- Expand the family of LBPs using oxiranes employed containing different functional groups under different reaction conditions to obtain LBPs “a la carte” with different compositions and microstructures.
- Study the scale-up of the reaction to produce LBPs on a pilot plant scale.
- Study the possible applications where LBPs can be introduced as intermediates for the synthesis of bio-based materials.
- Carry out an economic study based on the cost of the lignin production and the cost of the reagents to establish the final price of the potentially obtained LBPs in order to know their potential market.

## 5.3 Published research

### PAPERS IN SCIENTIFIC JOURNALS

---

---

**Perez-Arce, J.**, Centeno-Pedraza, A., Labidi, J., Ochoa-Gómez, José R., Garcia-Suarez, Eduardo J.

**A novel and efficient approach to obtain lignin-based polyols with potential industrial application. (Submitted)**

Year: 2020

**Perez-Arce, J.**, Serrano, A., Dauvergne, Jean-Luc, Centeno-Pedraza, A., Prieto, S., Palomo, E., Garcia-Suarez, Eduardo J.

**Sustainable Lignin-based polyols (LBPs) as promising energy storage materials. (Submitted)**

Year: 2020

**Perez-Arce, J.**, Centeno-Pedraza, A., Labidi, J., Ochoa-Gómez, José R., Garcia-Suarez, Eduardo J.

**Lignin-based polyols with controlled microstructure by cationic ring-opening polymerization. (Submitted)**

Year: 2020

### PATENTS

---

---

Ochoa-Gómez, José R., **Perez-Arce, J.**, B. Maestro-Madurga, and Garcia-Suarez, Eduardo J.

**Lignin-based polyols**

Application number: WO 2020/109460 A1

Year: 2020



CONTRIBUTIONS AT INTERNATIONAL SCIENTIFIC  
CONFERENCES

---

**Perez-Arce, J.**, Garcia-Suarez, Eduardo J, Labidi, J., Ochoa-Gómez, José R.

**A new synthetic route to obtain a family of lignin-based polyols.**

BIOPOL 2019. Stockholm (Sweden). 17-19/06/19

Poster

Garcia-Suarez, Eduardo J., Maestro-Madurga, B., **Perez-Arce, J.**, Henneken, H., Ochoa-Gómez, José R.

**Lignocellulosic biomass valorization by reductive depolymerization in supercritical ethanol.**

ISGC 2019. La Rochelle (France). 05/10/2019

Oral

# LIST OF FIGURES

<b>Chapter 1</b>	<b>Page</b>
<b>Figure 1.1</b> Energy consumption timeline by source (up) and annual percentage change in fossil consumption in 2019 (down) (data obtained from: 'https://ourworldindata.org/energy').	<b>3</b>
<b>Figure 1.2</b> Global production capacity of bioplastics (left) and global production capacity in 2019 (right), (adapted from https://www.european-bioplastics.org).	<b>7</b>
<b>Figure 1.3</b> Main compounds of the lignocellulosic biomass.	<b>10</b>
<b>Figure 1.4</b> Lignin monolignols precursors.	<b>12</b>
<b>Figure 1.5</b> Enzymatic formation of resonance monolignol radicals.	<b>13</b>
<b>Figure 1.6</b> Mayor linkages formed in the lignin formation.	<b>14</b>
<b>Figure 1.7</b> Proposed lignin structure [1.25].	<b>15</b>
<b>Figure 1.8</b> Number of research publications (left) and sorted by subject area (right) filtered with "lignin" as a keyword in the title (data obtained from Web Of Science).	<b>16</b>
<b>Figure 1.9</b> Lignin fractionation diagram to obtain added-value compounds and energy, (adapted from [1.37]).	<b>18</b>
<b>Figure 1.10</b> Lignin modification main approaches.	<b>21</b>
<b>Figure 1.11</b> Ring-opening polymerization of a) $\epsilon$ -caprolactone, b) lactide, and c) propylene oxide [1.65].	<b>23</b>
<b>Figure 1.12</b> Lignin oxypropylation by anionic ring-opening polymerization.	<b>26</b>
 <b>Chapter 2</b>	 <b>Page</b>
<b>Figure 2.1</b> Scheme of the biorefinery concept.	<b>45</b>
<b>Figure 2.2</b> Picture of the different lignin employed: a) Eucalyptus-HL, b) Pine-HL, c) Poplar-HL, d) Elm-KL, e) Eucalyptus-KL, f) Poplar-KL, g) Beech-OL, i) Mix-OL, and j) Olive-SL.	<b>57</b>

<b>Figure 2.3</b> Lignin solubility in different organic solvents.	<b>58</b>
<b>Figure 2.4</b> ATR-FTIR spectra of the Mix-OL.	<b>62</b>
<b>Figure 2.5</b> Mix-OL molecular weight distribution profile.	<b>64</b>
<b>Figure 2.6</b> Thermal profile of the Mix-OL: a) TG, b) dTG.	<b>65</b>
<b>Figure 2.7</b> DSC curve of the Mix-OL.	<b>66</b>

### **Chapter 3**

**Page**

<b>Figure 3.1</b> Set-up of the polymerization reaction.	<b>88</b>
<b>Figure 3.2</b> Mix-OL lignin and the LBP obtained (0.125 MR BF <sub>3</sub> /OH-L).	<b>92</b>
<b>Figure 3.3</b> Comparative ATR-FTIR spectra of Mix-OL and LBP (0.125 MR BF <sub>3</sub> /OH-L).	<b>94</b>
<b>Figure 3.4</b> a) Comparative MWD of Mix-OL and LBP (0.125 MR BF <sub>3</sub> /OH-L). b) Comparative DSC curves of Mix-OL and LBP (0.125 MR BF <sub>3</sub> /OH-L).	<b>94</b>
<b>Figure 3.5</b> Comparative TGA thermal profile of Mix-OL and LBP (0.125 MR BF <sub>3</sub> /OH-L): a) TG, b) dTG.	<b>96</b>
<b>Figure 3.6</b> a) Comparative ATR-FTIR spectra of the LBPs obtained with different Q <sub>s</sub> . b) Comparative MWD of the LBPs obtained with different Q <sub>s</sub> .	<b>98</b>
<b>Figure 3.7</b> Comparative TGA thermal profile of the LBPs obtained at different Q <sub>s</sub> : a) TG, b) dTG.	<b>99</b>
<b>Figure 3.8</b> Comparative MWD of the LBPs obtained with different MR BO/OH-L.	<b>101</b>
<b>Figure 3.9</b> a) Comparative ATR-FTIR spectra of the LBPs obtained with different MR BO/OH-L. b) Comparative TGA thermal profile of the LBPs obtained at different MR BO/OH-L.	<b>102</b>
<b>Figure 3.10</b> Comparative MWD of the LBPs obtained with different lignin concentration: a) MR BO/OH-L = 1, b) BO/OH-L = 2.	<b>104</b>
<b>Figure 3.11</b> Comparative ATR-FTIR spectra of the LBPs obtained with different lignin concentrations: a) MR BO/OH-L = 1, b) MR BO/OH-L = 2.	<b>106</b>

- Figure 3.12** Comparison of different LBPs states at room temperature (MR BO/OH-L = 1): a) [L] = 55 g/L, b) [L] = 110 g/L, and c) [L] = 274 g/L. **108**
- Figure 3.13** Comparative thermal profile of the LBPs obtained at different lignin concentration: a) MR BO/OH-L = 1, b) MR BO/OH-L = 2. **108**
- Figure 3.14** a) Comparative BO conversion along the reaction time at different temperatures. b) Comparative MWD of the LBPs obtained at different reaction temperatures. **110**
- Figure 3.15** a) Comparative ATR-FTIR spectra of the LBPs obtained at different reaction temperatures. b) Comparative thermal profile of the LBPs obtained at different reaction temperatures. **111**
- Figure 3.16** a) Comparative ATR-FTIR spectra of GL, GL-LBP, and Mix-OL-LBP-1, b) Comparative MWD of GL, GL-LBP, and Mix-OL-LBP-1. **117**
- Figure 3.17** a) Comparative DSC curves of GL and GL-LBP. b) Comparative thermal profile of GL and GL-LBP. **118**
- Figure 3.18** Comparison of the reaction with KL at different times: a) KL dissolved in THF, b) KL-LBP, and c) Glass balloon after pouring the KL-LBP without visible solids. **120**
- Figure 3.19** a) Comparison of BO conversion using different types of lignin. b) Comparison of BO conversion with different  $Q_5$  in the presence of KL. **120**
- Figure 3.20** a) Comparative ATR-FTIR spectra of KL, KL-LBP, and Mix-OL-LBP-2. b) Comparative MWD of KL-LBP and Mix-OL-LBP-2. **122**
- Figure 3.21** a) Comparative DSC curves of KL and KL-LBP. b) Comparative thermal profile of KL and KL-LBP. **123**
- Figure 3.22** Comparison of the LBPs melting temperature and associated enthalpy according to their BO/THF mass ratio. **128**
- Figure 3.23** Comparison of the LBPs crystallization temperature and associated enthalpy according to their BO/THF mass ratio. **130**
- Figure 3.24** Comparative ATR-FTIR spectra of the reaction with LBP and HDI: a) start of the reaction, b) end of the reaction. **133**
- Figure 3.25** Comparative images of reference RPU (left) and LBP-RPU (right). **134**

**Figure 3.26** Comparative images of reference FPU (left) and LBP-FPU (right). **135**

## **Chapter 4**

**Page**

**Figure 4.1** Monomers employed to obtain LBPs with different microstructures. **158**

**Figure 4.2** Comparative MWD of the LBPs obtained with different monomers. **163**

**Figure 4.3** Comparative ATR-FTIR spectra of the LBPs obtained with different monomers. **165**

**Figure 4.4** Comparative thermal profile of the LBPs obtained at different monomers: a) TG, b) dTG. **169**

**Figure 4.5** Schematic representation of different LBP types of polymerization: a) linear, b) branching. **170**

**Figure 4.6** a) Comparative ATR-FTIR spectra of the LBPs obtained with different MR GLY/OH-L. b) Comparative MWD of the LBPs obtained with different MR GLY/OH-L. **172**

**Figure 4.7** Comparative thermal profile of the LBPs obtained with different MR GLY/OH-L: a) TG, b) dTG. **173**

**Figure 4.8** a) Comparative MWD of the CO-LBPs and TER-LBPs. b) Comparative ATR-FTIR spectra of the CO-LBPs and TER-LBPs. **176**

**Figure 4.9** Comparative thermal profile of the CO-LBPs and TER-LBPs: a) TG, b) dTG. **177**

**Figure 4.10** a) Comparative ATR-FTIR spectra of TETRA-LBP at different reaction stages. b) Comparative MWD of TETRA-LBP at different reaction stages. **183**

**Figure 4.11** Comparative thermal profile of the TETRA-LBP at different reaction stages: a) TG, b) dTG. **184**

## **Chapter 5**

**Page**

**Figure 5.1** Graphical abstract of this thesis. **195**

# LIST OF TABLES

<b><i>Chapter 1</i></b>	<b><i>Page</i></b>
<b>Table 1.1</b> Biomass classification according to their biological diversity, source, and origin [1.10].	<b>6</b>
<b>Table 1.2</b> Monolignol distribution in different types of lignin [1.37, 1.38].	<b>13</b>
<b>Table 1.3</b> Percentage of linkages in softwood and hardwood lignins [1.34, 1.35, 1.40].	<b>15</b>
<b>Table 1.4</b> Main applications for lignin.	<b>17</b>
<b><i>Chapter 2</i></b>	<b><i>Page</i></b>
<b>Table 2.1</b> Lignin content in different biomass [2.2, 2.6-2.8].	<b>44</b>
<b>Table 2.2</b> Major industrial producers of various types of lignin, (adapted from [2.24]).	<b>51</b>
<b>Table 2.3</b> Chemical composition and properties of the technical lignins [2.11, 2.16].	<b>52</b>
<b>Table 2.4</b> Grafting reactions conducted with different technical lignins, (adapted from [2.30]).	<b>53</b>
<b>Table 2.5</b> Moisture content of different technical lignins.	<b>58</b>
<b>Table 2.6</b> Chemical composition of the Mix-OL.	<b>60</b>
<b>Table 2.7</b> Main compounds obtained in the pyrolysis of the Mix-OL (expressed as g/100 g lignin).	<b>61</b>
<b>Table 2.8</b> Wavenumber of the lignin Mix-OL ATR-FTIR spectra.	<b>63</b>
<b>Table 2.9</b> Molecular weight distribution of Mix-OL lignin.	<b>64</b>
<b><i>Chapter 3</i></b>	<b><i>Page</i></b>
<b>Table 3.1</b> Reagents, catalyst, and reaction parameters studied in the synthesis of LBPs.	<b>90</b>
<b>Table 3.2</b> Influence of the MR BF <sub>3</sub> /OH-L in the BO conversion at different reaction times.	<b>91</b>

<b>Table 3.3</b> LBP composition obtained with 0.125 MR BF <sub>3</sub> /OH-L.	<b>92</b>
<b>Table 3.4</b> $\overline{M_w}$ and PDI of Mix-OL and LBP (0.125 MR BF <sub>3</sub> /OH-L).	<b>95</b>
<b>Table 3.5</b> Thermal analysis of the LBP (0.125 MR BF <sub>3</sub> /OH-L).	<b>95</b>
<b>Table 3.6</b> LBPs properties obtained with different Q <sub>s</sub> .	<b>97</b>
<b>Table 3.7</b> LBPs properties obtained with different MR BO/OH-L.	<b>100</b>
<b>Table 3.8</b> LBPs properties obtained with different lignin concentrations with MR BO/OH-L = 1.	<b>103</b>
<b>Table 3.9</b> LBPs properties obtained with different lignin concentrations with MR BO/OH-L = 2.	<b>103</b>
<b>Table 3.10</b> LBP molecular weight analysis at different lignin concentration.	<b>105</b>
<b>Table 3.11</b> LBP thermal analysis with different lignin concentration.	<b>107</b>
<b>Table 3.12</b> LBPs properties obtained with different reaction temperatures.	<b>109</b>
<b>Table 3.13</b> LBPs properties obtained with GL and Mix-OL.	<b>117</b>
<b>Table 3.14</b> LBPs properties obtained with KL and Mix-OL.	<b>121</b>
<b>Table 3.15</b> Conditions summary, LBP composition and LBP thermal analysis employed in the LBP study as energy storage materials.	<b>127</b>

## **Chapter 4**

**Page**

<b>Table 4.1</b> Typical initiators, monomers (oxiranes), co-monomers, catalyst and solvents employed in the CROP and CROCOP reaction.	<b>153</b>
<b>Table 4.2</b> Reagents, catalyst, and reaction parameters employed in the synthesis of LBPs with different monomers.	<b>157</b>
<b>Table 4.3</b> LBPs properties obtained with different monomers.	<b>159</b>
<b>Table 4.4</b> LBPs properties obtained with different MR GLY/OH-L.	<b>171</b>
<b>Table 4.5</b> CO-LBPs and TER-LBPs properties obtained with different monomer addition.	<b>174</b>
<b>Table 4.6</b> LBP composition adding GLY as a monomer at different reaction conditions.	<b>178</b>

---

<b>Table 4.7</b> TETRA-LBP properties obtained at different reaction stages.	<b>180</b>
--	------------

<b><i>Appendix I</i></b>	<b><i>Page</i></b>
--------------------------	--------------------

---

<b>Table A.1</b> Standardized values of the F and C <sub>est</sub> parameters for the different monosaccharides, the acetic acid and the galacturonic acid.	<b>214</b>
---	------------



# LIST OF SCHEMES

<b><i>Chapter 3</i></b>	<b><i>Page</i></b>
<b>Scheme 3.1</b> CROP initiation by a Brønsted acid.	<b>81</b>
<b>Scheme 3.2</b> Propagation mechanisms in CROP.	<b>81</b>
<b>Scheme 3.3</b> CROP regiospecificity in the propagation step.	<b>82</b>
<b>Scheme 3.4</b> Different termination routes in the CROP in presence of hydroxyl groups.	<b>82</b>
<b>Scheme 3.5</b> Competitive reactions in CROP propagation leading to undesired side products.	<b>83</b>
<b>Scheme 3.6</b> Cyclic oligomer formation in CROP.	<b>83</b>
<b>Scheme 3.7</b> Disproportionation reactions in the CROP.	<b>84</b>
<b>Scheme 3.8</b> Formation of linear diols or homopolymers.	<b>85</b>
<b>Scheme 3.9</b> ACE and AM propagation competition.	<b>86</b>
<b>Scheme 3.10</b> Proposed mechanism to obtain LBPs by CROCOP.	<b>112</b>
<b>Scheme 3.11</b> Reaction scheme of the polyurethane synthesis employing a LBP.	<b>132</b>
<b><i>Chapter 4</i></b>	<b><i>Page</i></b>
<b>Scheme 4.1</b> Expected LBPs obtained with different monomers.	<b>162</b>
<b>Scheme 4.2</b> Different TER-LBPs structures according to the sequence of monomer addition.	<b>175</b>
<b>Scheme 4.3</b> Suggested TETRA-LBP final structures.	<b>182</b>

# APPENDIX I

## PROCEDURES FOR LIGNIN AND LIGNIN-BASED POLYOLS CHARACTERIZATION

---



In this appendix, the experimental procedure for the chemical and structural characterization of lignins and lignin-based polyols (LBPs) was detailed. For the selected lignin, the chemical characterization, monosaccharide, ash, acid-soluble lignin (ASL) and acid-insoluble lignin (AIL) content were determined. The monosaccharide, AIL, and ASL content were determined following the protocol NREL/TP-510-42618 [A.1], with a slight modification. The ASL was determined by TAPPI (TAPPI UM250 um-83) protocol [A.2], and the ash content was determined by modifying the procedure described by Liu et al. [A.3]. All measurements, except the determination of the ash content, were performed in triplicate, giving the results as the mean  $\pm$  standard deviation on an oven-dried basis.

Moreover, lignins and LBPs were characterized by means of their LBP structural determination, hydroxyl number (OH#), molecular weight distribution (MWD), average molecular weight ( $\overline{M}_w$ ) and polydispersity index (PDI). To complement the characterization, lignin and lignin-based polyols were analyzed their thermal properties by Differential Scanning Calorimetry (DSC) and Thermo-Gravimetric Analysis (TGA).

## Moisture content determination

The moisture contained (H) in the biomass is the water vapor retained by the material that is in equilibrium with the environment. It is, therefore, necessary to determinate since it will be taken into account in the subsequent analysis because of the results are typically reported on an oven-dried basis. The procedure used to determine the moisture content according to (TAPPI T264 cm-97) consists of:

- Prepare the recipient that will be used for the measurement. It needs to be clean and dry. The recipient is heated in an oven at  $105 \pm 3$  °C for 6 h. After that, cool it down until room temperature in a desiccator, and weigh it on the analytical balance to the nearest 0.1 mg ( $m_0$ ).
- Weigh accurately  $2.00 \pm 0.01$  g of sample in the previously tared recipient with the same analytical balance ( $m_1$ ).
- Place the recipient with the sample in the oven at  $105 \pm 3$  °C for 24 hours.
- Then, place the recipient with the sample in a desiccator until it is cooled down to room temperature. Finally, weigh the recipient with the sample ( $m_2$ ).

The moisture content was determined as follows:

$$\text{Moisture content (H) (\%)} = \frac{(m_2 - m_0)}{m_1} \cdot 100$$

## Lignin ash content determination

The ash consists on the inorganic matter present in the lignin isolated from biomass, and its presence is typically attributed to the procedure used in the isolation process. For the ash content determination in biomass, a modification of the procedure proposed by Liu et al. is used by thermogravimetric analysis [A.3]. To determine the ash content in lignin, the Thermo-Gravimetric Analysis (TGA) of the sample was performed on a TA instruments TG-DTA92 instrument under air atmosphere. In a typical experiment, an accurate amount of sample ( $m_0$ ) is heated from 20 °C to 100 °C at 5 °C/min. Then, the sample was dried at this temperature for 1 h in order to eliminate moisture and residual solvent, if any. Then,

it was heated from 120 to 700 °C at 10 °C/min while recording the final weight loss ( $m_1$ ). The Ash Content (AC) was determined as follows:

$$\text{Ash content (AC)}(\%) = 1 - \frac{m_1 (g)}{m_0 (g)} * 100$$

## Acid-insoluble lignin and carbohydrate content of lignin determination

The determination of the chemical composition of the lignin is an essential analysis, which permits the determination of the lignin purity. The lignin purity is estimated as the contribution of the Acid-Soluble Lignin (ASL) and Acid-Insoluble Lignin (AIL). The lignin could contain carbohydrates as impurities obtained in the extraction process. The AIL and carbohydrate content were determined according to the procedure described by Davila [A.4], which is based on the NREL/TP-510-42618 protocol (quantitative acid hydrolysis (QAH) determination) with a slight modification. This procedure consists in two consecutive acid hydrolysis, leading the estimation of the hemicellulosic content and the glucan content of the lignocellulosic biomass by determination of the concentration of monosaccharides. The modification in the procedure was realized in the second hydrolysis stage, where the sample was less diluted, with a concentration of  $\text{H}_2\text{SO}_4$  of 12.0 wt. % instead of 4.0 wt. %. In this thesis, the carbohydrate content was determined by HPLC analyses using a Jasco LC Net II/ADC chromatograph equipped with a refractive index detector and a photodiode array. The chromatographic column was a 300 x 7.8 mm Aminex HPX-87H column (Bio-Rad Laboratories, USA) working with a flow rate of 0.6 mL/min at 50 °C and eluting 20  $\mu\text{L}$  of the sample with a mobile phase of 0.005 M  $\text{H}_2\text{SO}_4$ .

The procedure to determine the ASL, AIL, and carbohydrates content consists of:

- Weigh accurately  $0.25 \pm 0.001$  g of the extract-free sample ( $m_0$ ) in a test tube. The particle size of the sample should be less than 0.5 mm, and the moisture of the sample (H) needs to be previously determined.
- Add 2.5 mL of 72.0 wt. %  $\text{H}_2\text{SO}_4$  to the test tube and stir the sample to ensure a homogeneous mixture. Then, place the test tube in a water bath at 30 °C for 1 h, and mixing it periodically.
- After this period of time, add distilled water to the mixture in order to stop the reaction. Then, transfer the content of the test tube to a previously tared pressure flask and add distilled water until the weight of the whole mixture is 74.33 g ( $m_1$ ), which corresponds to a  $\text{H}_2\text{SO}_4$  concentration of 12.0 wt. %.
- Weigh the pressure flask with the mixture ( $m_2$ ) and autoclave it for 1 h at 121 °C.
- After this period of time, cool down the pressure flask and note down the weight of the pressure flask ( $m_3$ ).
- Separate the mixture by filtration using a previously tared Gooch crucible N° 3. The Gooch crucible should be previously dried in an oven for 6 h at  $105 \pm 3$  °C, cooled down in a desiccator, and weighed ( $m_4$ ).
- Dry the solid residue contained in the Gooch crucible in an oven at  $105 \pm 3$  °C for 24 h.
- After this time, cool down to room temperature the Gooch crucible with the solid phase in a desiccator and weigh it ( $m_5$ ) until the weight of the sample is constant to  $\pm 0.2$  mg.

- Analyze the liquid phase obtained after the filtration by High Performance Liquid Chromatography (HPLC) to measure the concentration of monosaccharides, acetic, galacturonic acid, and degradation products (furfural and hydroxymethylfurfural (HMF)).

The AIL or Klason lignin content of the sample was estimated as follows:

$$\text{Acid - Insoluble Lignin (AIL)(\%)} = \left( \frac{m_5 - m_4}{m_0 \cdot \frac{(100 - H(\%))}{100}} \right) - AC(\%)$$

The structural carbohydrates content, measured as glucan, xylan, arabinosyl (ArOS), galactosyl (GalactOS), acetyl groups (AcOS), and galacturonic acids (GaAc), was estimated as follows:

$$\text{Glucan/xylan/ArOS/MaOS/GalactOS/AcOS/GaAc (\%)} = F \cdot C_{est} \cdot \frac{[X]}{\rho} \cdot \frac{P}{m_0 \cdot \left( \frac{100 - H(\%)}{100} \right)} \cdot 100$$

Where:

- F = degradation of the carbohydrates (standardized parameter (see **Table A.1**))
- C<sub>est</sub> considers the increase of the molecular weight of the monosaccharide during the hydrolysis (standardized parameter ((see **Table A.1**))
- [X] = concentration (g/L) of the monosaccharide or acids
- ρ = density of the liquid phase obtained in the QAH (1.022 g/L)
- P = weight of the liquid phase at the end of the QAH, considering the losses that could have taken place during the second stage of the QAH.



$$P = \left( m_1 - \left( m_0 \cdot \left( \frac{100 - H(\%)}{100} \right) \cdot \frac{AIL(\%)}{100} \right) \right) \cdot \frac{m_1 - (m_2 - m_3)}{m_1}$$

**Table A.1** Standardized values of the F and C<sub>est</sub> parameters for the different monosaccharides, the acetic acid, and the galacturonic acid.

	<b>Glucan/Manosyl/Galactosyl substituents</b>	<b>Xylan/Arabynosyl substituents</b>	<b>Acetyl substituents</b>	<b>Galaturonic acid substituents</b>
	<b>GC<sub>n</sub>/CMan<sub>n</sub>/CGa<sub>n</sub></b>	<b>CX<sub>n</sub>/CAr<sub>n</sub></b>	<b>CG<sub>A</sub></b>	<b>CG<sub>GaAc</sub></b>
	<b>Flucose/Mannose/galactose</b>	<b>Xylose/Arabinose</b>	<b>Acetic acid</b>	<b>Galacturonic acid</b>
<b>F</b>	1.04	1.088	1.00	1.00
<b>C<sub>est</sub></b>	162/180	132/150	43/60	212/230

The total carbohydrate content (TCC) was calculated as follow:

$$TCC (\%) = \text{Glucan}(\%) + \text{xylan}(\%) + \text{ArOS}(\%) + \text{MaOS}(\%) + \text{GalactOS}(\%) + \text{AcOS}(\%) + \text{GaAc}(\%)$$

## Acid-soluble lignin determination

The ASL determination is carried out by UV-vis spectrometry analysis using Jasco V-630 UV-VIS spectrophotometer. In this procedure, the liquid phase resulting from the lignin hydrolysis previously described was employed. The procedure was determined according to (TAPPI UM250 um-83) and consists of:

- Analyze the liquid phase by spectrophotometry (at 205 nm). Dilute the sample with 1 M H<sub>2</sub>SO<sub>4</sub> to bring the absorbance into the range 0.1-0.8 and measure it.

The ASL was determined as follows:

$$\text{Acid - Soluble Lignin (ASL)}(\%) = \frac{A \cdot V \cdot df}{a \cdot b \cdot W} \cdot 100$$

Where:

- A = Average UV-vis absorbance at 205 nm
- V = volume of filtrate (L)
- df = dilution factor
- a = average absorption coefficient ( $110 \text{ L} \cdot \text{g}^{-1} \cdot \text{cm}^{-1}$ )
- b = width of the cuvette (1 cm)
- W = weight of sample (g)

## Lignin purity determination

The lignin purity determination in a lignin sample ( $m_0$ ) is given as the sum of the Acid-Soluble Lignin (ASL) and Acid-Insoluble Lignin (AIL) as follows:

$$\text{Lignin purity (\%)} = \frac{AIL + ASL}{m_0} \cdot 100$$

## Pyrolysis-Gas Chromatography/Mass Spectrometry analysis

The Py-GC/MS analysis of the lignin provides information about its structure. The isolated lignin was analyzed by a 5150 Pyroprobe pyrolyzer (CDS Analytical In., Oxford, PA) connected to an Agilent 6890 gas chromatograph coupled to an Agilent 5973 (Agilent Technologies In., USA) mass spectrometer. The gas chromatograph was equipped with a 30 m x 0.25 mm x 0.25  $\mu\text{m}$  film thickness HP-5MS ((5.0 % phenyl)-methylpolysiloxane) column and employed helium as carrier gas. The pyrolysis was performed at 600 °C (15 s) using a heating ramp of 20 °C/ms, and maintaining the interface at 260 °C. The chromatographic method used for the separation of the pyrolysis products consisted of increasing the temperature from 50 °C to 120 °C (5 min) at 10 °C/min, then to 280 °C (8 min) at 10 °C/min and finally to 300 °C (2 min) at 10 °C/min. The

identification of the compounds was carried out using the National Institute of Standards Library (NIST-17). The concentration of each compound was estimated using the peak area ratio. It was calculated for the compounds with chromatographic peak areas bigger than 0.4 % and the sum of these peak areas was normalized to 100 % to calculate the relative abundance of each compound.

## Lignin solubility determination

The solubility determination of the different lignins was carried out in accordance with the following procedure:

- Dry the sample according to the procedure employed in the moisture content determination.
- Dissolve 1 gram weighed accurately ( $m_1$ ) in 5 mL ( $V_1$ ) of the selected solvent. Keep the sample under stirring 24 hours.
- Filter the sample employing a standard filter paper. The filter paper should be previously dried at 105 °C overnight, cooled down in a desiccator, and record its weight ( $m_2$ ).
- Dry the insoluble lignin fraction along the filter at 55 °C under vacuum for 24 hours. After that period, cool down the sample in a desiccator, and the record the final weight ( $m_3$ ). The solubility of the sample was calculated according to the following equation:

$$\text{Lignin solubility (g/L)} = \frac{m_1 - (m_3 - m_2)}{V_1}$$

## Differential Scanning Calorimetry analysis

The Differential Scanning Calorimetry (DSC) analysis is the most widely used technique to evaluate the thermal properties of a sample (glass transition temperature (T<sub>g</sub>), thermal stability, and heat capacity).

The DSC measures the energy necessary to maintain a sample and a reference at the same temperature, when they are both submitted to a temperature rise. DSC of the lignins and LBPs were carried out in a TA Instruments Q1000 Modulated Differential Scanning Calorimeter. Scans cycles consisted of heating the sample up to 100 °C followed by a cooling ramp between 100 °C and -80 °C and a subsequent heating ramp between -80 °C and 220 °C, both at 10 °C/min.

The glass transition temperature was determined as the onset of the change of slope of the measurement curve. The crystallization and melting temperatures of the samples were determined at the temperature where the maximum energy point associated with the phase change process was reached. The enthalpies associated with crystallization and melting processes were determined by integrating the normalized area associated with each process.

## Molecular weight analysis

Molecular weight distributions (MWD), the average molecular weights ( $\overline{Mw}$ ) and the polydispersity index (PDI) of the lignins and LBPs were determined by Size Exclusion Chromatography (SEC) using a Knauer Azura liquid chromatography equipment. The system consisted of two columns (Agilent ResiPore, 7.5 x 300 mm, 3  $\mu$ m) and a pre-column connected in series to an Azura RID 2.1L refractive index detector. Dried THF at a flow rate of 1 mL/min at 40 °C was used as the mobile phase. Calibration was carried out with an Agilent polymer polystyrene standard kit consisting of 15 standards with Mw ranging from 162 to 278700 g/mol.

The ( $\overline{Mw}$ ) and the PDI of the lignins were given by the total integration of the samples. The ( $\overline{Mw}$ ) and the PDI of the LBPs were given by partial

integration of the sample. The LBPs integration was done from the majority peak obtained at short elution times, including the possible formed shoulders.

## Lignin and LBP functional groups determination

The functional groups presented in the lignins and LBPs were analyzed by Attenuated Total Reflection Fourier Transform Infrared Spectroscopy (ATR-FTIR) analysis using an infrared spectrophotometer Bruker Instrument, model ALPHA-P in the range of 4000 to 400  $\text{cm}^{-1}$  at a resolution of 4  $\text{cm}^{-1}$  with 24 registered scans.

## Lignin-based polyol composition determination

The composition of the LBPs was determined according to the mass percentage of each compound. Three compounds composed the lignin-based polyols (LBPs): the lignin used, the employed monomer, and possible copolymerized solvent. To obtain the composition of the LBP it is necessary to remove previously the solvent used in the reaction by a rotary evaporator under vacuum at 55 °C until a constant weight is achieved.

The lignin weight content (L wt. %) in the LBP was calculated dividing the initial mass of lignin ( $m_L$ ) employed in the reaction by the total weight of the LBP obtained ( $m_{LBP}$ ) and multiplying the result by 100.

$$\text{Lignin content (L wt. \%)} = \frac{m_L}{m_{LBP}} \cdot 100$$

The monomer weight content in the LBP (MON wt. %) was calculated by dividing the difference between the monomer weight ( $m_{MON}$ ) used in the

reaction by the total weight of LBP ( $m_{LBP}$ ) obtained and multiplying the result by 100.

$$\text{Monomer content (MON wt. \%)} = \frac{m_{MON}}{m_{LBP}} \cdot 100$$

Copolymerizable solvent content was calculated by subtracting the sum of the two above percentage amounts from 100. In this thesis, only tetrahydrofuran (THF) was used as a solvent. Consequently, this value was given as the amount of THF polymerized (THF wt. %)

$$\text{THF content (THF wt. \%)} = (100 - (\text{L wt. \%}) - (\text{MON wt. \%}))$$

The average co-monomer/monomer molar ratio (MR THF/MON) was determined as the amount of co-comonomer (mol) polymerized by each mol of monomer employed. In this thesis, the co-monomer was the THF employed as a solvent in the reaction.

$$MR^{THF}/MON = \frac{m_{LBP} \cdot (\text{THF wt. \%}) / M_{w_{THF}}}{MON (mol)}$$

The average molar ratio as a function of the number of -OH groups proportioned by the lignin (OH:MON:THF) provides an insight of the average composition of the chains. This ratio was calculated as follows:

$$MR (OH:MON:THF) = \left( 1: MR \frac{MON}{OH-L} : MR \frac{MON}{OH-L} \cdot MR \frac{THF}{MON} \right)$$

The mass ratio employed in the study of the LBPs as phase change materials was calculated according to the weight content of the monomer and THF content in the LBP:

$$MON/_{THF} \text{ mass ratio} = \frac{THF \text{ content (THF wt. \%)}}{Monomer \text{ content (MON wt. \% )}}$$

– The term MON was substituted in **Chapter 3** by BO due to it was the only monomer used (Butylene oxide). In the same manner, in **Chapter 4**, the MON term can be substituted with any oxirane employed.

## Monomer conversion and unreacted monomer determination

The monomer conversion ( $conv_{MON}$ ) at a specific reaction time was determined taking into account the unreacted monomer, and the total theoretical monomer amount added. The unreacted monomer was determined using a HPLC instrument (Agilent 1260 Infinity) fitted with a 300 mm x 7.8 mm x 9  $\mu$ m Aminex HPX-87 column and a refractive index detector. The mobile phase was 0.01N aqueous sulphuric acid, and the flow rate of 0.7 mL/min. Column and detector temperatures were 65 °C and 50 °C, respectively. Samples were prepared diluting 0.200 mL aliquot of the reaction, 0.200 mL of malonic acid (9942 ppm in distilled water) in a 10 mL flask filled with the mobile phase. All samples were filtered to remove the insoluble fractions. The monomer conversion was calculated as follows:

$$Monomer \text{ conversion } (conv_{MON})(\%) = \left(1 - \frac{unreacted \text{ monomer (ppm)}}{total \text{ monomer added (ppm)}}\right) \cdot 100$$

The unreacted monomer concentration at a certain reaction time was calculated as follows:

$$Unreacted \text{ monomer concentration } (mol/L) = \frac{unreacted \text{ monomer (ppm)} / 1000}{Mw_{mon}}$$

## Hydroxyl number determination

The hydroxyl number (OH#), defined as the milligrams of potassium hydroxide (KOH) equivalent to the hydroxyl content of 1 g of sample is a suitable determination to evaluate the -OH content in a sample. The OH# of the lignins as well as the LBPs were determined according to ASTM E-1899-02 standard using THF as a solvent in a 702 SM Titrino equipment from Metrohm. Briefly, the determination was performed in accordance with the following procedure:

- Dissolve the sample (0.2-0.6 g) in THF (10 mL) under agitation, covering the beaker with a watch glass.
- When the sample is dissolved, add 10 mL of p-Toluenesulfonyl isocyanate (TSI) reagent (4 %V/V in acetonitrile) into the sample solution, and stir it slowly for 5 min.
- Then, add 0.5 mL of water to destroy the excess of TSI reagent, maintaining the solution 1 min under slow stirring.
- Add 30 mL of acetonitrile using a graduated cylinder.
- Place the beaker in the automatic titrator. Immerse the electrode and stir it with a gently stirring speed. Realize the titration with 0.1 N standardized Tetrabutylammonium hydroxide (Bu<sub>4</sub>NOH) solution (1M solution in methanol). The titrant normality should be verified each day by the analysis of a 1-Hexanol standard.
- Record the volume in mL of Bu<sub>4</sub>NOH employed to reach the first potentiometer endpoint (V<sub>1</sub>). Then, record the volume in mL of Bu<sub>4</sub>NOH employed to reach the second potentiometer endpoint (V<sub>2</sub>).

The hydroxyl number (OH#) was calculated according to the following equation:



$$\text{Hydroxyl numer (OH\#)} = \frac{(V_2 - V_1) \cdot N_{\text{Bu4NOH}} \cdot 56.1}{\text{sample weight (g)}}$$

## Thermo-Gravimetric Analysis

Thermo-Gravimetric Analysis (TGA) is used to determine the lignin thermal stability by monitoring sample weight loss as a function of temperature. TGA of lignins and LBPs were performed on a TA instruments TG-DTA92 instrument under air atmosphere. In a typical experiment, samples (10-20 mg) were heated from 20 °C to 100 °C at 5 °C/min. Then, the samples were dried at this temperature for 1 h in order to eliminate moisture and residual solvent, if any. Then, they were heated from 120 to 700 °C at 10 °C/min while recording the weight loss.

## References

- [A.1] “Determination of Structural Carbohydrates and Lignin in Biomass”, NREL, 2012.
- [A.2] “Test methods of the Technical Association of the Pulp and Paper Industry,” TAPPI Stand., 2007.
- [A.3] J. Liu, Y. Pan, C. Yao, H. Wang, X. Cao, and S. Xue, “Determination of ash content and concomitant acquisition of cell compositions in microalgae via thermogravimetric (TG) analysis,” *Algal Res.*, vol. 12, pp. 149–155, Nov. 2015.
- [A.4] I. Dávila Rodríguez, “High added-value compounds from the integral revalorisation of winery residues,” 2019.





---

---

The increase in the use of petrochemical-based products along with the oil depletion and the growing awareness of environmental issues has led to intense research for bio-based alternatives. The growing interest in green and sustainable chemistry has focused in the lignocellulosic feedstocks, being lignin one of the most promising biopolymers for its exploitation. However, the use of lignin for the production of bio-based materials is still hampered by its inherent low reactivity, its brittle and its complex structure. One way to boost the lignin is through its functionalization yielding lignin-based polyols with better properties. In this thesis, an industrially feasible alternative route is proposed. The new process allows to synthesize lignin-based polyols with controlled microstructure under mild conditions.

---

---

**Jonatan Pérez Arce**